Aus der Neurochirurgischen Klinik und Poliklinik
der Universitätsmedizin der Johannes Gutenberg-Universität Mainz

Effectiveness of ipsi- and contralateral approaches to the ophthalmic segment of the internal carotid artery: A comparative morphometrical characterization in anatomic specimens and 3D- virtual surgical simulations

Effektivität von ipsi- und kontralateralen Zugängen zum ophthalmischen Abschnitt der Arteria carotis interna: Eine komparative morphometrische Charakterisierung in anatomischen Präparaten und 3D-virtuelle chirurgische Simulationen

Dissertation
zur Erlangung des Doktorgrades der
Medizin

der Universitätsmedizin
der Johannes Gutenberg-Universität Mainz
vorgelegt von

Lucas Ezequiel Serrano Sponton
aus San Carlos de Bariloche, Argentinien

Mainz, 2019

Tag der Promotion: 20.11.2019

Index

Abbreviations used in this text

ACA	anterior cerebral artery
AChA	anterior choroideal artery
AcomA	anterior communicating artery
ACP	anterior clinoid process
C1	cervical segment of the internal carotid artery
C2	petrous segment of the internal carotid artery
C3	cavernous segment of the internal carotid artery
C4	supraclinoid segment of the internal carotid artery
FL	falciform dural fold (ligament)
HS	hypophyseal steal
ICA	internal carotid artery
MCA	middle cerebral artery
OA	ophthalmic artery
OCh	optic chiasm
oICA	clinoid and ophthalmic segment of the internal carotid artery
OlfN	olfactory nerve
ON	optic nerve
PB	perforant branches of the oICA
PComA	posterior communicating artery
PS	planum sphenoidale
rIOT	relative interoptic triangle
SHA	superior hypophyseal artery
SphS	sphenoidal sinus
STA	superficial temporal artery

$_i$	ipsilateral
$_c$	contralateral

F	Fisher test
IQR	interquartile range
M	median
ns	non-significant
r	Pearson's *r* correlation coefficient
η_p^2	partial eta-square
χ^2	chi-squared test
SD	standard deviation
T	Student t-test

1. Introduction and central objectives of the dissertation

Despite sophisticated surgical techniques, paraclinoid internal carotid artery (ICA) aneurysms remain a complex challenge to neurosurgeons. The complex anatomy of the clinoid and ophthalmic segments of the internal carotid artery (oICA) and its branches, its close relation to the optic apparatus and cavernous sinus and the surrounding bone contribute to this condition. Consequently, it is difficult to achieve proximal control and complex clip configurations as well as further surgical steps, like anterior clinoidectomy, are frequently required, all resulting in a high morbidity associated to these surgical procedures (Gelber 1980, Day 1990, de Oliveira 1996, Gibo 1981, Kobayashi 1989, Nishio 1985, Oikawa 1998, Nacar 2014).

Great advances in endovascular neurosurgery allow nowadays to effectively treat many paraclinoid aneurysms by these means, sparing the risks of open cranial surgery (Loumiotis 2012, Sun 2011, Wang 2013, Shimizu 2016, Lanzino 2012). However, endovascular techniques have their own limitations. Complex aneurysm and/or vessel configurations do not always allow complete occlusion, leaving a risk for recurrent bleeding (Loumiotis 2012). In addition, the occlusion of small perforant branches, not always visible on angiography, can cause ischemic complications with potential devastating consequences (Thornton 2000, Chen 2013b, Shimizu 2016). Furthermore, the use of stents or flow diverting devices implies the need of lifelong platelet antiaggregant therapy with its associated increased risk of intracranial haemorrhage (van den Brand 2017). Finally, endovascular techniques are unable to solve the problem of mass effects and compression of highly sensible neural structures, such as the optic nerve or chiasm, caused by some aneurysms.

In this context, surgery remains an important treatment modality and has turned into an even more demanding challenge. Neurosurgeons have to deal nowadays with selected cases that cannot be treated by endovascular means or after endovascular treatment has failed. Additionally, in many undeveloped countries endovascular techniques are not available in a vast majority of centres and surgery remains the only treatment option for patients presenting with this pathology. For all these facts, the study of the surgical anatomy and how to best approach the ophthalmic segment of the oICA remains a very important topic in vascular neurosurgery.

Traditionally, ipsilateral approaches have been applied to attempt surgical clipping of paraclinoid aneurysms (Yasargil 1984, Rhoton 2002, Hassoun-Turkmani 2016).

However, these approaches usually require oICA and optic nerve mobilization as well as anterior clinoidectomy, all associated with increased surgical risk and morbidity. Some surgeons have suggested that contralateral approaches may provide better exposure of the oICA's medial aspect and its branches, being therefore more effective for the treatment of paraclinoid aneuryms. The microsurgical anatomy of these contralateral approaches has however not yet been studied systematically.

The aim of the present work is to anatomically and morphometrically characterize the contralateral approach to the oICA and to systematically compare its effectiveness to ipsilateral approaches.

The main questions of the present study can be summarized as follows:

- Which are the optimal trajectories to access the superomedial aspect of the oICA when using approaches from the ipsilateral and contralateral side? Do these trajectories differ from each other? Which are the main surgical implications of this?
- Which are the exact morphometric and anatomic characteristics of the `conventional´ ipsilateral and `non-conventional´ contralateral approaches to the oICA? Which are the main anatomo-morphometrical differences between both approaches and which are their meaningful surgical implications? Allows a contralateral approach better exposure of the medial oICA aspect and its branches in comparison to ipsilateral approaches?
- To which extent is the exposure of the oICA influenced by removing the anterior clinoidal process in ipsilateral approaches?
- To which extent is the exposure of the oICA influenced by removal of the planum sphenoidale/tubecullum sellae and/or mobilizing the contralateral optic nerve in contralateral approaches?
- Which anatomical factors determine the feasibility and effectiveness of contralateral approaches to the oICA and its branches?

In order to address these issues, we studied the anatomy and morphometry of ipsi- and contralateral approaches to the oICA and the parasellar region in cadaveric specimens. Since moderate changes in vasculature morphology can occur after cadaveric conservation (Rozen 2009) we additionally studied these approaches in virtual 3D models based on MRT and CT data of alive subjects, which were not subjected to postmortem changes.

2. Literature discussion

2.1 Anatomy of the internal carotid artery's clinoid and ophthalmic segment

The internal carotid artery has been traditionally divided in four segments. The cervical segment (C1) extends from its origin at the common carotid bifurcation to the external orifice of the carotid canal, the petrous segment (C2) stretches along the carotid canal within the petrous bone and ends where the artery enters the cavernous sinus, the cavernous segment (C3) courses within the cavernous sinus and ends where the artery passes through the dura mater forming the roof of the cavernous sinus, and the supraclinoid segment (C4) begins where the artery enters the subarachnoid space and extends to its bifurcation into the anterior (ACA) and middle cerebral arteries (MCA) (Paullus 1977, Rosner 1984).

The C4 segment is subdivided into three portions according to the origin of the ophthalmic (OA), posterior communicating (PcomA) and anterior choroideal (AChA) arteries. The ophthalmic portion is the longest and comprehends the C4 segment from its origin at the dural sleeve to the origin of the PcomA, the communicating portion extends up to the origin of the anterior choroideal artery (AChA), and the choroideal portion includes the segment between the AChA and the ICA bifurcation (Gibo 1981).

As the carotid artery emerges from the cavernous sinus, it enters the dura and subarachnoidal space into the carotid cistern and follows a superior trajectory attached to the anterior clinoid process to its upper end, prior to acquire a superomedial relationship to it. This tiny portion of the carotid artery covered by the anterior clinoid process is referred as the clinoid segment and is regarded as a part of the ophthalmic segment of the C4 (Rhoton 2002). The clinoid segment of the internal carotid artery is located at the junction of the intracavernous and subarachnoid segments of the artery, between the dural folds coming from the upper and lower margins of the anterior clinoid process. The dura coming medially from the top of the anterior clinoid process forms the upper dural ring around the carotid artery. The dura coming medially from the lower margin of the anterior clinoid surrounds the artery to form the lower dural ring. Both rings mark respectively the upper and lower margins of the clinoid segment. The upper ring forms a tight collar around the artery, although there is usually in fact a narrow depression in the dura at

the site at which the ring reaches the anteromedial aspect of the artery, the so called carotid cave. This cave extends a variable distance below the level of the upper dural ring and is most prominent on the anteromedial side of the artery. The artery then follows a course upward, posterior and slightly lateral towards its bifurcation. The carotid artery is immediately lateral to the optic nerve and may course parallel to it, or it may describe a convex or concave curve in relation to the nerve. Often, this tortuosity described by the artery can indent the nerve as it enters the optic canal (Yasargil 1984).

The ophthalmic artery (OA) is the first branch of the supraclinoid internal carotid artery and is directed medially, a constant anatomic feature with relevant surgical implications. It arises in the majority of cases from the anteromedial (53.6%) or superomedial (31.5%) aspect of the C4 and even when the exact site of origin can be variable, none OA arise from the lateral third of the ICA (Hayreh & Dass 1962, Hayreh 1974, Rhoton 2002). Most OA arise anterior to the tip and approximately 5 mm medial to the anterior clinoid process (Harris 1976). According to old series reporting the study in 168 specimens, in 83% the origin of the artery was in the subdural space just at the point where the carotid artery enters the dura after leaving the cavernous sinus (clinoid portion), in 2% it arose just proximal to this point so the artery was partially subdural and partially extradural, in 7.5% the origin was even further proximally, so that it was intracavernous and completely extradural, and in the 6.5%, it arose within the most anterior portion of the carotid cistern within 1 mm of its most anterior portion (Hayreh & Dass 1962, Hayreh 1974). In extremely rare cases, the OA may arise from the middle meningeal artery (Liu 2001). The intracranial segment of the OA is usually very short. In 14% of the cases it enters the optic canal immediately after its origin from the internal carotid artery (Harris 1976). In the remaining 86%, the maximum length prior to the entrance into the optic canal has been found to be 7 mm with an average of 3 mm (Harris 1976). In its origin and initial course, the OA is in close contact with the planum sphenoidale, the tuberculum sellae and the proximal part of the supraclinoid internal carotid artery to which a section of the OA is frequently adherent (Hayreh 1974). Further, the OA is frequently attached to the inferior surface of the optic nerve during its entire intracranial course. The position of the OA in relation to the optic nerve is inferomedial in 43 % of cases, directly inferior in 37 %, inferolateral in 16 %, or in very rare cases (2%) directly medial or lateral (Hayreh & Dass 1962). It enters the optic canal beneath the optic

nerve following an inferolateral relationship in 26% of cases, directly inferior in 33% and inferomedial in 41% (Hayreh & Dass 1962). Within the optic canal it perforates the optic nerve dural sheath and lies between this sheath and the periosteum inferolaterally (84.5%) or inferomedially (15.5%) to the optic nerve (Hayreh & Dass 1962). As the OA enters the orbit, it crosses over (82.6%) or under (17.4%) the optic nerve and follows a more medial course. The OA has usually a diameter that varies between 1 and 2 mm and uncommonly gives rise to intracranial perforating branches, which run posteriorly and irrigate the ventral aspect of the optic nerve, the chiasm and the pituitary stalk.

An average of four perforating arteries arise from the oICA. Typically, most of these perforant branches arise from the posterior or medial aspect of the artery. These branches irrigate important structures such as the infundibulum and stalk of the pituitary gland, the optic chiasm, and less commonly, in descending order of frequency, the optic nerve, premamillary portion of the floor of the third ventricle, the optic tract and the parahippocampal uncus (Yasargil 1984, Rhoton 2002). Some small perforant branches terminate in the dura mater covering the anterior clinoid process, falciform fold, sella turcica, and tuberculum sellae. The superior hypophyseal arteries (SHA) correspond to the most relevant perforant branches arising from the oICA and are usually studied separately (Fuji 1980, Gibo 1981, Yasargil 1984, Rhoton 2002). In average there are two of these small but rather constant vessels leaving the inferomedial, posteromedial, medial or the posterior surface of the oICA and course beneath the optic nerves through the carotid and chiasmatic cisterns to irrigate the pituitary stalk, tuber cinereum, anterior lobe of the pituitary, the inferior surface of the optic nerves and chiasm (Stephens & Stilwell 1969, Rhoton 2002). The largest of these branches is often referred in surgical anatomy as `the´ superior hypophyseal artery (SHA) so that we have adopted this nomenclature for our present study (Rhoton 2002). As the SHA anastomose with contralateral vessels and with the inferior hypophyseal branches of the ICA (circuminfundibular anastomosis), they form a longitudinally oriented vascular plexus around and along the hypophyseal stalk corresponding to the hypophyseal portal system.

2.1.1 Osseous relationships: The sphenoid bone

The clinoidal and ophthalmic segments of the internal carotid artery are surrounded by tightly osseous structures belonging to the sphenoid bone. Observed from a superior view, the C3 portion of the internal carotid artery transverses the cavernous sinus, located on the lateral aspect of the pituitary fossa, and emerges posteromedially to the anterior clinoid process and posterolaterally to the planum sphenoidale and tuberculum sellae, all belonging to the sphenoid bone. The pituitary fossa occupies the central part of the sphenoid body and is limited anteriorly by the tuberculum sellae and posteriorly by the dorsum sellae. The chiasmatic groove, a slight transverse depression connecting both optic foramina, is limited posteriorly by the tuberculum sellae and anteriorly by the planum sphenoidale. The tuberculum sellae may vary from being almost flat to protruding upward as much as 3 mm (Renn 1975). The frontal lobes and the olfactory nerves rest against the smooth upper surface of the lesser sphenoidal wing and the planum sphenoidale. The posterior margin of the lesser wing forms the sphenoid ridge, a free edge which projects into the sylvian fissure to separate the frontal and temporal lobes. The anterior clinoid processes are located at the medial end of the lesser sphenoid wings, the middle clinoid processes are lateral to the tuberculum sellae, and the posterior clinoid processes are situated at the superolateral margin of the dorsum sellae. The anterior clinoid process provides the bony roof to the superior orbital fissure and the anterior portion of the cavernous sinus. The optic strut extends from the inferomedial surface of the anterior clinoidal process towards the body of the sphenoid bone, providing a separation between the optic canal from the superior orbital fissure. As mentioned before, these bony landmarks surround the ICA in a tight manner as the vessel arises from the cavernous sinus and interfere with any surgical approach to the anterior, lateral and especially medial borders of the ICA. Superomedially, the anterior clinoid process is connected to the planum sphenoidale through a bone layer corresponding to the roof of the optic canal. The most posterior portion of the optic canal roof is formed by a dural fold called the falciform ligament.

2.1.2 Neural relationships

The cranial nerves included within the cavernous sinus or running through its lateral dural envelope, i.e. III, IV, V and VI, are rarely affected by pathology of the clinoidal

or ophthalmic segments of the ICA, since paraclinoid aneurysms generally project superiorly or medially away from the superior orbital fissure and lateral cavernous sinus wall. However, given their close proximity to the anterior clinoid process the knowledge of their anatomy becomes relevant to avoid injury if an anterior clinoidectomy must be performed. The oculomotor nerve perforates the roof of the cavernous sinus within a triangular depression (oculomotor cistern/triangle) limited by the anterior petroclinoidal, posterior petroclinoidal and interclinoidal dural folds and turns downward in the superolateral corner of the cavernous sinus. It courses anteriorly just beneath the anterior clinoidal process and enters the orbit through the superior orbital fissure within the Zinn anulus. The trochlear nerve is also located within the lateral cavernous sinus wall, traveling just beneath and parallel to the oculomotor nerve and enters the orbit through the superior orbital fissure but lateral to Zinn´s anulus. The first division of the trigeminal nerve (V1) courses several millimeters below the oculomotor and trochlear nerves within the lateral sinus wall, whereas the abducens nerve enters the cavernous sinus through Dorello's canal and courses within the cavernous venous compartment accompanying the ICA to reach the orbit through the superior orbital fissure within Zinn´s anulus. Finally, sympathetic fiber plexus course along the cavernous and clinoidal ICA, usually leaving the carotid artery proximal to the carotid collar to project into the orbit.

In contrast, the optic nerves or the chiasm are often directly in line with aneurysms arising from the clinoidal and ophthalmic segment of the ICA. The optic nerve leaves the orbit through the medial part of the annular tendon. After passing through the optic canal, which forms a prominence in the upper part of the sphenoid sinus in front of the sella turcica and along the medial aspect of the anterior clinoid process, the intracranial portion of the nerve is directed posteriorly, superiorly, and medially toward the optic chiasm and crosses the anterior incisural space. After leaving the optic canal and proximal to its entrance into the subarachnoid space, the optic nerve is covered by a leaf of dura mater, previously mentioned as the falciform ligament. The length of nerve covered only by falciform ligament's dura may vary from less than 1mm to 10 mm (Renn 1975). The existence of the falciform ligament acquires surgical relevance since coagulation of the dura above the optic nerve just proximal to the optic canal can lead to nerve injury. Furthermore, compression of the optic nerve against the sharp edge of the falciform ligament may also result in nerve damage and visual deficits.

Both optic nerves join in the midline into the optic chiasm, which is situated at the junction of the anterior wall and floor of the third ventricle. The ACA and anterior communicating artery (AcomA), the lamina terminalis and the third ventricle are located immediately above the chiasm. Posteriorly the chiasm is related to the tuber cinereum and the infundibulum, while both ICAs are lateral and the diaphragma sellae and pituitary gland are situated below. The third ventricle forms the suprachiasmatic recess between the chiasm and lamina terminalis and the infundibular recess extends into the base of the pituitary stalk posteriorly to the optic chiasm.

2.2 The anatomy of paraclinoid internal carotid artery aneurysms

Many authors have suggested sophisticated classifications of aneurysms arising in this region based on variations in clinical and anatomic features (Rodhan 1993, Barami 2003, Batjer 1994, Day 1990, Giannotta 2002, Heros 2002, Kinouchi 2002, Kobayashi 1989, Oshiro 1997, Raco 2008). Basically, aneurysms of the C4 segment of the internal carotid can arise at five sites: the upper surface of the ICA at the origin of the OA, the medial wall at the origin of the SHA, the posterior wall at the origin of the PcomA, the posterior wall at the origin of the AChA and the apex of the ICA bifurcation into the ACA and ACM (Rhoton 2002). Paraclinoid aneurysms are defined as those arising from the ICA in close relationship to the anterior clinoid process. As pointed out by other authors, using this broad definition, aneurysms arising from the intracavernous, clinoidal, ophthalmic and posterior communicating C4 segments could be included as paraclinoid aneurysms. However, in practical terms paraclinoid aneurysms comprehend aneurysms arising from the clinoidal and ophthalmic ICA portion (Hassoun-Turkmani 2016).

2.2.1 Clinoidal Segment Aneurysms

These aneurysms arise between the upper and lower dural ring of the clinoid segment of the ICA and due to the strong and fixed bony relationships surrounding the short clinoidal segment of the internal carotid artery, the frequency of these aneurysms is very low. They can be classified in anterolateral and medial variants (Hassoun-Turkmani 2016).

2.2.1.1 Anterolateral Variant

This variant constitutes the least common form of clinoidal segment aneurysms. It arises from the anterolateral surface of the clinoid segment as it obliquely ascends toward the dural ring under the anterior clinoid process. Given the superiorly and slightly medially directed course of the segment, an aneurysm that expands lateral and anterior to the ascending ICA tends to project superiorly toward s or into the anterior clinoid process. These aneurysms may erode the optic strut and the anterior clinoid process causing optic nerve compression within the optic canal and monocular ipsilateral visual loss. These aneurysms are associated mostly with the hemodynamic stress associated with the anterior ascending vertical segment of the cavernous ICA and rarely with a low origin of the ophthalmic artery, given the medial origin of this artery.

2.2.1.2 Medial Variant

The medial variant constitutes the most common form of clinoid segment aneurysms. These aneurysms enlarge toward the sphenoid sinus and the sella turcica as the ICA turns from lateral to medial during its ascent toward and through the dural ring. They can expand beneath the diaphragma sellae into the pituitary fossa, causing hypopituitarism. In rare cases aneurysm rupture into the sella and pituitary gland may simulate pituitary apoplexy. Extension and rupture into the sphenoid sinus may cause life-threatening epistaxis. Visual loss from this aneurysm type does not occur with small lesions, but field cuts resembling those of pituitary tumors may occur with giant lesions invading the suprasellar space.

2.2.2 Ophthalmic Segment Aneurysms

These aneurysms constitute the vast majority of paraclinoid aneurysms, exceeding in frequency the clinoid aneurysms. Three variants can be differentiated according to their origin, projection and relationships to arterial branches and the adjacent dural- and osseous structures (Hassoun-Turkmani 2016).

2.2.2.1 Ophthalmic Artery Aneurysms

These lesions typically arise along the posterior aspect of the ICA just distal to the OA and dural ring. They project dorsally or dorsomedially and can press the lateral edge of the nerve against the falciform ligament. The pressure from the falciform

ligament against the superior surface of the nerve results in a monoocular inferior nasal visual field defect. As the lesion enlarges, the entire nasal visual field can be affected, followed by a superior temporal field loss in the contralateral eye. If this condition is left untreated, ipsilateral blindness with marked contralateral deficits can occur. If the ophthalmic artery has an even longer subarachnoid segment and arises distal to the upper ring along the superomedial side of the carotid artery, the aneurysm may project medially under the optic nerve in the anterior pre-sellar area and mimic an anteriorly situated superior hypophyseal aneurysm, although it arises at the origin of the OA.

2.2.2.2 Superior Hypophyseal Artery Aneurysms

Superior hypophyseal artery aneurysms arise in association with the SHA along the medial surface of the ICA, usually just distal to the upper dural ring. There are two main variants: the parasellar variant projects inferiorly toward the sella into the carotid cave, whereas the suprasellar variant projects superiorly into the suprasellar space. Their medial projection and proximity to ICA perforators renders an ipsislateral approach difficult. These aneurysms tend to elevate the optic chiasm and produce visual changes similar to those seen with pituitary tumors. Larger SHA aneurysms tend to develop thickenings or calcifications in their wall along the anteromedial aspect, near their origin from the ICA, similar to OA aneurysms. Because these lesions can extend medially to the optic chiasm, they can result in bilateral visual field defects. Many small lesions project inferiorly and medially toward and beneath the diaphragma sellae, expanding the carotid cave. These lesions, termed parasellar variant of SHA aneurysms, have also been called carotid cave aneurysms and discussed as a distinct variant (Rhoton 2002). Superior hypophyseal artery lesions can cause visual deficits by expanding into the suprasellar space and compressionof the optic chiasm, producing superior bitemporal visual field deficits or other patterns more suggestive of pituitary tumors.

2.2.2.3 Dorsal variant aneurysms

Dorsal variant aneurysms are rare and arise along the dorsal surface of the ICA distinctly distal to the ophthalmic artery origin, unrelated to any arterial branch point (Hassoun-Turkmani 2016). Many are thought to be the result of hemodynamic forces caused by accentuated turbulences in the ICA as the vessel courses laterally to form the communicating segment. Others appear as blister-like aneurysms on the dorsal

carotid surface of the ophthalmic segment. Visual loss or a reliable relationship with the optic nerve or chiasm is not consistently seen with the rare dorsal variant.

2.3 Surgical approaches to paraclinoid aneurysms

Traditionally, ipsilateral surgical approaches have been performed to treat paraclinoid aneurysms and other pathologies of the oICA (Yasargil 1984, Rhoton 2002, Hassoun-Turkmani 2016). For this approach the patient is positioned supine, the head is elevated above the heart, fixed in a head clamp and turned 45 to 60 degrees toward the contralateral side. The vertex is lowered in order that the maxilla is at the highest point in order to use gravitational retraction of the frontal and temporal lobes. Most surgeons drape out the cervical carotid region to gain proximal control of the ICA if required. The skin incision depends on the craniotomy to be performed. For the pterional craniotomy with its variations, advocated by the majority of cerebrovascular surgeons, the skin is incised from the midline to the zygoma, just behind the hairline.

For paraclinoid aneurysms the skin and galea are usually incised and retracted as one single layer and the temporalis muscle and fascia are treated as a second layer. This two-layer scalp opening provides a lower exposure and better access for removing the anterior clinoid process and adjacent part of the orbital roof than the single-layer flap which is nevertheless preferred by other surgeons (Rhoton 2002). A craniotomy centred below the pterion is then performed. Typically, it extends inferiorly and medially to the sphenoid ridge and the orbital roof can then be thinned (Yasargil 1984). The orbitozygomatic osteotomy, an extended modification of the traditional pterional approach, has been used with increasing frequency, mostly in the USA, arguing that it reduces the need for brain retraction, increase the width of the operative route, and broaden the angle for dissection and clip application (Rhoton 2002). For this variant, a variable amount of the upper and lateral orbital rim and zygomatic arch are removed as a single piece in continuity with the bone flap, or as a second step after elevation of a pterional bone flap. However, the incidence of weakness of the frontalis muscle is higher for orbitozygomatic osteotomy because the manipulation of the facial nerve branches to the frontal muscle within the superficial temporal fascia and fat pad is greater than for pterional craniotomies. Furthermore, extended dissection around the temporalis muscle needed for an orbitozygomatic osteotomy increases the incidence of contractures that limit opening

of the mouth. This must be added to the higher incidence of cosmetic deformities caused by scarring and atrophy of the temporalis muscle as well exophthalmos, enophthalmos, diplopia and persistent periorbital and eyelid swelling which is associated with the orbitozygomatic craniotomy (Boari 2017). After the pterional or orbitozygomatic bone flap is elevated and the dura opened, the dissection is performed straightforward through the Sylvian fissure to expose the carotid artery. The frontal lobe may be elevated to expose the sphenoid ridge to the depth of the anterior clinoid process. To get access to aneurysms arising from the OA and SHA, which tend to originate and point medially, ipsilateral approaches require the removal of the anterior clinoid process (usually performed intra- rather than extradurally), the optic strut, opening the falciform dural fold, unroofing the optic canal and mobilization of the optic nerve and the C4 segment of the ICA and its branches (Hassoun-Turkmani 2016).

Some experienced neurosurgeons have advocated the use of contralateral approaches to paraclinoid aneurysms and the oICA, arguing that the anatomy of the oICA and specifically its medial wall, where most ophthalmic and superior hypophyseal artery aneurysms arise, can be better exposed from the contralateral side (van Lindert 1998, de Oliveira 1996, Fries 1997, Nakao 1981, Nishio 1985, Perneczky 1985, Shiokawa 1988, Vajda 1988). Furthermore, the high incidence of multiple aneurysms observed in patients with paraclinoid aneurysms encourage neurosurgeons to be able to approach them bilaterally through a one-sided craniotomy (Fries 1997, Nankao 1981, Vajda 1998, Sheick 200b).

Along decades of aneurysm surgery, only some sporadic small case-series and case-reports have been published reporting the use of a contralateral approach to treat paraclinoid aneurysms (*Table 1*). In these reports, a contralateral pterional craniotomy has been applied in the majority of cases. This includes some variations, such as surgery in semi-sitting position in order to reduce the venous pressure in the cavernous sinus (Sheick 2000b) or reducing the extent of craniotomy to only its supraorbital portion (Fries 1997, Andrade-Barazarte 2015). All authors conclude that the use of this approach can be highly effective and associated with very good clinical and surgical results if patients are carefully selected. However, to date there is a lack of systematic studies assessing the surgical anatomy and morphometry of contralateral approaches to the oICA and there are no studies comparing the visualization of the oICA through ipsilateral vs. contralateral approaches.

Ref	N	Median (Min/Max) age	Sex (%)		Aneurysm distribution (%)		Aneurysm size	Aneurysm localization	Projection	Approach	Complete occlusion?	Contralateral optic nerve mobilization	Way to achieve proximal control	Complications	Outcome
			M	F	Unilateral	Bilateral									
Nakao 1981	2	40.5 (36/45)	0	100	50	50	NS	OA	Posteromedial	Pterional	Yes	Not required	NS	None	Good
Milenkovic 1982	1	48	0	100	0	100	NS	OA	NS	Pterional	Yes	NS	NS	Intraoperative bleeding from other aneurysm	Good
Yamada 1984	4	51.5 (32/57)	0	100	75	25	NS	OA	Medial	Pterional	Yes	Not required	NS	Vasospasm: 25% Mild hemiparesis: 25%	Good: 50% Fair: 50%
Nishio 1985	1	55	0	100	0	100	10 mm	OA	Inferomedial	Pterional	Yes	Not required	NS	None	Good
Shiokawa 1988	1	44	0	100	0	100	NS	OA	Medial	Bifrontal	Yes	NS	NS	None	Good
Vajda 1988	23	NS	NS	NS	50	50	4-35 mm	OA	NS	Pterional	NS	Slight mobilization if aneurysm > 15 mm	NS	NS	NS
Oshiro 1997	1	NS	NS	NS	0	100	NS	OA	NS	Pterional	Yes	NS	NS	None	NS
Fries 1997	10	53.5 (33/64)	20	80	90	10	<10 mm: 60% 10-24 mm: 40%	OA: 60% SHA: 40%	Medial: 60% Superomedial: 20% Anteromedial: 10% Superior: 10%	Supraorbital	Yes 80% Wrapping 20%	NS	Ballon occlusion + clinoid segment exposure	Visual deficits: 10%	Good: 70% Fair: 10% Poor: 10% Dead: 10%
Kakizawa 2000	11	60 (55/76)	18	82	37	63	<5 mm	OA	Superomedial: 45% Inferomedial: 55%	Pterional	Yes	Not required: 73% Slight mobilization: 27%	Cervical exposure	None	NS
Sheick 2000b	4	55.5 (48/60)	50	50	100	0	<5 mm	CC	Inferomedial: 25% Medial: 75%	Pterional / Bifrontal	Yes	Slight mobilization	Ballon occlusion	None	Good
Hongo 2001	1	69	0	100	0	100	25 mm	OA	Superomedial-posterior	Pterional	Yes	Not required	Clinoid segment exposure	None	Good
McMahon 2001	9	44 (38/60)	22	78	0	100	NS	OA: 77% SHA: 23%	NS	Pterional	Yes	Not required	NS	Visual deficits: 11% Artery dissection: 11% N. caudatus infaction: 11%	Good: 78% Fair: 11% Dead: 11%
Pereira 2006	13	NS	NS	NS	0	100	NS	OA: 84% SHA: 16%	NS	Pterional		NS	NS	Visual deficits: 23%	Good
Park 2009	2	44 (25/63)	0	100	0	100	NS	OA: 50% SHA: 50%	NS			NS	NS	Anosmia: 50%	Good
Chandela 2011	1	37	0	100	0	100	NS	OA	Medial	Pterional	Yes	NS	Cervical exposure	None	NS
Chen 2013	8	60.5 (28/77)	25	75	100	0	<5 mm	SHA	Inferomedial: 75% Superomedial: 25%	Pterional	Yes	Not required: 62% Slight mobilization: 25% Significant mobilization: 13%	Ballon occlusion	None	NS
Nacar 2014	11	47 (24/62)	11	89	0	100	<6 mm	OA	Superior: 64% Medial: 18% Superomedial: 9% Anteromedial: 9%	Pterional	Yes 91% Wrapping 9%	Not required: 82% Sligth mobilization: 18%	NS	Pneumonia: 9% Visual deficits: 9%	Good: 91% Dead: 11%
Andrade-Barazarte 2015	30	45 (19/79)	17	83	15	85	<7 mm: 96% 7-14 mm: 4%	OA	Superomedial: 76% Medial: 13% Superior: 10%	Supraorbital	Yes	NS	ns	CSF leackage: 7% Wound infection: 7% Visual deficits: 3%	Good: 93% Poor: 7%
Yu 2017	5	54 (47/65)	NS	NS	0	100	2-14 mm	OA	Medial	Pterional	NS	NS	NS	NS	Good

Table 1. A survey of published studies that investigate contralateral approaches to paraclinoid aneurysms. Relevant articles were first identified in a Pubmed search by the following Boolean search terms: {"aneurysm" AND (“approach” OR “approaches”) AND ("contralateral" OR "unilateral" OR "bilateral")} on the 11th of November 2017. The articles were then screened to exclude studies in which (i) no paraclinoid aneurysms had been treated, (ii) no contralateral approaches were used, (iii) no epidemiological or surgical data from patients were available. Furthermore, after having identified relevant works, additional articles could be identified by a systematic cross reference search. *M*, male; *F*, female; *NS*, not specified; *OA*, ophthalmic artery; *SHA*, superior hypophyseal artery; *CC*, carotid cave.

3. Materials and methods

3.1 Anatomical study in cadaveric specimens

3.1.1 Set-up of the experimental microsurgical laboratory

All cadaveric dissections were performed in our experimental microsurgical research laboratory at the University of Mainz Medical Center. The facility was equipped with 2 surgical lightheads and a fixed operating table. For cadaveric dissections, complete sets of surgical and microsurgical instruments were used. Craniotomies and skull base bone removal were accomplished with a craniotome and a high speed surgical drill (ELAN-EC, Aesculap®).

Microsurgical dissections were carried out using an operative microscope (Carl Zeiss Set NC 4 Multivision), protected with the adequate plastic coverage to avoid contact with cadaveric specimens.

3.1.2 Cadaveric specimens

Eight adult head cadaver specimens conserved in a formaldehyde solution of 40 g/L were used for 16 craniotomies in this study. All ethical and hygienic procedures for obtaining and conservation of cadaveric specimens followed the standard rules set up by the Hygiene and Health Department of the University of Mainz.

Craniometric measurements on the sagittal, coronal and axial planes were estimated for each head to rule out significant anthropometric differences between specimens as well as asymmetry between the right and left skull halves.

3.1.3 Ipsi- and contralateral pterional approach to the internal carotid artery

Each specimen was subjected to classical bilateral pterional craniotomies (Yasargil 1984) and microsurgical dissections directed to the oICA following a systematic stepwise manner:

The head was mounted in a 19 × 19 cm quadrangular holder and fixed in 4 points with adjustable pins in supine position. Head fixation resembled the classical positioning used for in-vivo pterional approaches, directed about 20° vertex down, elevated slightly, and rotated about 45° to bring the malar eminence to the superior point of the operating field. This position allows the frontal lobes to fall away from the orbital roof, the sphenoid ridge is directed vertically in the operating field and establishes an unobstructed visual axis through the surgical microscope along the sphenoid ridge to the anterior clinoid and parasellar area.

Dissections started with a curvilinear skin incision starting approximately 1 cm inferior to the zygomatic arch and 1 cm anteriorly to the tragus (*Figure 1*). The incision extended to the temporal crest in a direction perpendicular to the zygoma. From the temporal crest, the incision curved sharply anterior, ending in cadaveric specimens 1-2 cm beyond the midline and hairline. Due to the reduced distensibility of the tissue induced by formaline conservation, the skin incision had to be slightly broader than when performed in living patients. The incision sacrificed in all cases only collateral branches of the superficial temporal artery, leaving the main trunk of this vessel undamaged *(Figure 1)*. The skin flap was reflected anteroinferiorly to expose the epicranial aponeurosis (galea aponeurotica) and the temporal muscle covered by the superficial temporal fascia. An incision along the superficial temporal fascia was performed just above the superior border of the fat pad that covers the temporal and zygomatic branches of the facial nerve. Following this step, the temporal muscle was detached and reflected posteroinferiorly, providing a wide exposure of the skull surrounding the pterion.

A burr hole was then placed at the MacCarty's keyhole point, located at the anterior junction of the zygoma and the frontal bone (MacCarty 1972) and a pterional craniotomy was extended anteriorly above the orbital roof up to the supraorbital foramen, as well as posteriorly up to 4 cm along the temporal squama *(Figure 2)*. After elevating the bone flap, the temporal squama and greater wing of the sphenoid bone were rongeured further inferiorly toward the floor of the middle fossa, thereby allowing more mobility of the anterior temporal lobe if necessary. With the aid of a high-speed electric drill and gentle frontal lobe retraction, the rough bone of the posterolateral orbital roof was smoothened. In a similar fashion the posterior ridge of

the lesser wing of the sphenoid bone was progressively flattened until the orbital-meningeal fold was reached.

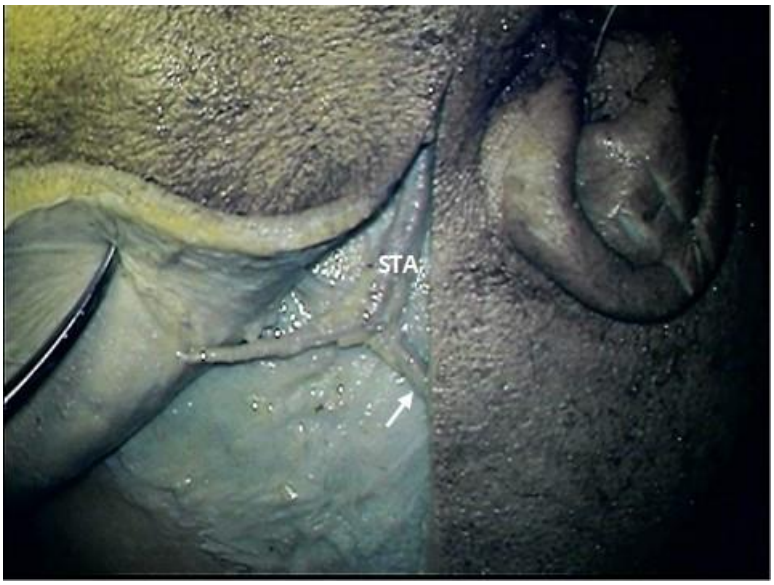

Fig. 1. In order to perform pterional craniotomies, skin insicion started 1 cm anterior to the tragus an was directed perpendicular to the zygoma until it reached the superior temporal line, where it sharply curved rostrally towards the midline. The main trunk of the superficial temporal artery (STA) was left intact and access to deeper planes of dissection was gained by dividing the posterior branches of the STA (arrow).

After bone removal, the dura mater, containing the branches of the medial meningeal artery, was incised and opened in a semicircular fashion around the Sylvian fissure. The incision arched toward the sphenoid ridge and orbit and reflected anteroinferiorly. At this stage the operative microscope was set on the operative field and the following steps of dissection were carried on in microsurgical technique:

The further dissection was performed stepwise and straightforward towards the anterior parasellar region of the skull base to approach the supraclinoidal segment of the ICA and its neighbor structures *(Figure 2)*. The approaches were directed both through opening the sylvian cistern, entering at the level of the opercular part of the inferior frontal gyrus (*transsylvian route*), as well as through a corridor above the orbital roof allowing retracting the frontal lobe up to a maximum of 15 mm (*subfrontal/supraorbital route*) (*Figure 2 to 5*).

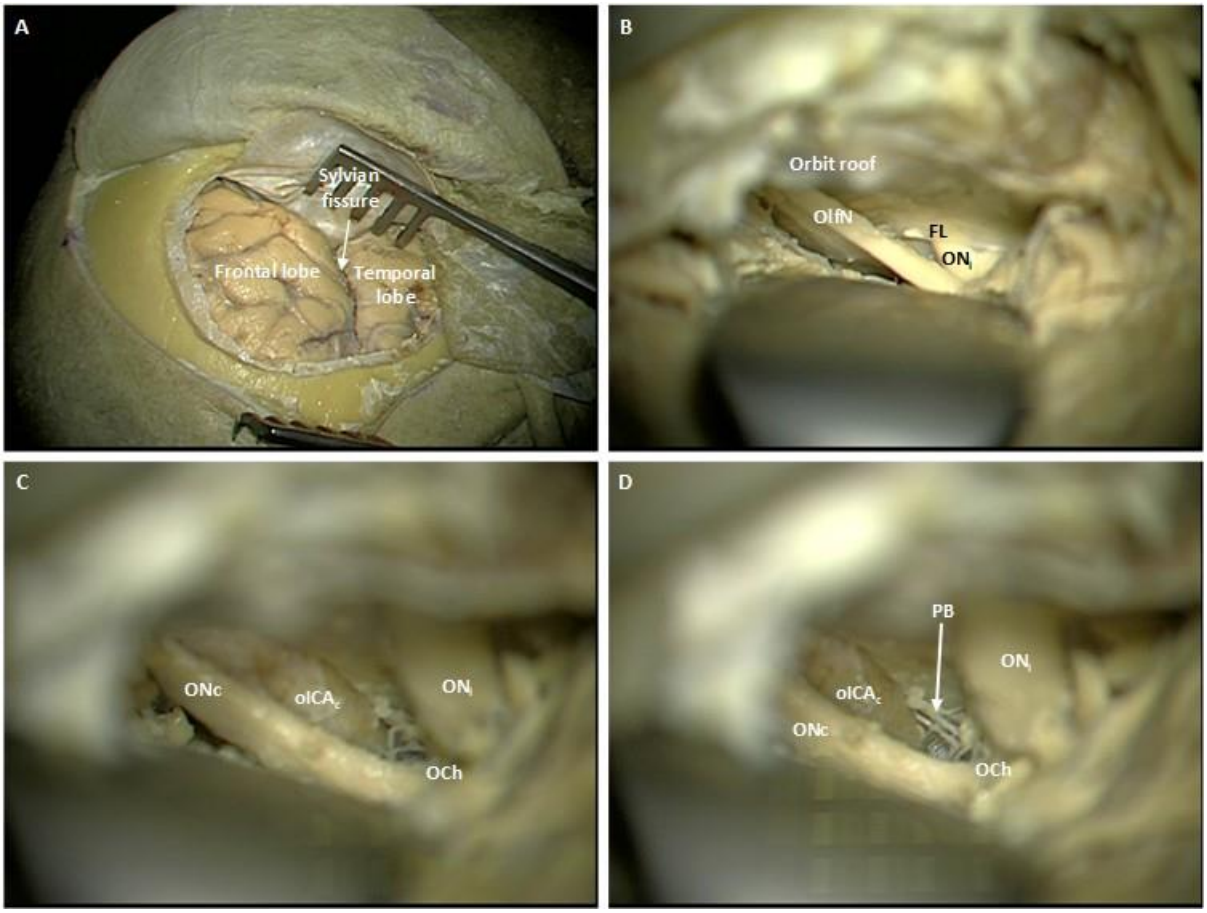

Fig. 2. After two-layer scalp opening and posteroinferior re-flexion of the temporal-muscle flap a pterional craniotomy was performed. The dura was folded anteriorly and the frontal and temporal lobes, divided by the sylvian fissure, were exposed (*A*). To approach the medial aspect of the contralateral internal carotid artery, the frontal lobe was retracted and the orbit roof smoothened (*B*). The olfactory nerve was identified lying on the straight gyrus of the frontal lobe, and the optic nerve furhter down. The interoptic space provided access to the medial wall of the contralateral internal carotid artery and exposed several of its perforating branches (*C, D*). *OlfN,* olfactory nerve; *FL,* falciform dural fold (ligament); *ON$_i$*, ipsilateral optic nerve; *ON$_c$*, contralateral optic nerve; *OCh,* optic chiasm; *oICA$_c$,* ophthalmic segment of the contralateral internal carotid artery; *PB,* perforant branches of the oICA.

The following structures could be exposed by careful microsurgical dissection:

- Ipsilateral olfactory nerve
- Ipsi- and contralateral optic nerves
- Optic chiasm
- Ipsi- and contralateral supraclinoid segments of the internal carotid arteries

- Ipsi- and contralateral superior hypophyseal arteries
- Perforant branches of the contralateral supraclinoid segment of the internal carotid arteries
- Ipsi- and contralateral ophthalmic arteries

3.1.3.1 Approaching the internal carotid artery through a transsylvian route

For this approach, the first step consisted in identifying the anterior sylvian point, recognizable as a broadening of the subarachnoidal space inferiorly to the apex of the pars triangularis of the inferior frontal gyrus, where the emergence of the MCA on the surface of the brain and the entrance of the medial cerebral vein into the sylvian fissure is observed.

After opening the arachnoidal layer, the MCA was dissected proximally towards the internal carotid artery bifurcation (*Figure 3C,D and 5B*). Throughout this approach the lenticulostriatal arteries had to be carefully preserved. As soon as the ICA bifurcation was reached, a gentle elevation of the frontal lobe enabled the observation of the precommunicating segment of the ACA (A1 segment) following an anteromedial and superior trajectory crossing above the optic chiasm and optic nerve. A slightly retraction of the temporal lobe enabled to follow in the depth the C4 segment of the ICA proximally, giving rise to the AChA, PcomA, OA, SHA and several perforant arteries. In relationship to the C4, the cavernous sinus, optic nerve, optic chiasm, anterior clinoid process and hypophyseal steal were also visualized.

3.1.3.2 Subfrontal/supraorbital approach to the internal carotid artery

The oICA was additionally approached following a more anteriorly corridor above the orbital roof. For this route, gentle retraction of the orbital gyri of the frontal lobe of up to a maximum of 15 mm was required (*Figure 2, 3A,B, 4, 5A*). The olfactory nerve was identified attached to the olfactory sulcus of the frontal lobe separating the straight gyrus from the medial orbital gyrus. It was then mobilized superiorly to proceed with the dissection posteromedially. This allowed exposure of both optic nerves, the optic chiasm, the C4 segment of both ICAs with the above-mentioned branches and the hypophyseal steal. This corridor enabled the visualization of the ipsilateral anterior clinoid process, the falciform ligament covering the entrance of the

optic nerve and the OA into the optic channel, the planum sphenoidale and the tuberculum sellae.

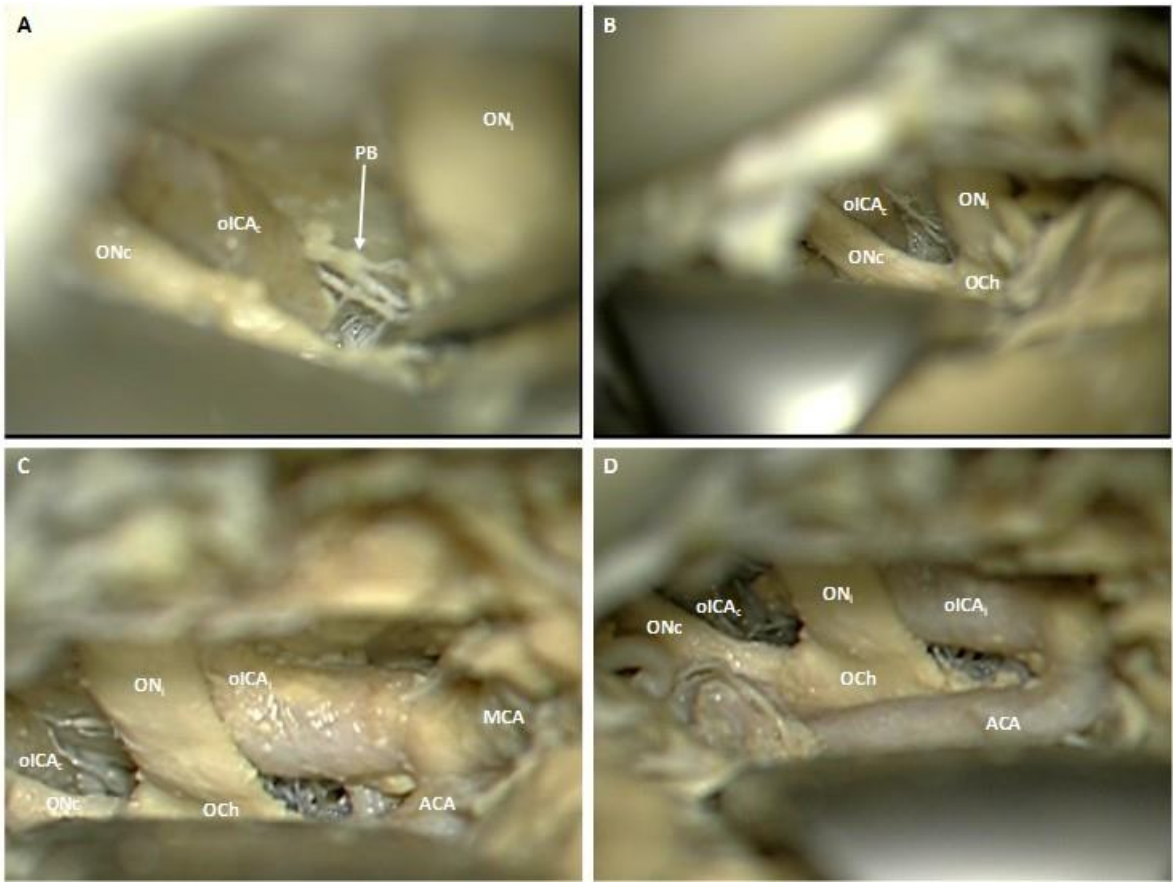

Fig. 3. Amplified view of the interoptic space providing access to the medial wall of the contralateral oICA and perforating arteries destined mostly to the optic apparatus (*A, B*). A transsylvian approach trajectory allowed the exposure of the lateral aspect of the ipsilateral internal carotid artery and its bifurcation into the middle and anterior cerebral arteries (*C, D*). *ON_i* , ipsilateral optic nerve; *ON_c* , contralateral optic nerve; *Och,* optic chiasm; *$oICA_i$* , ophthalmic segment of the ipsilateral internal carotid artery; *$oICA_c$,* ophthalmic segment of the contralateral internal carotid artery; *PB,* perforant branches of the oICA; *ACA,* anterior cerebral artery.

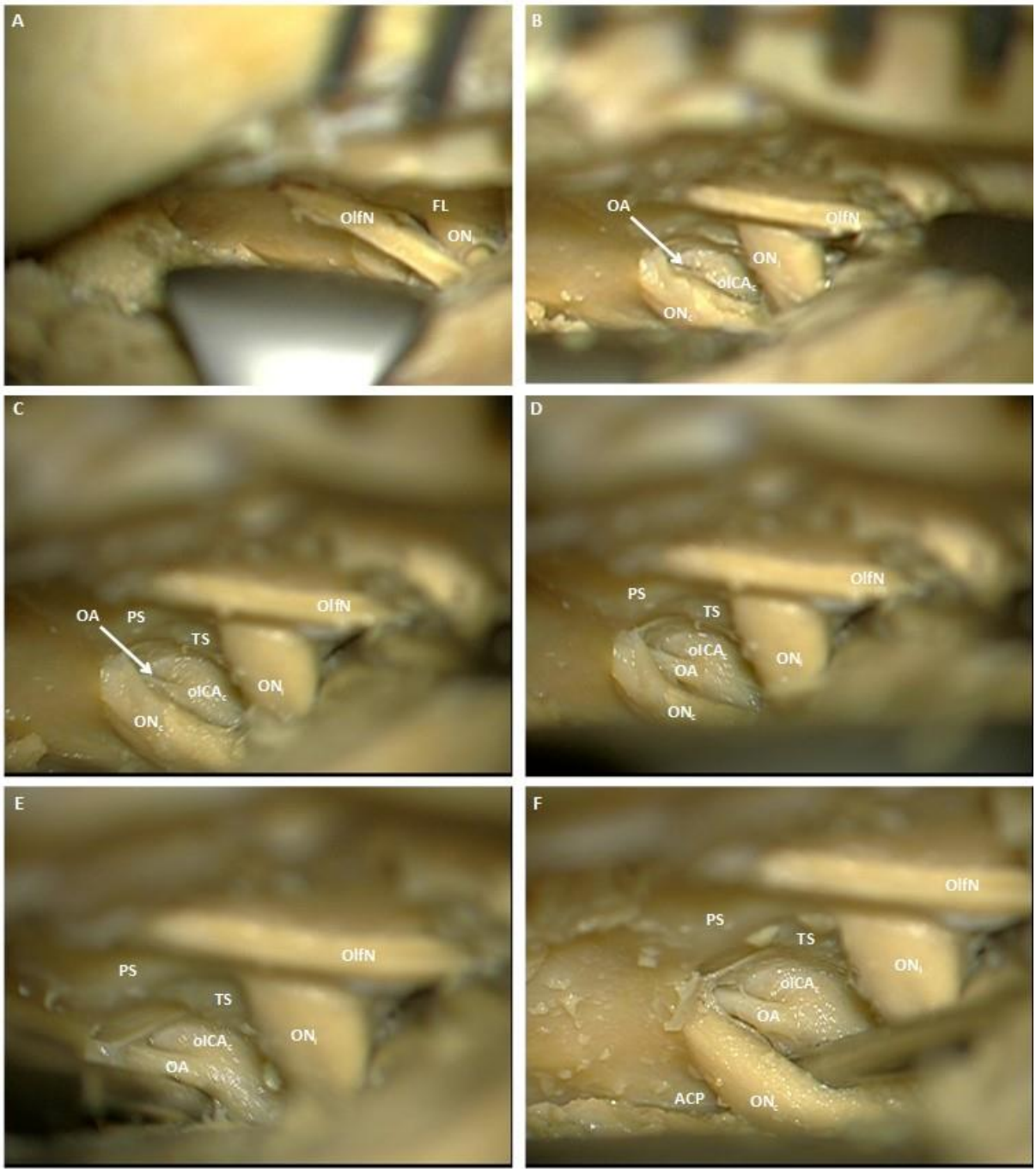

Fig. 4. Images acquired from another specimen. Again, a dissection directed through a subfrontal/supraorbital trajectory exposing the olfactory nerve and the optic apparatus (*A, B*). The medial aspect of the contralateral internal carotid and the origin of the ophthalmic artery could be effectively exposed through the interoptic triangle without the need of optic nerve mobilization (*B, C, D*). The mobilization of the contralateral optic nerve did not result in a significant enhancement of ophthalmic artery 's exposure (*E,F*). *OlfN,* olfactory nerve; *FL,* falciform dural fold (ligament); *ON$_i$,* ipsilateral optic nerve; *ON$_c$,* contralateral optic nerve; *OA,* contralateral ophthalmic artery; *oICA$_i$* , ophthalmic segment of the ipsilateral internal carotid artery; *oICA$_c$,* ophthalmic segment of the contralateral internal carotid artery; *PS,* planum sphenoidale; *TS,* tuberculum sellae; *ACP,* contralateral anterior clinoid process.

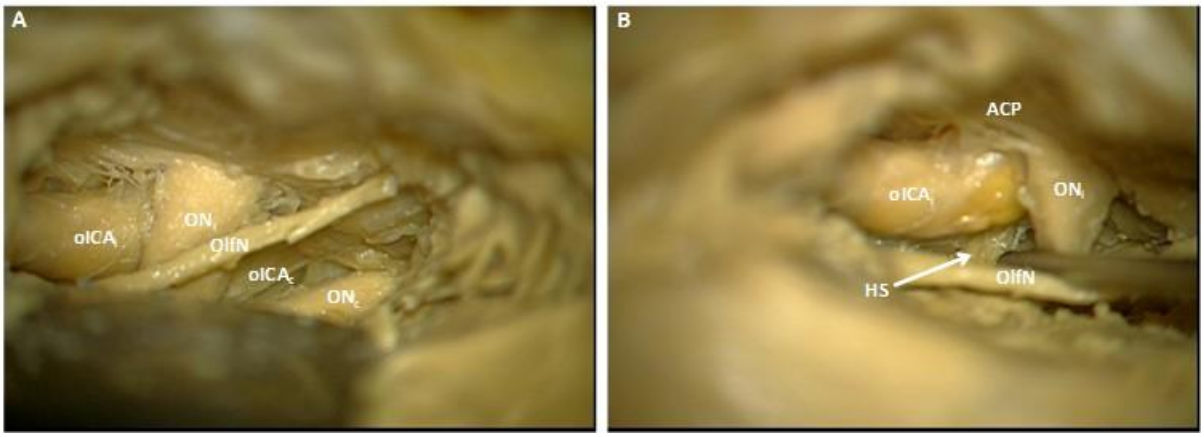

Fig. 5. Left side approach exposing the ipsilateral carotid artery along its lateral aspect and the medial aspect of the contralateral carotid (*A*). Prior to anterior clinoidectomy, to gain access to the medial wall of the ipsilateral internal carotid artery, an unacceptable optic nerve mobilization was required (*B*). *OlfN,* olfactory nerve; ON_i , ipsilateral optic nerve; ON_c , contralateral optic nerve; $oICA_i$, ophthalmic segment of the ipsilateral internal carotid artery; $oICA_c$, ophthalmic segment of the contralateral internal carotid artery; *HS,* hypophyseal steal; *ACP,* ipsilateral anterior clinoid process.

3.1.4 Anatomical and morphometrical characterization of neurovascular structures

Once the C4 segment of the ICA and the parasellar region were exposed, the interoptic space was carefully dissected and the falciform dural fold was opened above both optic nerves. Then, following anatomical and morphometrical parameters were measured and recorded:

- Distance from the MacCarty's keyhole to the supraorbital foramen, i.e.supraorbital nerve
- Percentage of cases in which the frontal sinus was opened
- Optimal approach angle to the oICA: An imaginary line crossing the MacCarty's keyhole point and the apex of the ipsilateral anterior clinoid process was established as 0° reference. From this line, we determined separately the angle at which the ipsilateral and contralateral oICA were maximally visualized and exposed. Positive angles were considered anteriorly to the reference line and negative angles posteriorly to it (*Figure 6*)
- Distance to the ipsilateral olfactory nerve

- Ipsilateral olfactory nerve's mobilization needed to approach the oICA
- Distance to the ipsi- and contralateral optic nerve
- Distance to the medial wall of the ipsi- and contralateral oICA
- Optic nerve's length between the anterior border of the optic chiasm and the entrance into the optic channel
- Optic nerve's mobilization needed to maximally expose the ipsi- and contralateral oICA
- oICA mobilization needed to maximally expose the OA, SHA and perforant branches arising from the oICA segment
- oICA length
- Visualization of the ipsi- and contralateral OA origin
- Maximal ipsi- and contralateral OA length exposed
- Visualization of the ipsi- and contralateral SHA origin
- Maximal ipsi- and contralateral SHA length exposed
- Number of perforant branches of the ipsi- and contralateral oICA visualized
- Relative interoptic triangle's area (*Figure 7*): The interoptic triangle is defined as the subarachnoidal space between both optic nerves in their intracranial course. The apex of this triangle is constituted by the confluence of both optic nerves into the chiasm and the base is formed by the line binding both optic foramina, corresponding to the chiasmatic groove limited posteriorly by the tuberculum sellae. This space constitutes the key anatomical landmark enabling to approach the oICA contralaterally. We now denominated as relative interoptic triangle's area, the 2-dimensional projection of this triangle to the surgeon's view. In this case, the area measured depends on the angulation of the operative microscope in relation to the anatomic triangle. If the microscope is orientated tangential to the interoptic space, the projected 2-dimensional area of this space in surgeon's view decreases independently of its absolute extension. On the way round, a more orthogonal microscope's orientation increases the area of the interoptic triangle 2-dimensional projection to surgeon's view. We measured the relative interoptic triangle's area after having aligned the microscope with the optimal approach angle to the contralateral oICA.

The identification, exposure and morphometric characterization of the above-listed parameters was repeated after each of the following steps (*Figure 8*):

1. Prior to removal of any bony structure.
2. After ipsilateral intradural anterior clinoidectomy and opening of the falciform ligament.
3. After removing the contralateral half of the planum sphenoidale and tuberculum sellae.

Additionally, the exposure of the contralateral vascular elements was quantified prior and after mobilization of the contralateral optic nerve.

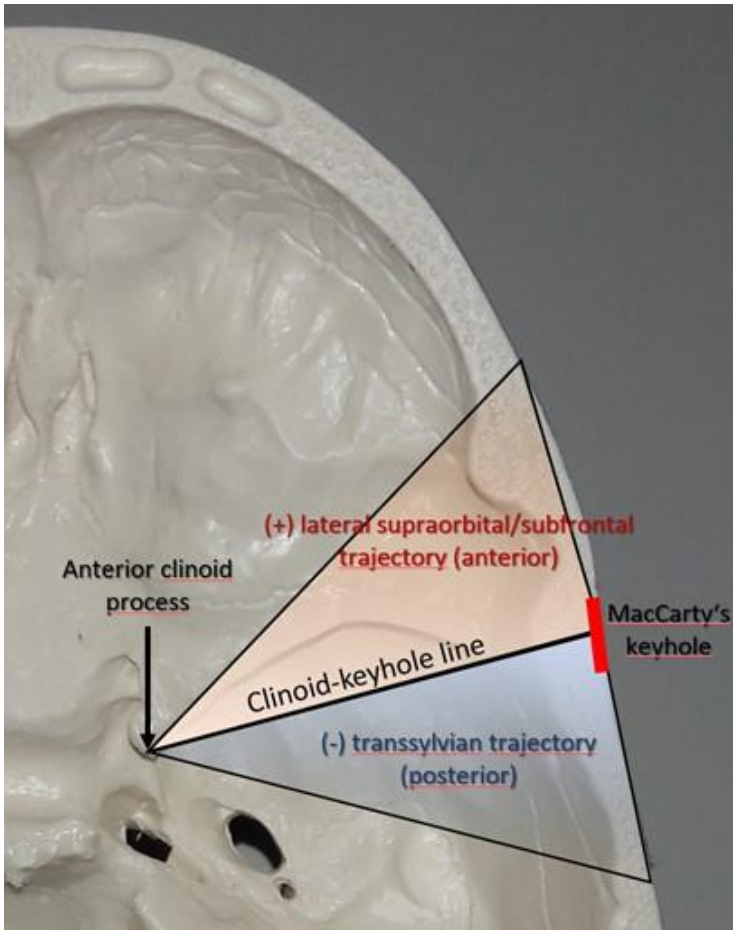

Fig. 6. Calculation of the optimal approach angle to the oICA. The clinoid-keyhole line was established as 0° reference. The optimal trajectory to the ipsilateral a contralateral oICA was determined in relationship to this line. Approach angles directed anteriorly to the reference line were considered positive, while those directed posteriorly to the reference were negative.

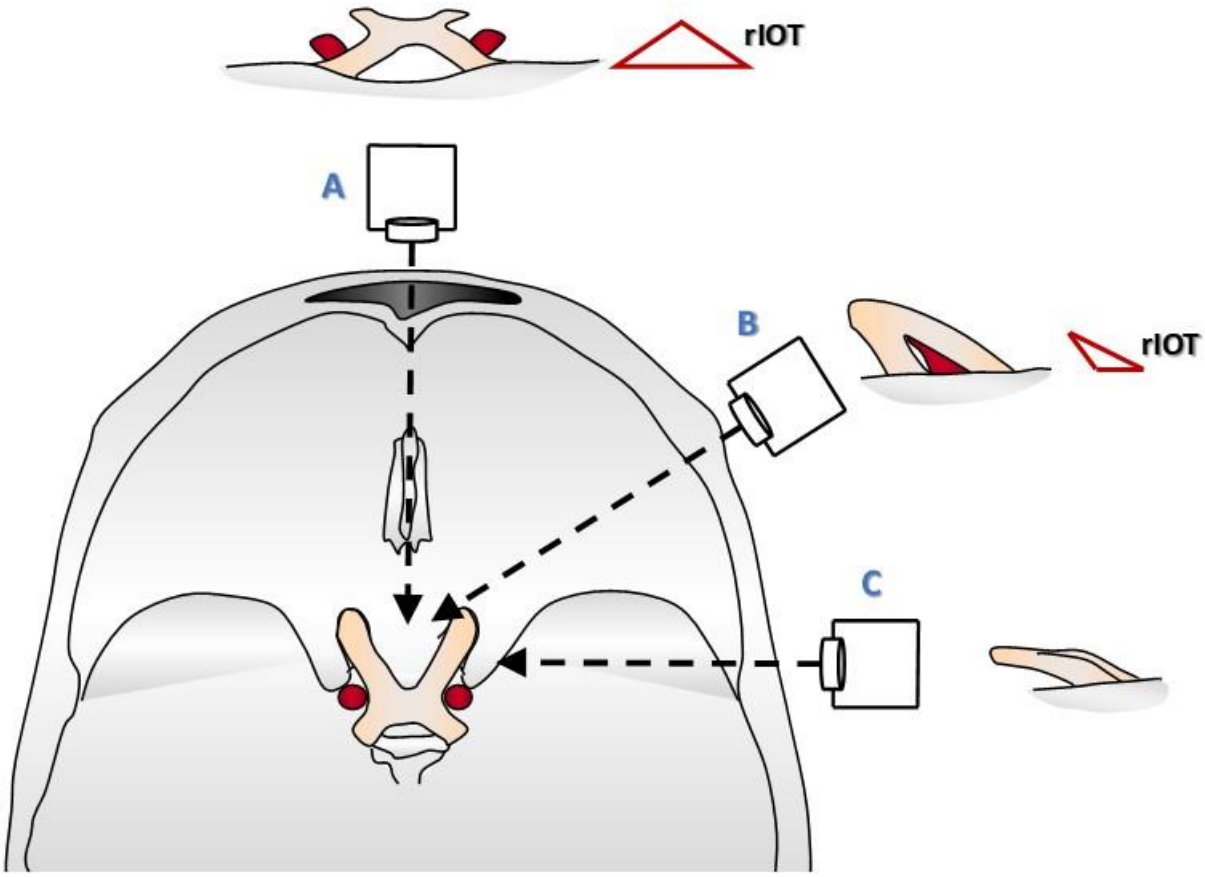

Fig. 7. Schematic illustration of the relative interoptic triangle (rIOT). The triangular space between both optic nerves in their intracranial course acquires a different 2-dimentional projection to microscopic's view according to the axial angle of approach selected. This was defined as the relative interoptic triangle (rIOT). Theoretically, if the view is orthogonal to interoptic triangle's axis, the 2-dimentional workspace, i.e. rIOT, is maximal (*A*). If the trajectory is tangential to interoptic triangle's axis, the 2-dimentional workspace between both optic nerves is minimal (*C*). To approach the medial wall of the contralateral oICA, a subfrontal trajectory is needed and the 2-dimentional projection of the interoptic triangle to surgeon's view differs according to the approach angle adopted (*B*).

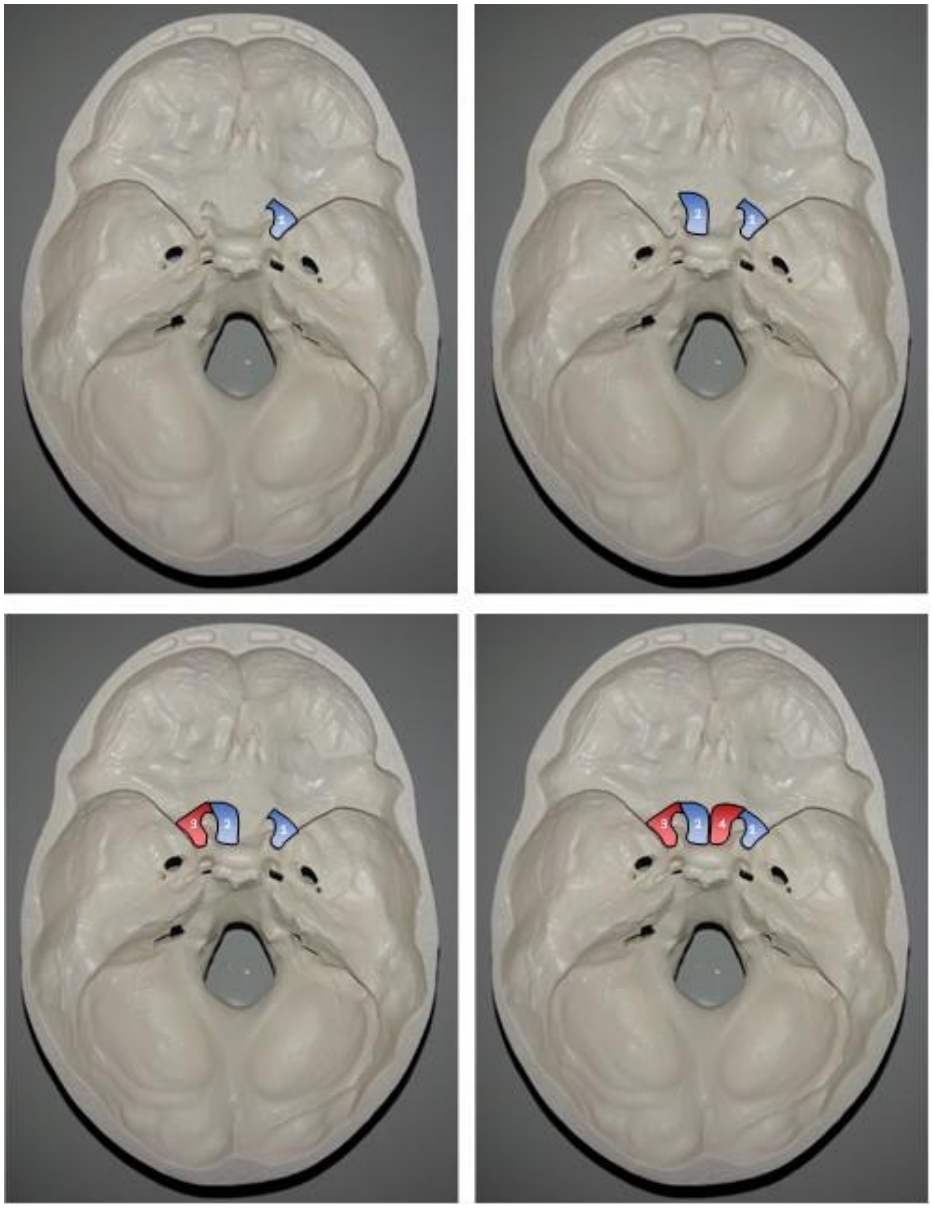

Fig. 8. Steps of bony resections performed in cadaveric and virtual dissections. First a right- sided pterional craniotomy was performed to approach the ipsi- and contralateral oICA, their branches and the optic apparatus. In a first instance, morphometric measurements of the ipsilateral and contralateral neurovascular elements were accomplished in native conditions avoiding bone removal or optic nerve mobilization. After this, the morphometric characterization was repeated, following mobilization of the contralateral optic nerve. The next measurement was performed following ipsilateral intradural anterior clinoidectomy. This was again repeated prior and after mobilization of the contralateral optic nerve (*1*). The last measurement was performed after removal of the contralateral half of the planum sphenoidale and tuberculum sellae with and without contralateral optic nerve mobilization (*2*). Identical steps were now repeated through a left-sided craniotomy (*3→4*).

3.2 3D virtual surgical approach simulation in alive subjects

3.2.1 Patient selection

We randomly selected preoperative cranial image-data-sets from 10 patients and performed bilateral virtual 3D dissections and surgical simulations with the dextroscope® (20 individual approaches).

3.2.2 Data Acquisition

All CT and MRI scans were performed at the Institute of Neuroradiology at the University of Mainz Medical Center. Magnetic resonance imaging was performed using 3 Tesla systems, either on a Magnetom Vision (Siemens, Munich) machine with gradients of 25 mT/m and standard head coil or on a Magnetom Sonata (Siemens, Munich) machine with gradients of 40 mT/ m. On the Magnetom Sonata, we applied a parallel imaging technique by means of an 8-channel head coil and generalized autocalibrating partial parallel acquisition (the acceleration factor was 2). Magnetic resonance imaging was performed with a 2-mm slice thickness without gap. Magnetic resonance time of flight angiography was performed with a transverse 3D FLASH tilt-optimized nonsaturated excitation sequence of the carotid siphon and the circle of Willis (TR/TE: 4.1/1.5 ms [Vision], and 3.0/1.2 ms [Sonata]), 1 to 1.5-mm slice thickness without gap. Due to technical reasons, contrast-enhanced MR angiography with coronal 3D FLASH sequences (TR/ TE/Flip 3.14/1.35 millisecond/20°, field of view 230 mm) was performed only with the Sonata to demonstrate veins and sinuses. The standard protocol included 3D data record with 2-mm slice thickness, 2- mm index and 230 field of view. All imaging series were stored on the system server in DICOM 3 format. The data was transferred to the Dextroscope via ethernet (100 Mbit/second).

3.2.3 Dextroscope Hardware

With the Dextroscope® (Volume Interactions Pte. Ltd., Singapore), the user works with both hands inside a stereoscopic virtual workspace. This is achieved by reflecting a computer-generated 3D scenario via a mirror into the user's eyes. Wearing liquid display shutter glasses synchronized with the time split display, the user reaches with both hands behind the mirror into the "floating" 3D data.

Electromagnetic sensors in both hands convey the interaction and allow manipulation of the 3D data in real time. One hand holds an ergonomically shaped handle to move the 3D data freely as if it were an object. The other hand holds a pen-shaped instrument, which appears inside the virtual reality workspace as a computer-generated instrument that can be used to perform detailed data manipulations.

3.2.4 Dextroscope Software

The virtual workspace inside the Dextroscope® provides all the tools necessary for surgical planning. By lowering the hand-held pen onto the physical bottom of the workspace inside the Dextroscope, a virtual tool automatically appears consisting of virtual buttons and sliders, which can be activated with the virtual instrument. The software tools for colour and transparency coding, manual and semiautomatic segmentation, image fusion, curved, linear and volumetric measurements, virtual tissue removal (virtual drilling and suctioning) and reconstruction, as well as snapshot and video reporting tools, are available.

3.2.5 Image Processing

The images transferred into the Dextroscope are displayed by 3D volume rendering. In case of multimodality visualization, the CT and MR imaging data are automatically co-registered and displayed as one. The segmentation of structures that were demarcated by their outstanding intensity on the grey scale, such as vessels, optic apparatus, brain, bone or skin surface, is achieved by semiautomatic adjustments of the colour lookup tables or interactive region-growing algorithms. Other structures are generated with the help of manual outlining tools. The resulting multimodal and multisegmented 3D data set is typically a mix of volume-rendered and polygonal surface structures, displayed in stereo and shaded to various degrees.

3.2.6 Virtual surgery/dissection simulations

The procedure of anatomical dissection was accomplished in an identical stepwise manner as for cadaveric specimens. Using the hand-held pen eraser tool into the virtual matrix, we firstly removed the skin and temporal muscle covering the pterion and performed a virtual craniotomy following exactly the same anatomical landmarks as for cadaveric specimens (*see above*). The standard pterional craniotomy was

completed with the removal of the sphenoidal ridge up to the lateral border of the superior orbital fissure and smoothing of the roughness along the orbital part of the frontal bone. The duramater was now removed and the brain was exposed (*Figure 9*).

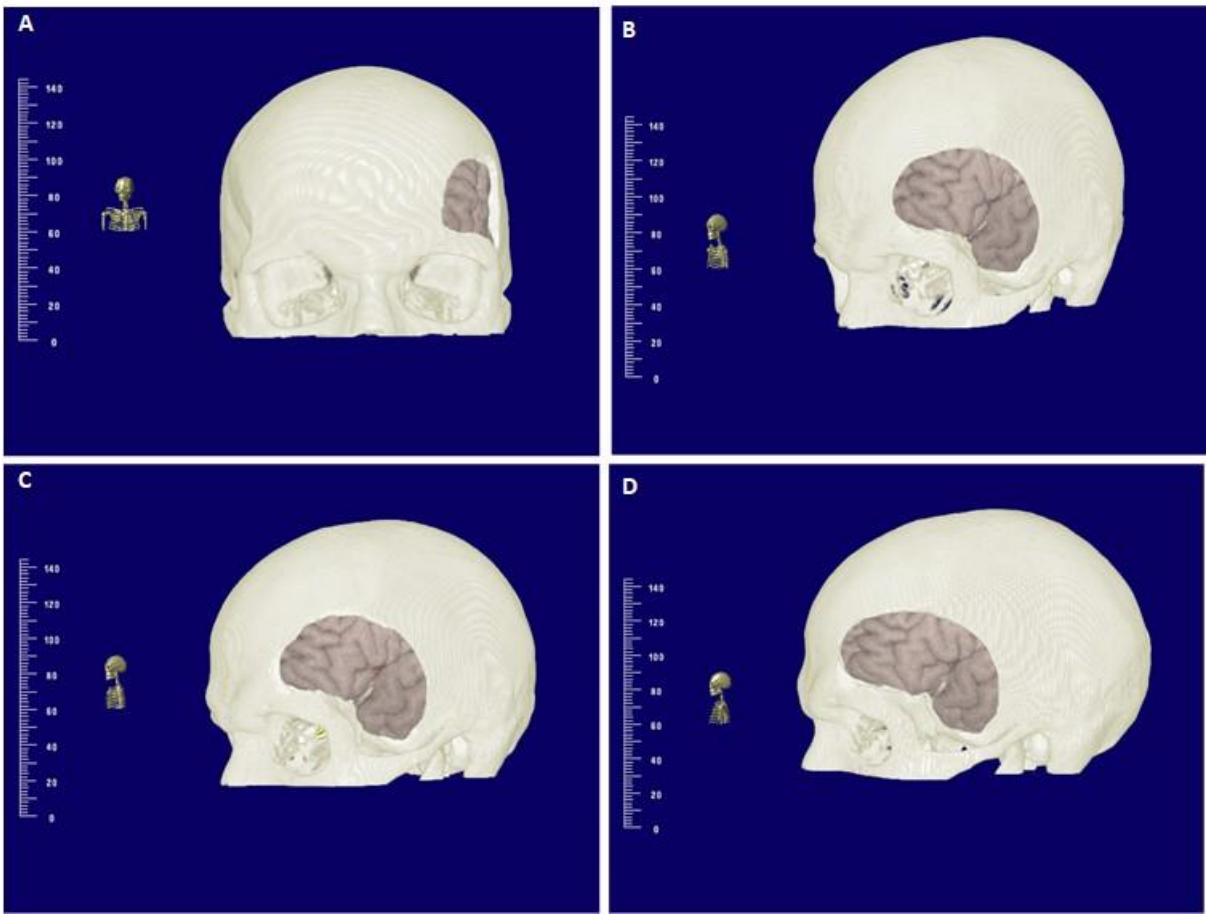

Fig. 9. Exposure of the brain after performing a left-sided pterional cranoitomy in a 3-D virtual specimen. The direction of the approach angle differed when intended to expose de contralateral or ipsilateral oICA. Whilst a supraorbital trajectory was optimal for approaching the contralateral oICA (*B*), the ipsilateral oICA was better exposed by opening the Sylvian fissure and therefore opting for a more posterior angle with respect to de clinoid-keyhole line (D).

Since brain retraction cannot be simulated in the Dextroscope, this was compensated by virtual resection of a 15-mm layer of brain parenchyma of the orbitofrontal cortex which was displaced in conventional operations by gentle retraction (*Figure 10 and 11*).

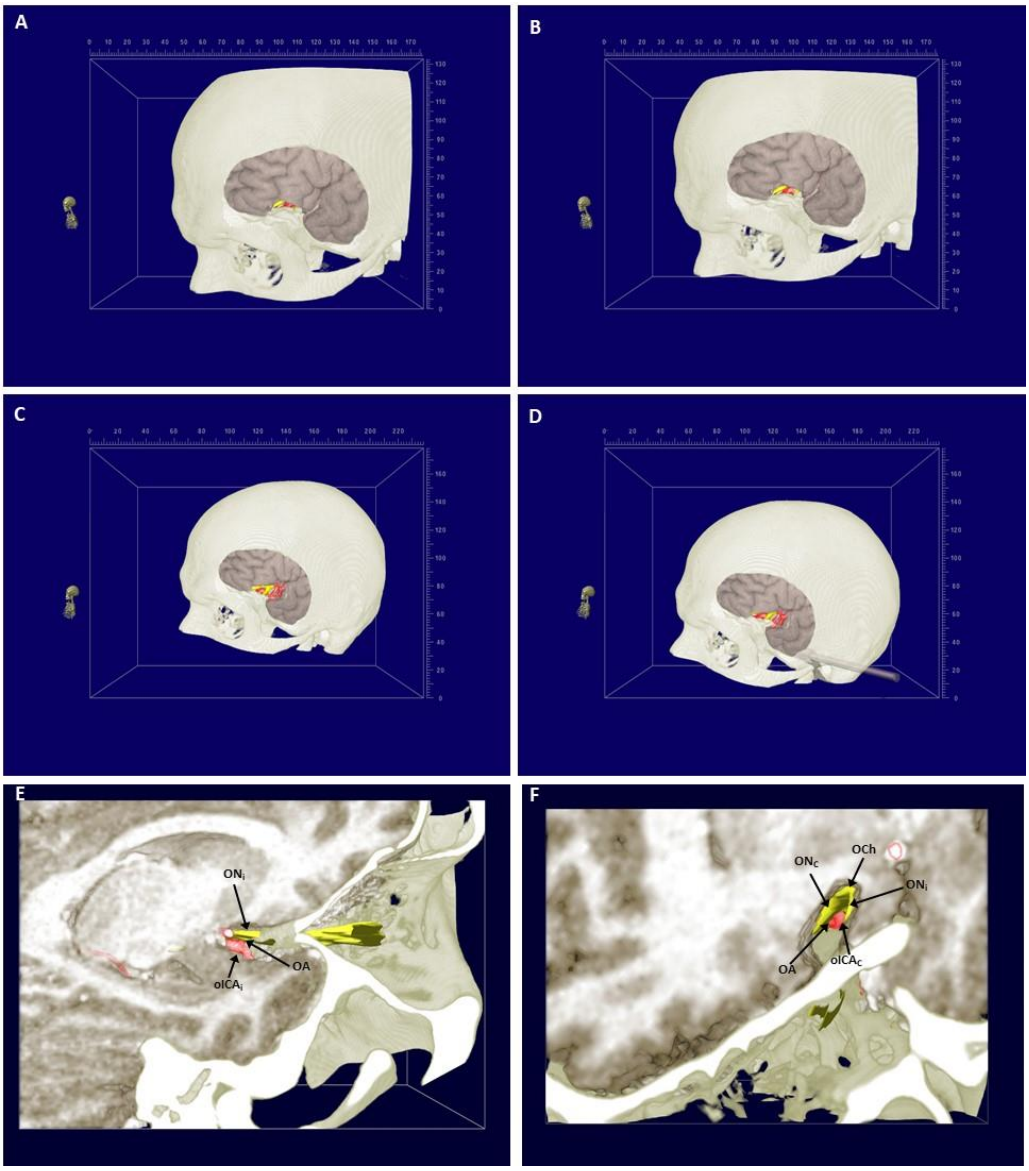

Fig. 10. Approach to the ipsi- and contralateral oICA through a left pterional approach. Now, the orbital gyri of the frontal lobe were partially removed in order to simulate gentle brain retraction. A supraorbital trajectory was adopted to approach the contralateral oICA through the interoptic space (*A, B, C*). A further sylvian fissure opening was accomplished to better approach the ipsilateral oICA (*C, D*). Ipsilateral approaches provided a wide exposure of the oICA's lateral aspect and the OA was best visualized under the ON when its origin was localized on the superomedial aspect of the oICA (E). Contralateral approaches allowed a direct visualization of the oICA's medial surface as well as the OA without ON manipulation, even in cases of more inferior OA's origin on oICA's medial aspect (F).

For a transsylvian approach we erased a brain layer of 5 mm superior and inferior to the Sylvian fissure. In each case, we erased selectively brain parenchyma leaving the segmented vessels and optic apparatus intact. Using the Dextroscope, we

exposed both ipsi- and contralateral supraclinoid segments of the internal carotid arteries, ipsi- and contralateral optic nerves, the optic chiasm and ipsi- and contralateral ophthalmic arteries.

Due to the limited resolution of the underlying MR-images, very fine structures such as the olfactory nerves (attached to the brain), the superior hypophyseal arteries and the tiny perforant branches of the oICA could not be segmented.

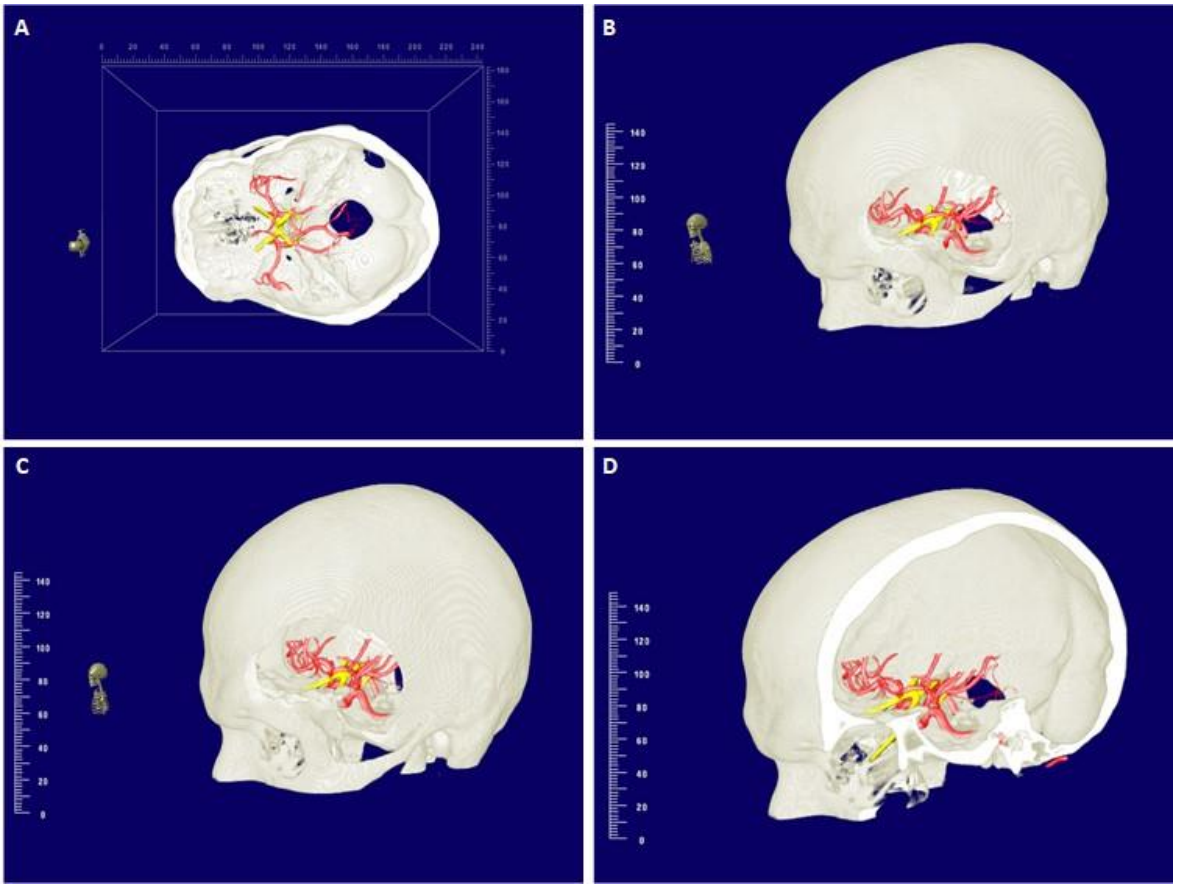

Fig. 11. 3-D virtual dissections to the ipsi- and contralateral oICA through a left pterional approach. In these images the brain parenchyma has been rendered transparent.

Identical to the proceedings on cadaveric specimens, we performed an anatomical and morphometric characterization of previously listed neurovascular structures through the ipsi- and contralateral routes as described above for conventional procedures. The identification, exposure and morphometric characterization of these parameters was repeated in the same modus as applied in conventional procedures.

Since optic mobilization was not replicable with the dextroscope, the contralateral vascular elements were characterized with no modifications of optic nerve's natural anatomic position.

3.3 Statistical analysis

3.3.1 Test of goodness of fit

For each variable, we performed first a Shapiro Wilk goodness of fit test to determine its parametric or non-parametric distribution. The test of Shapiro Wilk is well known as one of the most powerful tests for contrast of normality, especially for a sample size lower than 50, as in our study.

$$W = \frac{\left(\sum_{i=1}^{n} a_i x_{(i)}\right)^2}{\sum_{i=1}^{n} (x_i - \overline{x})^2}$$

In this test, the null-hypothesis is that the sample follows a normal distribution. Therefore, *p* values greater than the one defined as alpha level indicates that the sample is distributed normally, while *p* values lower than the alpha level allow to reject the null-hypothesis and it may be assumed a non-parametric distribution of the sample (Shapiro & Wilk 1965).

3.3.2 Descriptive statistics

For variables following a normal distribution we expressed the central tendency measure as the arithmetic mean and its dispersion as standard deviation.

The arithmetic mean is formally defined as the sum of the numerical values of each observation divided by the total number of observations.

$$\bar{x} = \frac{1}{n}\sum_{i=1}^{n} x_i = \frac{x_1 + x_2 + \cdots + x_n}{n}$$

The standard deviation is equal to the square root of the variable's variance, being this the expectation of the squared deviation of the variable from its mean.

$$\sigma = \sqrt{\frac{1}{N}\left[(x_1 - \mu)^2 + (x_2 - \mu)^2 + \cdots + (x_N - \mu)^2\right]}$$

where

$$\mu = \frac{1}{N}(x_1 + \cdots + x_N)$$

For variables following non-parametric distributions, the central tendency measure was expressed as the median of the sample and its dispersion as interquartile ranges.

The median is the value separating the higher half of a data sample from the lower half and is obtained by arranging all the numbers from smallest to greatest. If there is an odd number of numbers, the middle one is picked. If there is an even number of observations, then there is no single middle value and the median is then defined to be the mean of the two middle values.

After setting the median, the quartiles of a ranked set of data values are the three points that divide the data set into four equal groups, each group comprising a quarter of the data. The first quartile (Q1) is defined as the middle number between the smallest number and the median of the data set. The second quartile (Q2) is the median and the third quartile (Q3) is the middle value between the median and the highest value of the data set. The interquartile range (IQR), also known as H-spread, is a measure of statistical dispersion based on dividing a data set into quartiles, being equal to the difference between upper and lower quartiles.

3.3.3 Statistical tests of significance

For comparing the means of two variables following a normal distribution we used either Student-t test or one-way ANOVA. For comparison the means of two or more than two normal distributed variables we used ANOVA. The effect size for significant *p* values was expressed as partial eta square (η_p^2) values.

The *t* statistic to test whether the means are statistically different can be calculated as follows:

$$t = \frac{\bar{X}_1 - \bar{X}_2}{s_p\sqrt{2/n}}$$

where

$$s_p = \sqrt{\frac{s_{X_1}^2 + s_{X_2}^2}{2}}$$

On the other hand, the analysis of variance (ANOVA) represents a collection of statistical tests to compare means of several groups for statistical significance generalizing the *t*-test to more than two groups. ANOVA is conceptually similar to multiple two-sample t-tests, but is more conservative, resulting in less type I errors.

For variables following non-parametric distributions, we used the Mann-Whitney-Wilcoxon-U test to assess significance between two samples. The Mann-Whitney-Wilcoxon-U test represents the non-parametric version of the Student-t test and is nearly as efficient as the *t*-test on normal distributions. For more than two samples following non-parametric distributions we used the Kruskal–Wallis test. This method extends the Mann-Whitney-Wilcoxon-U test when there are more than two groups and corresponds to the non-parametric equivalent of one-way ANOVA.

For frequency distributions we elaborated contingency tables, i.e. crosstabs, and the significance of the difference between the proportions was assessed with Pearson's chi-squared (χ^2) test.

For analysis of correlation we performed scatter plots and calculated Pearson's *r* correlation coefficient, as a measure of the linear correlation between two variables. The values can variate between +1 and −1, where 1 is total positive linear correlation, 0 is no linear correlation, and −1 is total negative linear correlation.

3.3.4 Post-hoc analysis

To set our alpha levels, post-hoc Bonferroni corrections were performed. The Bonferroni correction is a mathematical method to counteract the problem of multiple comparisons. Since the probability of a rare event increases when multiple hypotheses are tested, the likelihood of incorrectly rejecting a null hypothesis also increases. The Bonferroni correction compensates this increase by testing each individual hypothesis with a significance level of α/m, being α the desired overall alpha level and m the number of hypothesis tested.

$$1 - \frac{\alpha}{m}$$

3.3.5 Statistics software

For statistical work we used the software package SPSS Statistics v23 (IBM, Armonk/NY/USA). The rights and licences for the use of this software were enabled by the Johannes Gutenberg University of Mainz, Germany.

4. Results

4.1 Effectiveness assessment of ipsi- and contralateral approaches to the oICA and related neurovascular structures in cadaveric specimens

4.1.1 Anthropometric measurements of cadaveric specimens

In order to rule out bias given by asymmetry between both right and left skull halves as well as other significant anthropomorphic differences between subjects, several measurements were performed in each cadaveric specimen. A survey of the measured values is depicted in Table 2.

Anthropometric measure	Mean ± SD		
Cephalic perimeter	53.63 ± 1.22		
Biauricular breadth	24.13 ± 1.36		
External biorbital breadth	11.25 ± 1.09		
	Rigth	Left	T-Tests
Vertex-zygomatic length	15.75 ± 0.66	15.88 ± 0.6	ns
External obito-auricular length	6.88 ± 0.78	6.75 ± 0.66	ns
Internal orbito-auricular length	11.38 ± 0.78	11.25 ± 0.66	ns
External orbito-midline length	6.25 ± 0.43	6.38 ± 0.48	ns

Table 2. Anthropometric measurements ruled out the possibility of significant asymmetries between both halves of the skull in cadaver specimens (ns: non-significant).

4.1.2 Determination of the optimal approach angle to the ipsi- and contralateral oICA

As standard our pterional craniotomies were extended anteriorly up to the supraorbital foramen, which was found 34,75 ± 1,39 mm anterior to the anterior margin of the MacCarty's keyhole (ranging between 33 and 37 mm). Using this standard anterior extension of the craniotomy, the frontal sinus was opened in 25% of the cases.

We determined for each approach the optimal angle to expose the oICA and nearby structures relatively to the reference line crossing the MacCarty's keyhole and the

apex of the ipsilateral anterior clinoid process. The optimal angle to expose the oICA through an ipsilateral or contralateral approach differed significantly (*Figure 12*). The maximal exposure of the ipsilateral oICA was obtained with an angle of -15.44° ± 4.11° posterior to the keyhole, while the contralateral oICA was maximally exposed using angles of 17.56° ± 4.34° anterior to the keyhole. A main effect of approach angle for oICA exposure was evidenced in one way ANOVA analysis with a large effect size [$F(7,127)=293,235$, $p<0.001$, $\eta_p^2=0.945$]. Approach routes aiming posterior from MacCarty´s keyhole required opening of the Sylvian fissure, whilst approaches aiming anterior of it required a corridor between the orbital roof and the frontal lobe. Therefore, the application of trans-Sylvian approaches maximizes the exposure of the ipsilateral oICA, while a supraorbital/subfrontal approach maximizes exposure of the contralateral oICA.

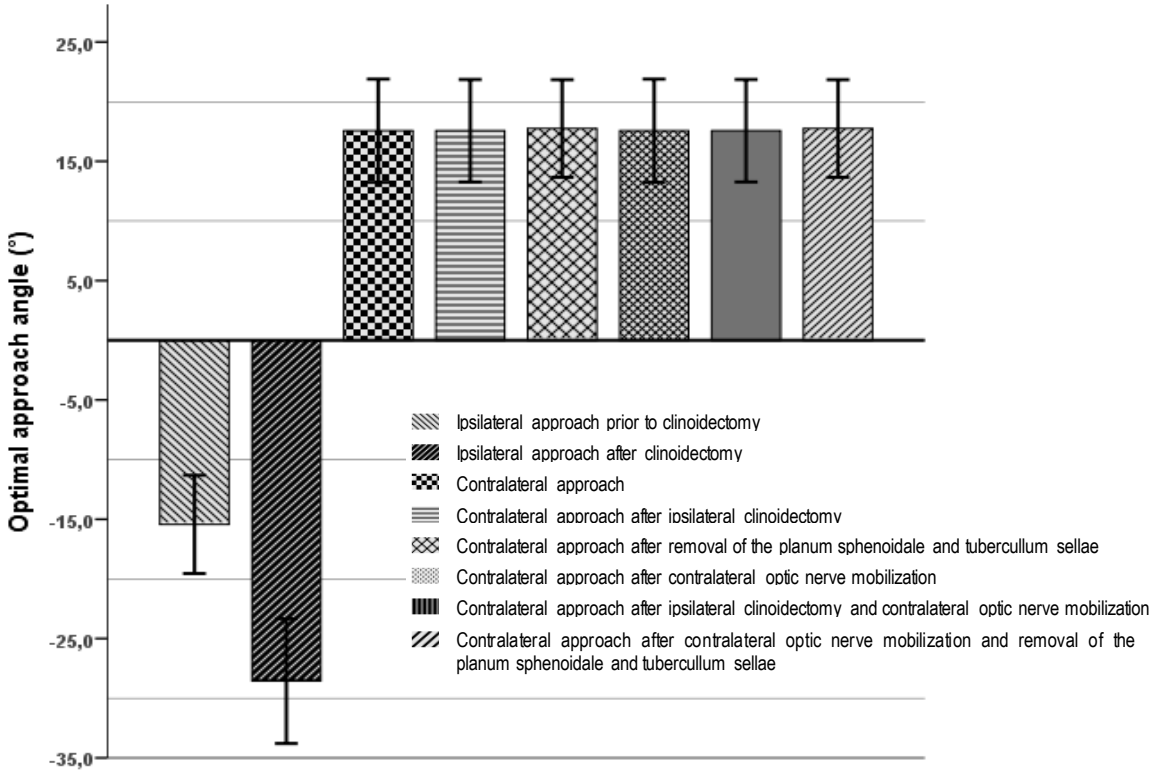

Fig. 12. The optimal approach angle in relation to the clinoid-keyhole line measured in cadaveric specimens. Exposure of the oICA from the ipsilateral side was better accomplished through slightly posterior (negative) trajectories to the reference line, whilst contralateral approaches to the oICA benefited from anterior (positive) supraorbital trajectories. All values express mean ± 2 SD.

After performance of an intradural anterior clinoidectomy, the maximal exposure of the oICA using an ipsilateral approach was obtained again with a negative angle of -28.56° ± 5.24° posterior to the MacCarty's keyhole. This projection reached statistical significance in comparison to the optimal approach angle determined prior to anterior clinoidectomy [$F(1,31)=62,089$, $p<0.001$, $\eta_p^2=0.674$]. For approaches to the oICA and neighbor structures from the contralateral side, neither bone removal nor optic nerve mobilization induced significant variations in terms of optimal approach angle to the target zone.

4.1.3 Comparative morphometric and anatomic characterization of ipsilateral and contralateral approaches to the oICA and nearby neurovascular structures

After having identified the optimal angles to approach ipsi- and contralaterally the oICA, a stepwise anatomic and morphometric characterization was separately performed to compare both approaches. In the trans-sylvian corridor, targeting the oICA from the ipsilateral side, the olfactory nerve was found at the depth of 44.38 ± 1.75 mm, while in the subfrontal/supraorbital corridor directed to the oICA contralaterally, the ipsilateral olfactory nerve was found at 43.13 ± 2.13mm. A Student-t test for independent samples revealed no significant differences in the distance to the ipsilateral olfactory nerve by using any of both surgical routes [$T(30)=1.818$, $p=0.79$] (*Figure 13*).

Given the use of a trans-Sylvian route to the ipsilateral oICA and a subfrontal/supraorbital route to the contralateral oICA, the mobilization of the ipsilateral olfactory nerve needed to approach the contralateral oICA was significantly higher than for approaches to the ipsilateral oICA [$F(7,96)=54,046$, $p<0.001$, $\eta_p^2=0.811$]. While a passive mobilization of the olfactory nerve of 5.50 ± 2.02 mm prior anterior clinoidectomy and 3.17 ± 2.17 after anterior clinoidectomy was induced by dissecting the Sylvian cistern and elevating minimally the frontal operculum, the subfrontal/supraorbital corridor to the contralateral oICA required active mobilization and elevation of the olfactory nerve of 11.08 ± 0.9 mm. Bone removal along the planum sphenoidale and tuberculum sellae did not significantly reduce the need of olfactory nerve mobilization (10.58 ± 1.38 mm, $p>0.05$).

The distance to the ipsilateral optic nerve was 46.56 ± 1.67 mm using the optimal approach angle and trans-Sylvian corridor for the ipsilateral oICA and 46.56 ± 2.19 mm using the optimal subfrontal/supraorbital approach angle to the contralateral oICA. The superomedial aspect of the ipsilateral oICA was reached at 49.25 ± 1.84 mm through the trans-Sylvian route and at 48.94 ± 1.88 mm through the subfrontal/supraorbital approach. Separate Student-t tests revealed no statistical difference between a trans-Sylvian or subfrontal/supraorbital trajectory in terms of both distance to the ipsilateral medial wall of the oICA and optic nerve. In terms of length of optic nerve exposed, as expected, performing an anterior clinoidectomy significantly increased optic nerve exposure from 11.25 ± 1 mm to 13,69 ± 1.25 mm independently of the approach used as shown by separate ANOVA analysis [$F(1,31)=37,098$, $p<0.001$, $\eta_p^2=0.553$] (*Figure 14*).

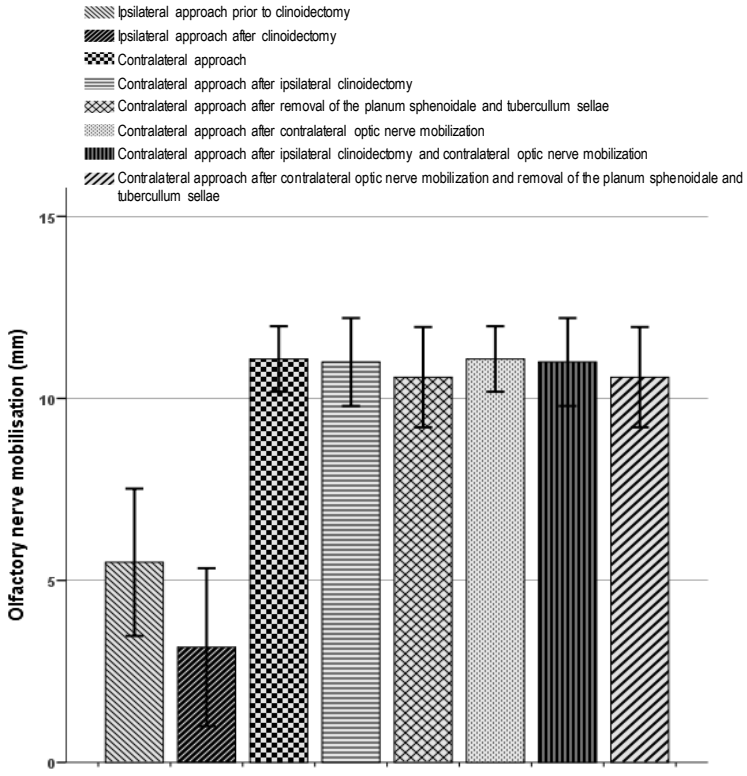

Fig. 13. Olfactory nerve mobilization needed was higher in contralateral than ipsilateral approaches to the oICA as shown by morphometric measurements in cadaveric specimens. All values express mean ± 2 SD.

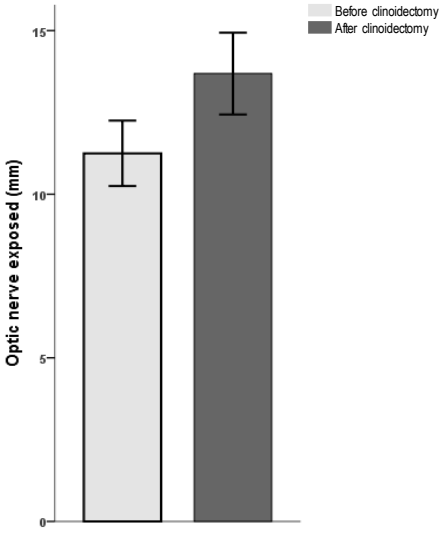

Fig. 14. Ipsilateral optic nerve exposure prior and after anterior clinoidectomy in cadaveric specimens. Removal of the anterior clinoid process increases significantly the exposure of the ipsilateral optic nerve. All values express mean ± 2 SD.

Contralateral approaches enabled a greater exposure of the oICA superomedial aspect than ipsilateral approaches, as demonstrated by separate Kruskal Wallis test [χ^2 (7)=107.58, p<0.001] (*Figure 15A*). The classical pterional approach enabled the exposure of 2.063 ± 0.57 mm (M=2 mm ± IQR 0 mm) of the superomedial aspect of the ipsilateral oICA, which could be increased after anterior clinoidectomy to 2.44 ± 0.51 (M=2 mm ± IQR 1 mm), though this tendency yielded to reach statistical significance as revealed by Mann-Whitney-Wilcoxon test comparing the exposure prior and after clinoidectomy (p=0.128). Using a contralateral subfrontal/supraorbital approach, the exposure of the superomedial aspect of the oICA was 7.25 ± 0,86 mm (M=7.5 mm ± IQR 1.8 mm). This was significantly higher than the ipsilateral exposure of the oICA before and after anterior clinoidectomy, as revealed by separate Mann-Whitney-Wilcoxon analysis for both independent comparisons (p<0.001).

As expected, ipsilateral anterior clinoidectomy did not influence the exposure of the contralateral oICA. Removal of the contralateral half of the planum sphenoidale and tuberculum sellae significantly increased the exposure of the contralateral oICA to 8.31 ± 0.79 mm (M=8,5 mm ± IQR 1 mm; p<0.005).

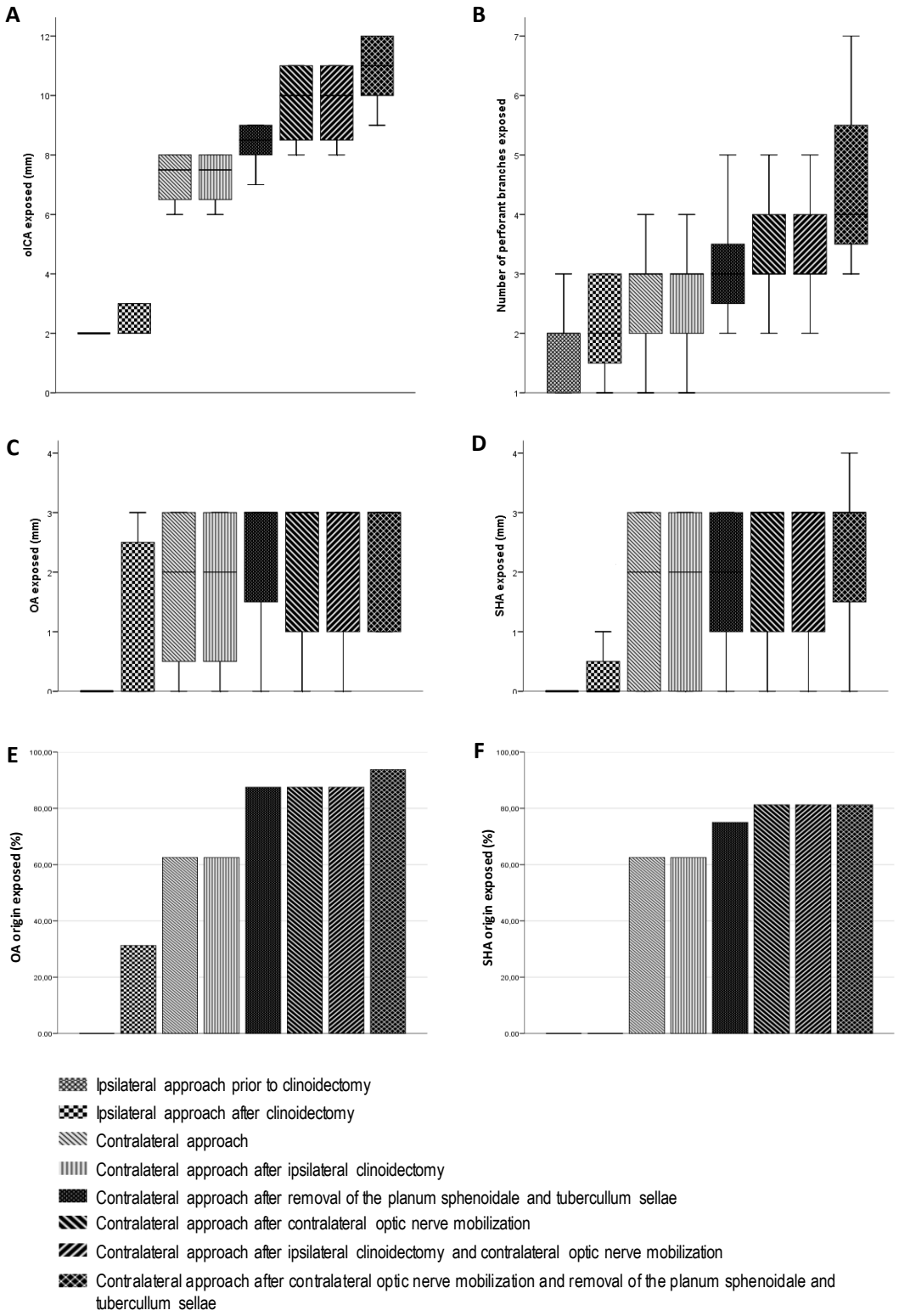

Fig. 15. Exposure of the oICA, OA, SHA and perforant arteries through ipsilateral and contralateral approaches assessed in cadaveric specimens. The use of contralateral approaches increased significantly the exposure of the oICA's superomedial aspect (*A*), the number of perforant branches visualized (*B*), the OA and SHA length (*C, D*), as well as the percentage of visualization of OA and SHA origin (*E, F*). Values from *A* to *D* express median ± IQR., whilst *E* and *F* express percentages.

A minimal mobilization of the contralateral optic nerve significantly increased the exposure of the contralateral oICA to 9,68 ± 1,19 mm (M=10 mm ± IQR 2.8 mm; p<0.001). Mobilization of the optic nerve provided an even significantly better exposure of the contralateral oICA than removal of the contralateral half of the planum sphenoidale and tuberculum sellae (p<0.005). The combination of both further increased the exposure of the contralateral oICA significantly to 10.75 mm ± 0.28 (M=11 mm ± IQR 2 mm) compared to each maneuver alone as demonstrated by separate Kuskall-Wallis analysis [χ^2 (2)=22,924, p<0.001].

Likewise, contralateral approaches enabled a larger exposure of the ophthalmic artery (OA) demonstrated by Kruskal-Wallis analysis for all approaches [χ^2 (7)=35,197, p<0.001] (*Figure 15C*). Pterional ipsilateral approaches were able to expose in average 0.31 ± 0.7 mm of the OA prior to anterior clinoidectomy with a maximal exposure of 2 mm in 2 specimens. Anterior clinoidectomy increased the average exposure of the OA to 0.88 ± 1.36 mm with a maximal exposure of 3 mm in 3 specimens. Although a tendency to greater OA exposure was observed after anterior clinoidectomy, separate Mann-Whitney-Wilcoxon analysis failed to prove statistical significance (p=0.402). Contralateral approaches without removal of the planum sphenoidale and tuberculum sellae or optic nerve mobilization enabled an OA exposure of 1.87 ± 1.25 mm (M=2 mm ± IQR 2.8 mm). This exposure reached statistical significance in a separate Mann-Whitney-Wilcoxon analysis when compared to the traditional ipsilateral pterional approach prior to clinoidectomy (p<0.001) but yielded no statistical difference when compared to OA exposure after anterior clinoidectomy (p=0.67). As expected, performing an ipsilateral anterior clinoidectomy did not influence OA exposure in contralateral approaches. Removal of the planum sphenoidale and tuberculum sellae tended to increase the OA length exposed to 2.19 ± 1.22 mm (M=3 mm ± IQR 1.8 mm), although Mann-Whitney-Wilcoxon test failed to show statistical significance in comparison to the OA exposure prior to bone removal (p=0.423). The mobilization of the contralateral optic nerve did not significantly increase OA exposure during contralateral approaches and the combination of bone removal and optic nerve mobilization did not provide a better OA exposure than bone removal alone. However, separate Mann-Whitney-Wilcoxon analysis of contralateral approaches after removal of the planum sphenoidale and tuberculum sellae and/or mobilization of the contralateral optic

nerve demonstrated a significant larger OA exposure compared to ipsilateral approaches after anterior clinoidectomy (all *p* values <0.01).

Given that aneurysms arise usually at sites of artery bifurcation or at the origin of collateral branches, we assessed the effectiveness of ipsi- and contraleral approaches to expose the OA origin (*Figure 15E*). In classical ipsilateral pterional approaches prior to anterior clinoidectomy, the origin of the OA could not be visualized in any of cadaveric dissections. Performing an ipsilateral anterior clinoidectomy increased significantly the likelihood of visualizing the origin of the OA to 31% [χ^2 (1)=5,926, p<0.01] and the contralateral approach enhanced the visualization of OA origin to 62.5% of the cases. For contralateral approaches, either mobilization of the contralateral optic nerve or removal of the planum sphenoidale and tuberculum sellae increased the visualization of the OA origin to 87.5% and both maneuvers together raised the likelihood of exposing OA origin to 93.75%. A main effect of visualization of OA origin was clearly seen favoring contralateral approaches [χ^2 (7)=53,616, p<0.001]. The contralateral approach without optic nerve mobilization or bone removal was able to significantly increase the exposure of the OA origin in comparison to the conventional ipsilateral pterional approach [χ^2 (1)=14,545, p<0.001].

A similar pattern was found when the exposure of the SHA was assessed. The advantage of contralateral approaches for a wider exposure of the SHA was demonstrated by a Kruskal Wallis analysis [χ^2 (7)=39,437, p<0.001] (*Figure 15D*). Ipsilateral pterional approaches enabled only a poor exposure of the SHA (1 mm in only 3 specimens). Anterior clinoidectomy increased the exposure of this vessel only to 1-2 mm (1 mm length in 2 specimens and 2 mm in other 2 specimens), while Mann-Withney-Wilcoxon test did not prove a significant increase of the SHA exposure using ipsilateral approaches with or without anterior clinoidectomy (p=0.96). When approached from the contralateral side, the median exposure of the SHA was increased to 2 mm ± IQR 3 mm. When approaching the contralateral oICA, removal of the planum sphenoidale and tuberculum sellae did not increase the SHA exposure (M=2 mm ± IQR 2.5 mm). Contralateral optic nerve mobilization increased the median length of exposed SHA to 3 mm ± IQR 2 mm, although statistical analysis could not show a significant difference (p=0.239). Likewise, the combination of optic nerve mobilization and planum sphenoidale/tuberculum sellae removal in

contralateral approaches did not result in a significant increase of SHA exposure (M=3 mm ± IQR 1.8 mm).

We also assessed the likelihood of visualizing the SHA origin arising from the C4 segment of the ICA. Ipsilateral approaches before and after anterior clinoidectomy were unable to expose the SHA origin in any of the examined specimens. The visualization of the SHA arising from the ICA was improved significantly by application of contralateral approaches [χ^2 (7)=55,887, p<0.001] (*Figure 15F*). The contralateral subfrontal/supraorbital corridor increased the visualization of SHA origin so that it could be surgically exposed in 62.5% of cases [χ^2 (1)=14,545, p<0.001] and removal of the planum sphenoidale and tuberculum sellae increased this value further to 75%. Contralateral optic nerve mobilization increased it further to 81.25%, a proportion that remained the same when both removal of the planum sphenoidale/tuberculum sellae and optic nerve mobilization were applied together. Nevertheless, in ipsilateral approaches neither mobilization of the contralateral optic nerve nor removal of the sphenoidal plane/tuberculum sellae contributed significantly to the exposure of SHA origin, compared to the contralateral approach without the need for these maneuvers (all p values > 0.05). For contralateral approaches, the extent of exposure of the oICA was significantly higher in those specimens in which the origin of the ophthalmic and superior hypophyseal arteries was visualized as demonstrated in separate Mann-Whitney-Wilcoxon analysis (p<0.001).

Another key point of our study was to assess how many perforant vessels arising from the oICA were exposed by application of ipsi- and contralateral approaches. A higher number of perforant branches was visualized with contralateral compared to ipsilateral approaches, as demonstrated by a main effect of approach variants in a separate Kruskal Wallis analysis [χ^2 (7)=65,189, p<0.001] (*Figure 15B*). The median number of perforant branches observed through pterional approaches was 2 ± IQR 1, which did not variate significantly after anterior clinoidectomy (p=0.095). The contralateral supraorbital/subfrontal corridor enabled exposure of a significantly higher number of perforant branches (M=3 ± IQR 1) compared to the pterional ipsilateral trans-Sylvian corridor (p<0.005). Contralateral optic nerve mobilization during contralateral approaches increased the number of exposed perforant branches significantly compared to approaches sparing this maneuver (p<0.005).

This effect was not observed after removal of the contralateral half of the planum sphenoidale and tuberculum sellae (p=0.128).

In order to expose the ophthalmic segment of the internal carotid artery and specially its superomedial aspect, ipsilateral approaches required optic nerve manipulation and mobilization. To achieve maximal exposure of the oICA, the mean optic nerve mobilization for ipsilateral approaches was 2.375±0.5 mm (M= 2 mm ± IQR 1 mm) prior to anterior clinoidectomy. After anterior clinoidectomy the mobility of the optic nerve increased. The average mobilization of the optic nerve required to achieve the best oICA's superomedial aspect exposure was 2.06 ± 0.57 mm only (M=2 mm ± IQR 0 mm). The maximal optic nerve mobilization required to maximally expose the oICA was 3 mm independently of whether an anterior clinoidectomy was performed or not. However, the need of a full mobilization of 3 mm of the optic nerve was reduced to 50% of the cases (from 6 to 3 cases) by performing an anterior clinoidectomy. In ipsilateral approaches anterior clinoidectomy also significantly reduced the need for carotid artery mobilization from 3 mm ± IQR 1 to 2 mm ± IQR 1 in order to maximize the visualization of oICA's medial wall (p<0.001).

The mean distance from the skull niveau to the contralateral optic nerve using the optimal contralateral supraorbital/subfrontal corridor was 62.75 ± 1.39 mm, while the distance to the medial aspect of the contralateral ophthalmic artery was found to be 65.18 ± 1.51 mm. For this approach, in average, a contralateral optic nerve mobilization of 2.44 ± 0,51 mm was required. The optic nerve length exposed through the contralateral approach was 12.94 ± 1.06 mm. The removal of the planum sphenoidale/tuberculum sellae significantly increased the length of the exposed part of the contralateral optic nerve to 15.43 ± 0.96 mm as demonstrated by one-way ANOVA analysis [F(1, 31)=48,583, p<0.001, η_p^2=0.618] (*Figure 16*).

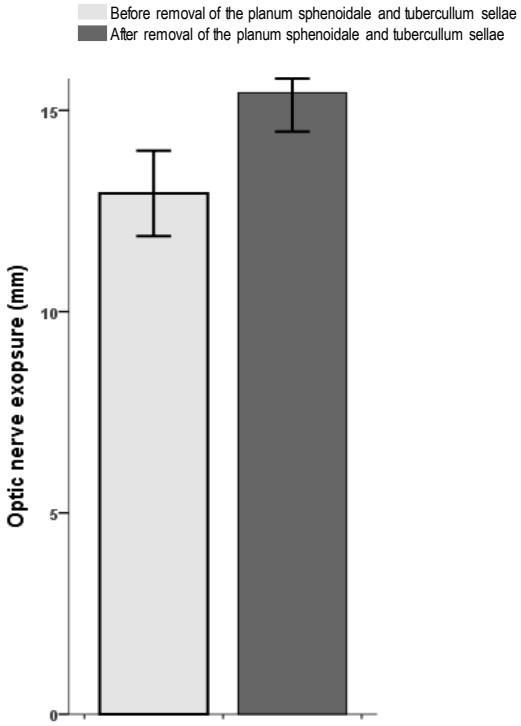

Fig. 16. Contralateral optic nerve exposure prior and after removal of the planum sphenoidale and tuberculum sellae in cadaveric specimens. Removal of the contralateral half of the planum sphenoidale and tuberculum sellae increased significantly the exposure of the contralateral optic nerve. All values express mean ± 2 SD.

4.1.4 Morphometric analysis of the relative interoptic triangle

The access to the oICA through a contralateral pterional approach using the optimal subfrontal/supraorbital route is limited by both optic nerves. Hence forward we call this space, which is defied by the bone of the skull base and both optic nerves from their emergence from the optic canal up to the chiasm, respectively its 2-dimensional projection in operative microscope (already aligned with the optimal approach angle to the contralateral oICA), the `relative intraoptic triangle´ (*see methods*).

The mean area of the relative interoptic triangle calculated for contralateral approaches directed through the optimal subfrontal/supraorbital angle was 81.19 ± 9.52 mm^2. As expected, an ipsilateral anterior clinoidectomy did not enlarge the relative interoptic triangle. Bone removal of the planum sphenoidale and tuberculum sellae increased the area of the relative interoptic triangle significantly to 98.12 ± 11.15 mm^2 [$F(1, 31)=21,355$, $p<0.001$, $\eta_p^2=0.416$]. Even greater was the effect of

optic nerve mobilization, increasing the area of the interoptic triangle to 107.5 ± 10.69 mm^2 [F(1, 31)=54,047, p<0.001, η_p^2=0.643]. A separate analysis of interoptic triangle's area after planum sphenoidale removal and optic nerve mobilization revealed an even significantly greater area provided compared to all manipulations alone [F(2, 47)=22,102, p<0.001, η_p^2=0.496]. As expected, combination of both optic nerve mobilization and planum sphenoidale removal resulted in the largest interoptic triangle's area of 124.44 ± 12.15 mm^2 compared to all other combinations [F (1, 31)=5,896, p<0.01, η_p^2=0.164] (*Figure 17*).

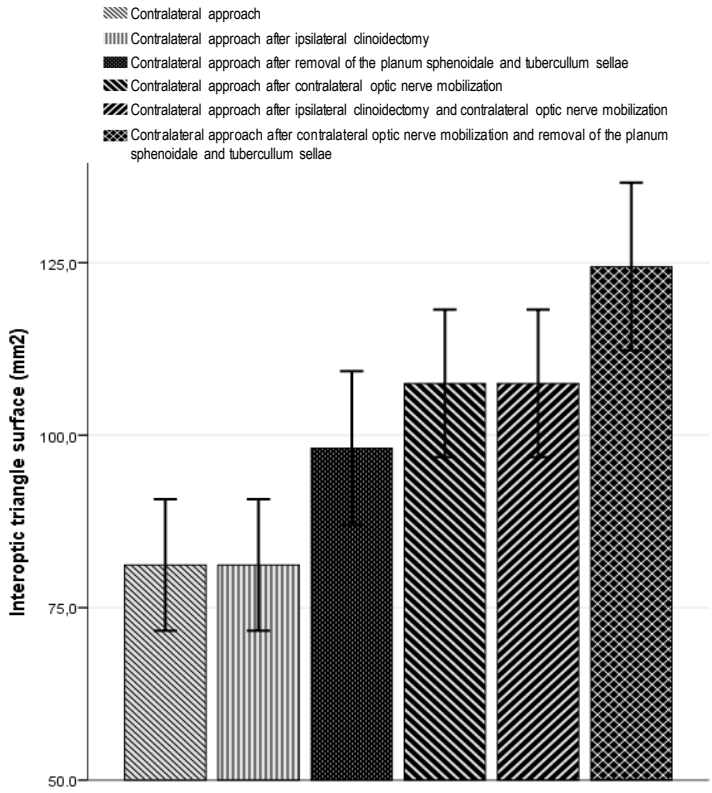

Fig. 17. Extension of the relative interoptic triangle area for contralateral approaches in cadaveric specimens. All values express mean ± 2 SD.

A larger relative interoptic triangle's area correlated positively with the exposure of the contralateral oICA (r=0.967, p<0.001) (*Figure 18*), OA (r=0.92, p<0.001) (*Figure 19*), SHA (r=0.917, p<0.001) (*Figure 20*) as well as the number of exposed perforant vessels arising from the oICA (r=0.862, p<0.001) (*Figure 21*). The exposed length of oICA increased from 6.2 ± 0.44 mm for specimens with relative interoptic triangle areas lower than 75 mm^2, to 7 ± 0.1 mm for interoptic triangle areas between 75 and

85 mm^2 and 8 ± 0.1 mm for interoptic triangle areas larger than 85mm^2. The same pattern was observed for the exposed OA length (<75 mm^2: 0.4 ± 0.89 mm; 75 – 85 mm^2: 1.66 ± 0.57 mm; >85 mm^2: 2.87 ± 0.35 mm) and SHA length (<75 mm^2: 0 mm; 75 – 85 mm^2: 1.33 ± 1.15 mm; >85 mm^2: 2.62 ± 0.51 mm). While relative interoptic triangle area <75 mm^2 allowed the visualization of 2 perforant branches from de oICA in 40% and 3 in 60% of cases, for relative interoptic triangle areas >85 mm^2 3 perforant branches were observed in 87% and 4 in 13% of our cases dissected. Furthermore, specimens in which the origin of the OA and SHA could be visualized, the relative interoptic triangle area was significantly higher than in those specimens in which the origin of these vessels was not observable as shown in separate Mann-Whitney-Wilcoxon tests (p<0.001) (*Figure 22 and 23*).

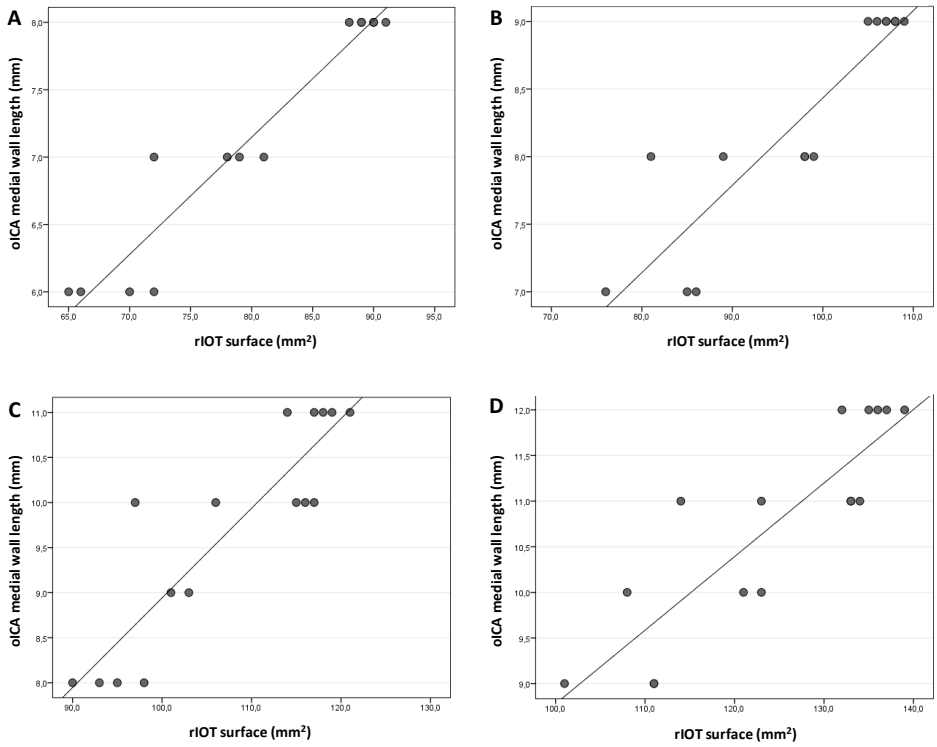

Fig. 18. Scatter plots showing correlation patterns between relative interoptic triangle (rIOT) extension and the extent of exposure of the contralateral oICA's medial aspect before removal of the contralateral half of the planum sphenoidale and tuberculum sellae as well as prior to contralateral optic nerve mobilization (*A*); after removal of the contralateral half of the planum sphenoidale and tuberculum sellae (*B*); after contralateral optic nerve mobilization (*C*); and after the combination of both removal of the contralateral half of the planum sphenoidale/tuberculum sellae and contralateral optic nerve mobilization (*D*).

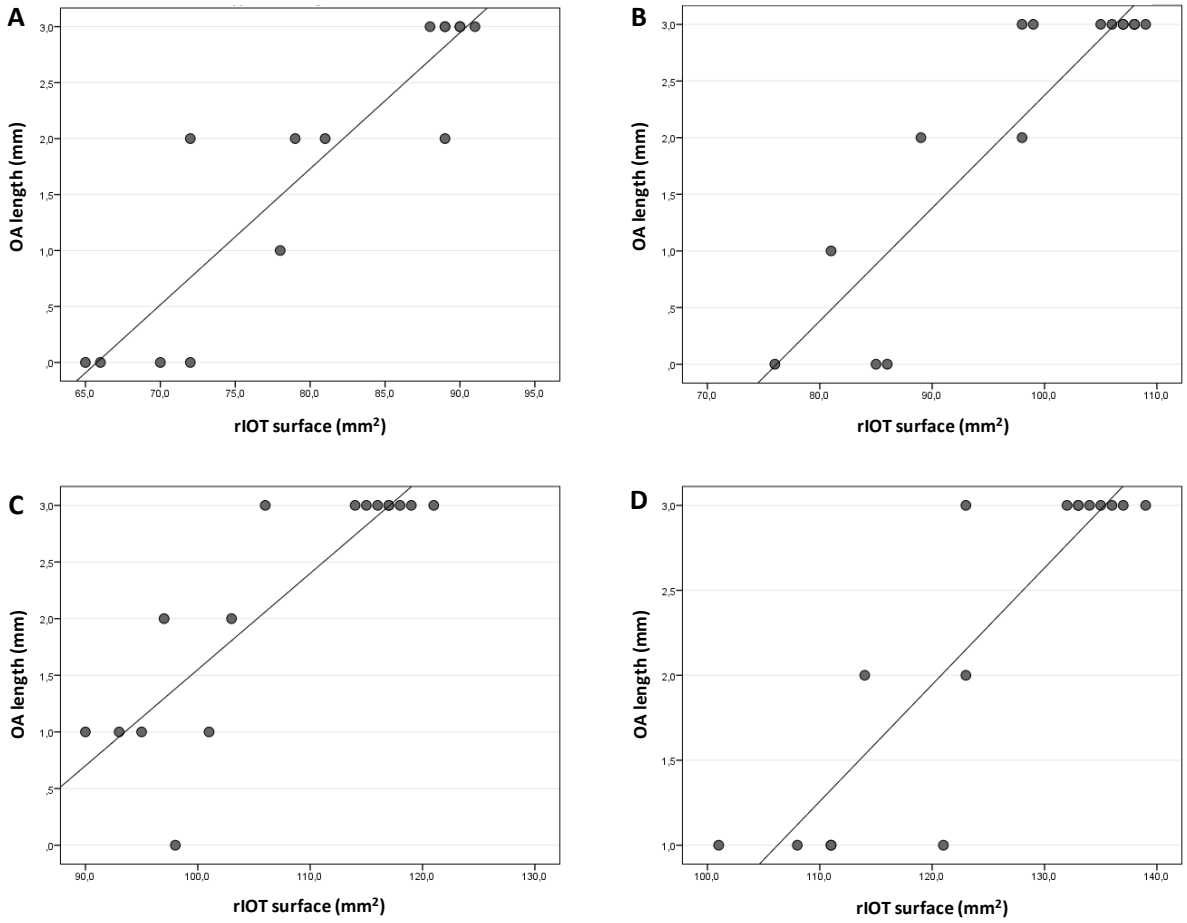

Fig. 19. Scatter plots showing correlation patterns between relative interoptic triangle (rIOT) extension and the extent of exposure of the contralateral OA before removal of the contralateral half of the planum sphenoidale and tuberculum sellae as well as prior to contralateral optic nerve mobilization (*A*); after removal of the contralateral half of the planum sphenoidale and tuberculum sellae (*B*); after contralateral optic nerve mobilization (*C*); and after the combination of both removal of the contralateral half of the planum sphenoidale/tuberculum sellae and contralateral optic nerve mobilization (*D*).

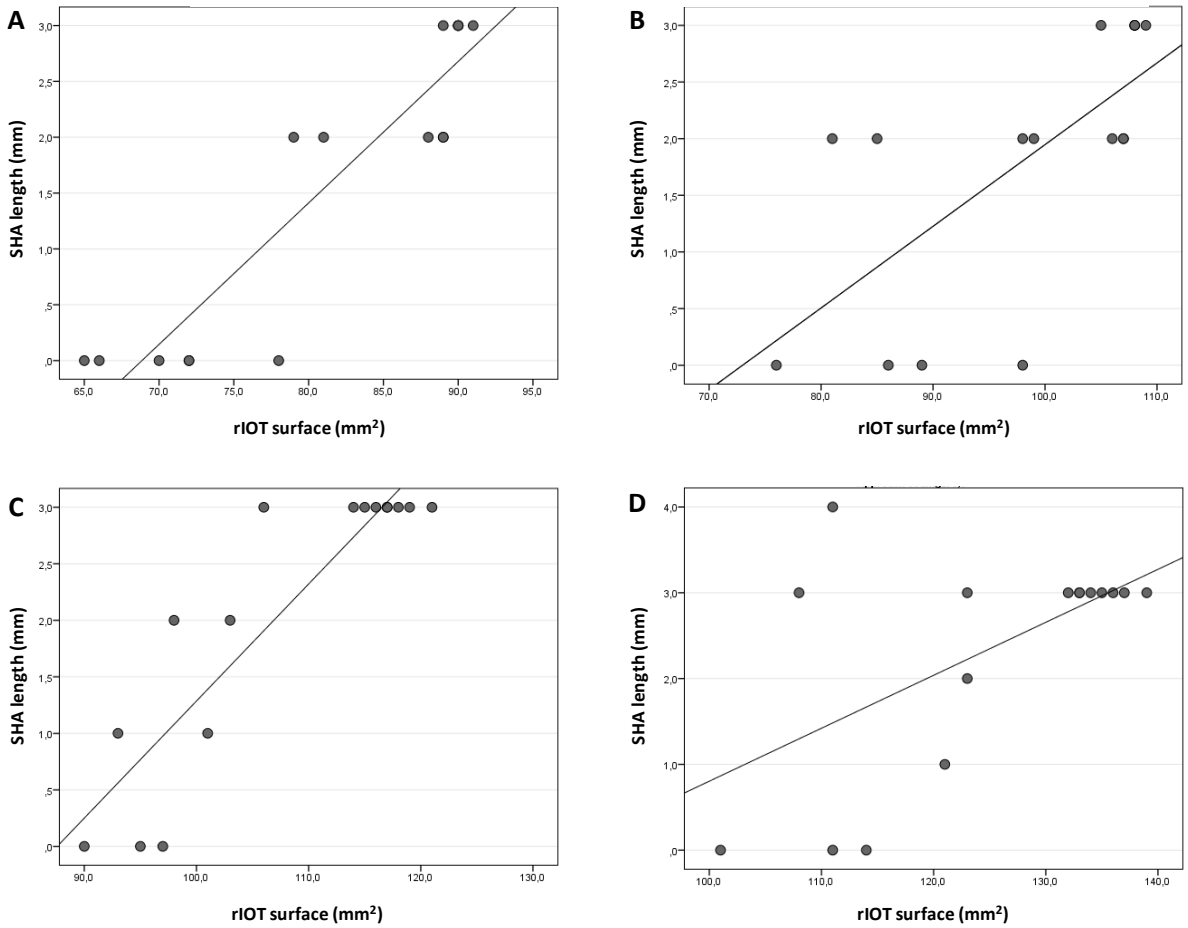

Fig. 20. Scatter plots showing correlation patterns between relative interoptic triangle (rIOT) extension and the extent of exposure of the contralateral SHA before removal of the contralateral half of the planum sphenoidale and tuberculum sellae as well as prior to contralateral optic nerve mobilization (*A*); after removal of the contralateral half of the planum sphenoidale and tuberculum sellae (*B*); after contralateral optic nerve mobilization (*C*); and after the combination of both removal of the contralateral half of the planum sphenoidale/tuberculum sellae and contralateral optic nerve mobilization (*D*).

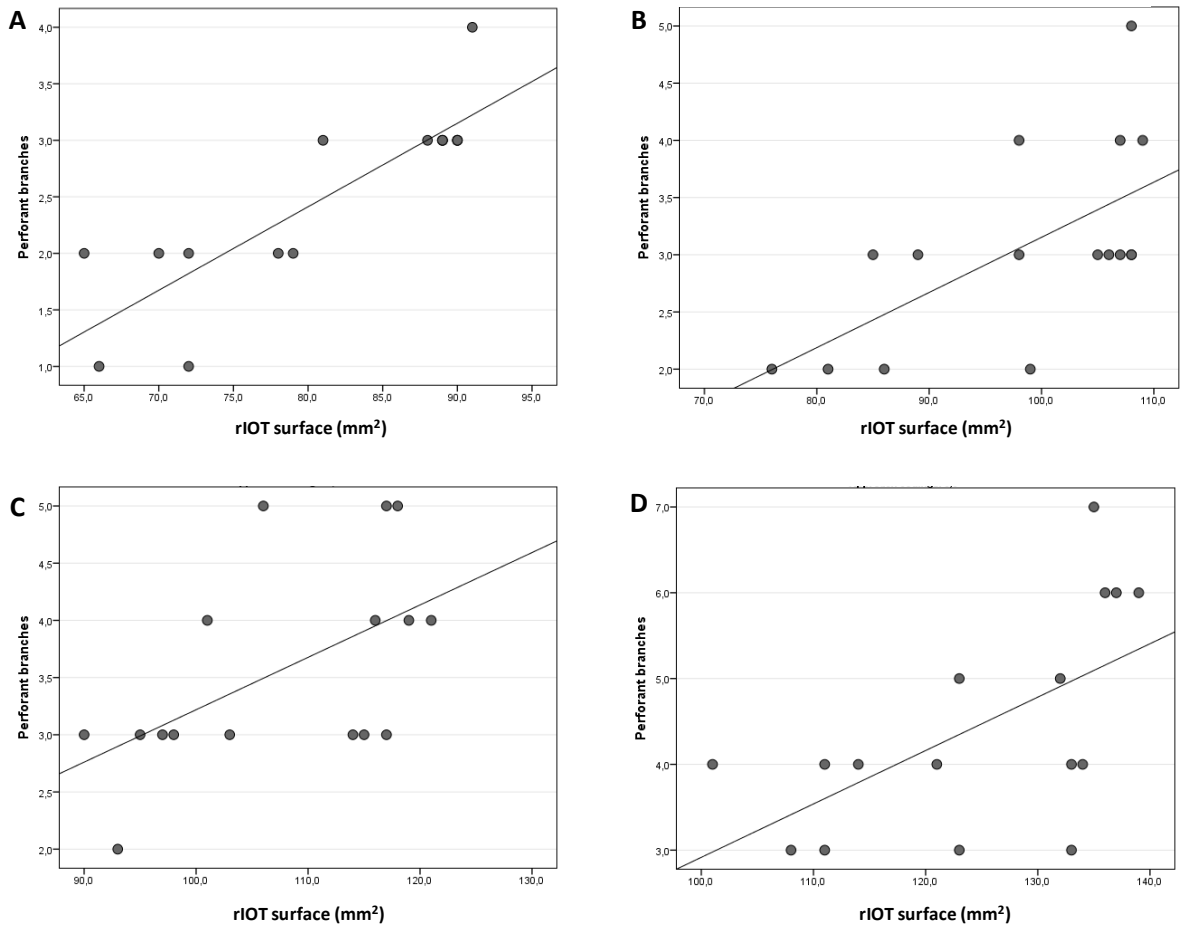

Fig. 21. Scatter plots showing correlation patterns between relative interoptic triangle (rIOT) extension and the number of perforant branches of the oICA exposed before removal of the contralateral half of the planum sphenoidale and tuberculum sellae as well as prior to contralateral optic nerve mobilization (*A*); after removal of the contralateral half of the planum sphenoidale and tuberculum sellae (*B*); after contralateral optic nerve mobilization (*C*); and after the combination of both removal of the contralateral half of the planum sphenoidale/tuberculum sellae and contralateral optic nerve mobilization (*D*).

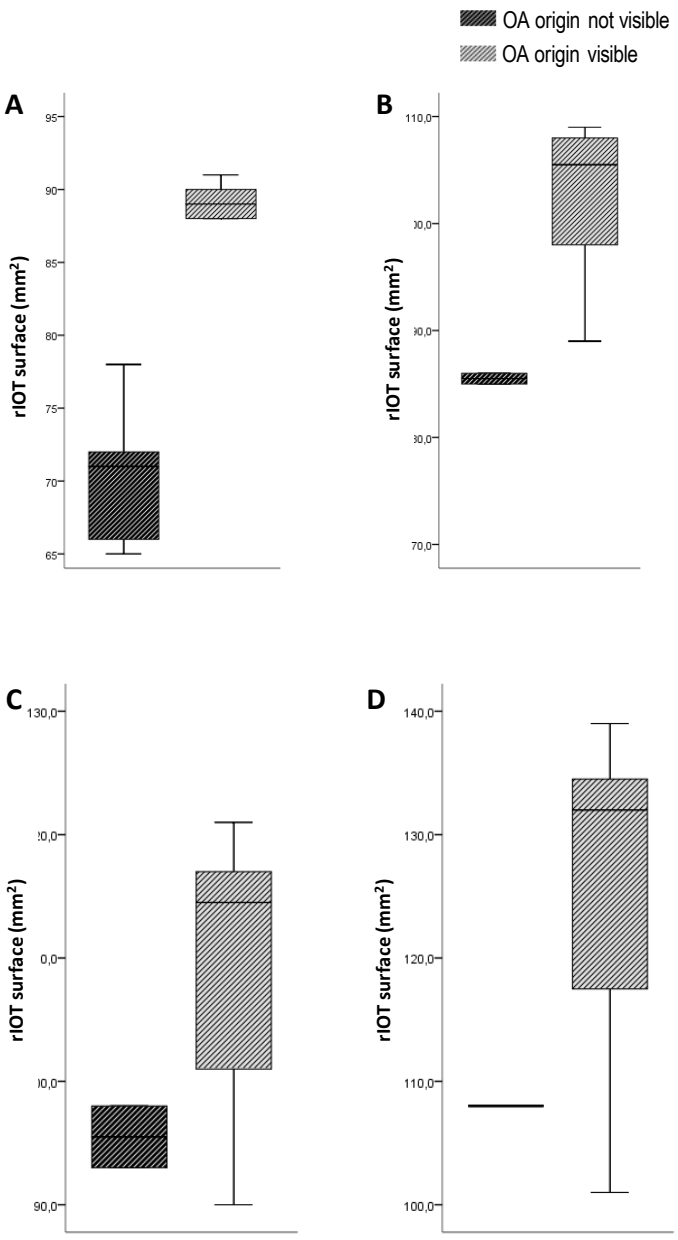

Fig 22. Relative interoptic triangle (rIOT) area in cadaver specimens in which the origin of the contralateral OA could be exposed or not. The measurements were obtained again before removal of the contralateral half of the planum sphenoidale and tuberculum sellae as well as prior to contralateral optic nerve mobilization (*A*); after removal of the contralateral half of the planum sphenoidale and tuberculum sellae (*B*); after contralateral optic nerve mobilization (*C*); and after the combination of both removal of the contralateral half of the planum sphenoidale/tuberculum sellae and contralateral optic nerve mobilization (*D*). All values express median ± IQR.

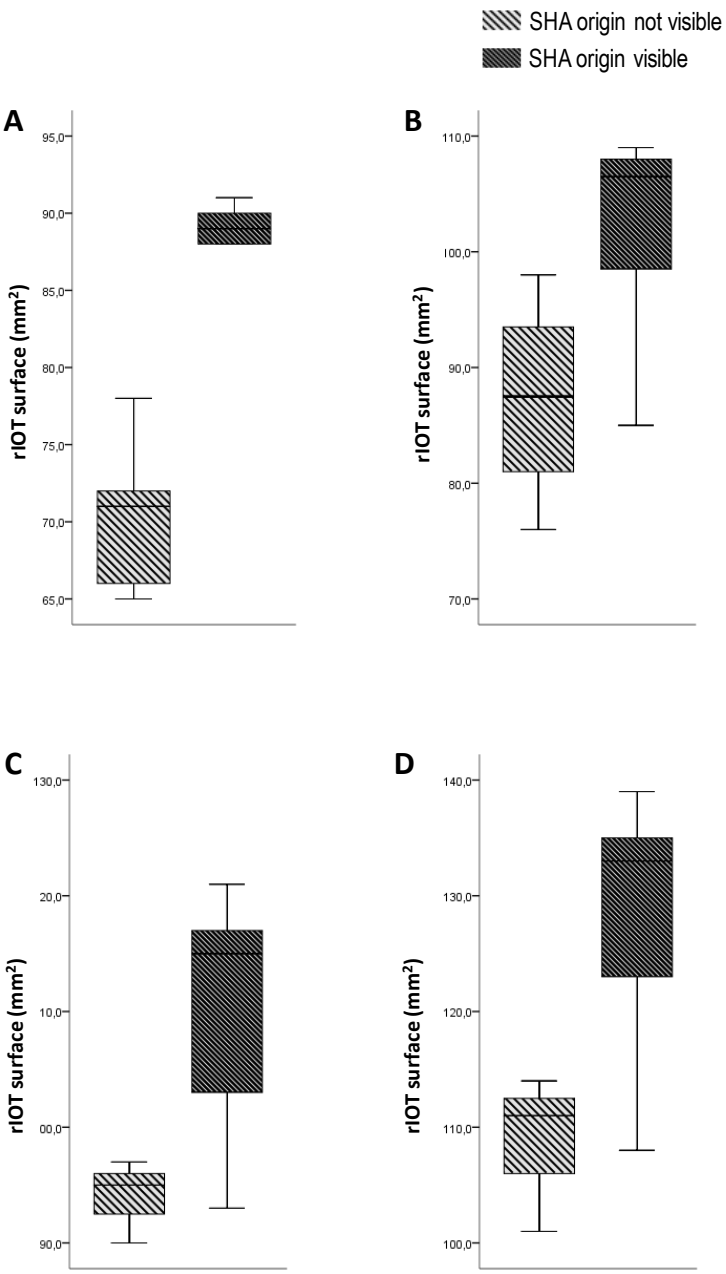

Fig 23. Relative interoptic triangle (rIOT) area in cadaver specimens in which the origin of the contralateral SHA could be exposed or not. The measurements were obtained again before removal of the contralateral half of the planum sphenoidale and tuberculum sellae as well as prior to contralateral optic nerve mobilization (*A*); after removal of the contralateral half of the planum sphenoidale and tuberculum sellae (*B*); after contralateral optic nerve mobilization (*C*); and after the combination of both removal of the contralateral half of the planum sphenoidale/tuberculum sellae and contralateral optic nerve mobilization (*D*). All values express median ± IQR.

4.2 Effectiveness of the assessment of ipsi- and contralateral approaches to the oICA and parasellar region in alive patients using a virtual 3D surgical simulation software

4.2.1 Anthropometric measurements of selected patients

First, we analyzed anthropometric parameters of the skull of the cases analyzed to rule out bias given by asymmetry between both right and left skull halves. A survey of the corresponding parameters is depicted in Table 3.

Anthropometric measure	Mean ± SD		
Cephalic perimeter	54.3 ± 0.78		
Biauricular breadth	24.6 ± 1.2		
External biorbital breadth	11.54 ± 1.18		
	Rigth	Left	T-Tests
Vertex-zygomatic length	15.88 ± 0.66	15.84 ± 0.56	ns
External obito-auricular length	6.95 ± 0.51	6.82 ± 0.72	ns
Internal orbito-auricular length	11.45 ± 0.73	11.32 ± 0.68	ns
External orbito-midline length	6.33 ± 0.44	6.47 ± 0.39	ns

Table 3. Anthropometric measurements ruled out the possibility of significant asymmetries between both halves of the skull in 3D virtual dissections. ns: non-significant.

4.2.2 Assessment of effectiveness given by ipsi- and contralateral approaches to the oICA

In our virtual pterional craniotomies the mean distance measured from the MacCarty's keyhole to the supraorbital foramen, i.e. supraorbital nerve, was 36.1 ± 2.4 mm. Extending the craniotomy anteriorly up to the lateral limit of the supraorbital foramen resulted in frontal sinus opening in 30% of the cases.

Similarly to our observations in the first part of the study, the optimal approach angle directed to the ipsilateral oICA and parasellar space was negative, i.e. posterior, to the reference line linking the keyhole with the apex of the ipsilateral anterior clinoid process. The other way round, positive, i.e. anterior, angles with respect to the reference line were found to be optimal while approaching the oICA and nearby

structures from the contralateral side (*Figure 24*). Separate one-way ANOVA analysis demonstrated a main effect of the applied approach variant on the optimal angle to reach the target structures [$F(4, 95)=648.568$, $p<0.001$, $\eta_p^2=0.965$]. The optimal approach angle to the ipsilateral oICA prior to anterior clinoidectomy was -14.8 ± 2,42°, with a minimum of -18° and a maximum of -12°. After performing anterior clinoidectomy, the optimal approach angle to expose the ipsilateral oICA was calculated on -24.5 ± 18.82°, variating between -22° and -28°. A separate Student-t test showed a significant change on optimal approach angle induced alone by having performed an ipsilateral anterior clinoidectomy [$T(38)=14,326$, $p<0.001$].

Fig. 24. The optimal approach angle in relation to the clinoid-keyhole line measured in 3D virtual dissections. Exposure of the oICA from the ipsilateral side was better accomplished through slightly posterior (negative) trajectories to the reference line, whilst contralateral approaches to the oICA benefited from anterior (positive) supraorbital trajectories. All values express mean ± 2 SD.

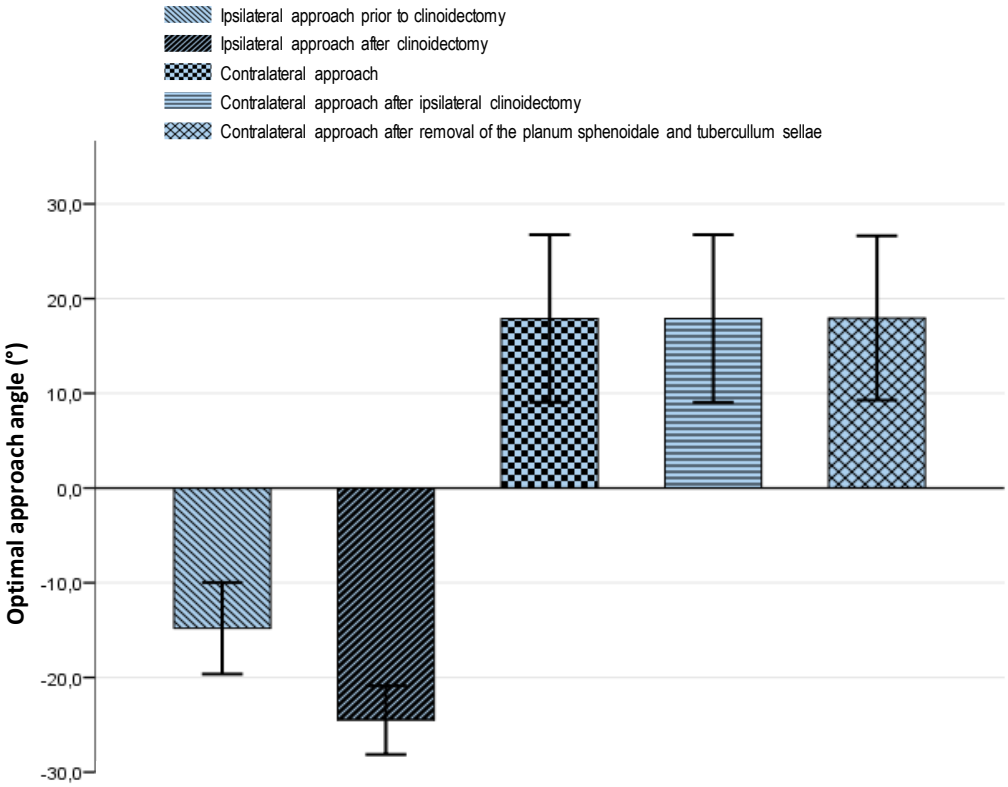

The angle of when the optimal route to the oICA from the contralateral side was positive, averaging 17.9 ± 4,42° and variating from a minimum of 11° and a maximum of 24°. Comparisons of the optimal trajectory angle between ipsilateral approaches prior and after anterior clinoidectomy with contralateral approaches confirmed the highly significant difference between ipsilateral and contralateral approaches (all *p* values <0.001). These findings were consistent with our observations in cadaveric specimens and demonstrate that the trans-Sylvian route enables the highest exposure of the oICA when the approach is directed from the ipsilateral side, while the subfrontal/supraorbital corridor enables a better exposure of the oICA when approached from the contralateral side.

On ipsilateral approaches to the oICA, the mean distance to the ipsilateral optic nerve through the optimal trans-Sylvian corridor was 45.9 ± 2.91 mm, variating minimally when a subfrontal/supraorbital corridor was used (46.6 ± 3.27 mm). Similarly, ipsilateral oICA's superomedial aspect was reached at 50.1 ± 2.92 mm by trans-Sylvian trajectories and at 49.9 ± 3.25 mm by subfrontal/supraorbital trajectories.

The mean ipsilateral optic nerve's length exposed was 11.05 ± 0.76 mm, variating between a minimum of 10 mm and a maximum of 12 mm. As expected, removal of the ipsilateral anterior clinoid process significantly increased the length of optic nerve exposed to 13.05 ± 1.05 mm (minimum 12 mm and maximum 15 mm) as shown by Student-t test for comparisons prior and after clinoidectomy [$T(38)=8.283$, $p<0.001$] (*Figure 25*).

The visualization and exposure of the oICA significantly differed according to the approach selected as observed in Kruskall Wallis analysis [$\chi^2(4)=88.067$, $p<0.001$] (*Figure 26A*). The median exposure of the oICA through an ipsilateral trans-Sylvian approach was 2 mm ± IQR 1 mm with a maximal exposure of 3 mm. Ipsilateral anterior clinoidectomy significantly increased the exposure to a median value of 3 mm ± IQR 2 mm with a maximum of 4 mm as show by Mann-Whitney-Wilcoxon test ($p<0.001$).

The contralateral approach significantly increased the oICA visualization to a median of 6 mm ± IQR 1 mm in comparison to ipsilateral approaches with or without anterior clinoidectomy as shown by Mann-Whitney-Wilcoxon tests ($p<0.001$). Furthermore,

the removal of the contralateral half of the planum sphenoidale and tubecullum sellae increased oICA exposure furhter to a median of 9 mm ± IQR 1.75 mm, being statistical significant in comparison to the contralateral approach prior to bone removal (p<0.001).

Fig. 25. Ipsilateral optic nerve exposure prior and after anterior clinoidectomy in 3D virtual dissections. Removal of the anterior clinoid process increases significantly the exposure of the ipsilateral optic nerve. All values express mean ± 2 SD.

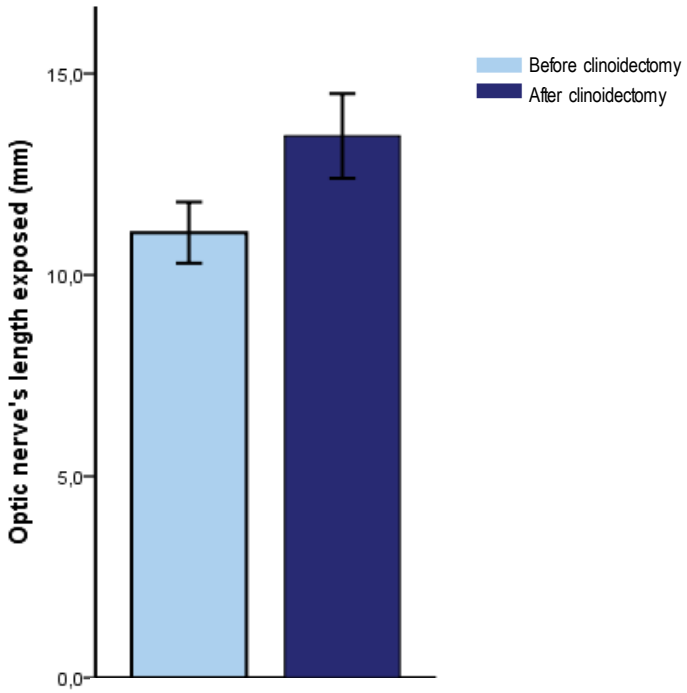

Again, a general increase in OA exposure as a main effect of approach variants was demonstrated by Kruskall Wallis analysis [$\chi^2(4)=21.122$, p<0.001] (*Figure 26B*). In this case, the absolutely lack of OA exposure through ipsilateral approaches prior to anterior clinoidectomy was overcome by anterior clinoidectomy. This maneuver enabled to visualize a segment of the OA in 40% of the cases with a maximal length of 3 mm in one subject. This increase in OA exposure was significant as confirmed by Mann-Whitney-Wilcoxon test between ipsilateral approaches with or without anterior clinoidectomy (p<0.01). Contralateral approaches to the oICA enabled

exposure of an OA segment in 50% of the cases with a maximum of 3 mm in 2 cases. Removal of the contralateral half of the planum sphenoidale and tubeculum sellae increased the proportion of cases in which the OA was exposed to 65% with a maximum of 3 mm in 7 virtual cases. Despite this rather evident trend, separate Mann-Whitney-Wilcoxon tests comparing the contralateral approach alone against ipsilateral approaches after clinoidectomy or with the contralateral approach after removal of the contralateral half of the planum sphenoidale and tuberculum sellae failed to demonstrate statistical significance (both $p>0.05$).

Fig. 26. Exposure of the superomedial aspect of the oICA and OA through ipsilateral and contralateral approaches assessed in 3D virtual dissections in the dextroscope. The use of contralateral approaches increased significantly the exposure of the oICA's superomedial aspect (*A*), the OA (*B*) and the percentage of visualization of OA origin (*C*). Values from *A* and *B* express median ± IQR., whilst *C* express percentages.

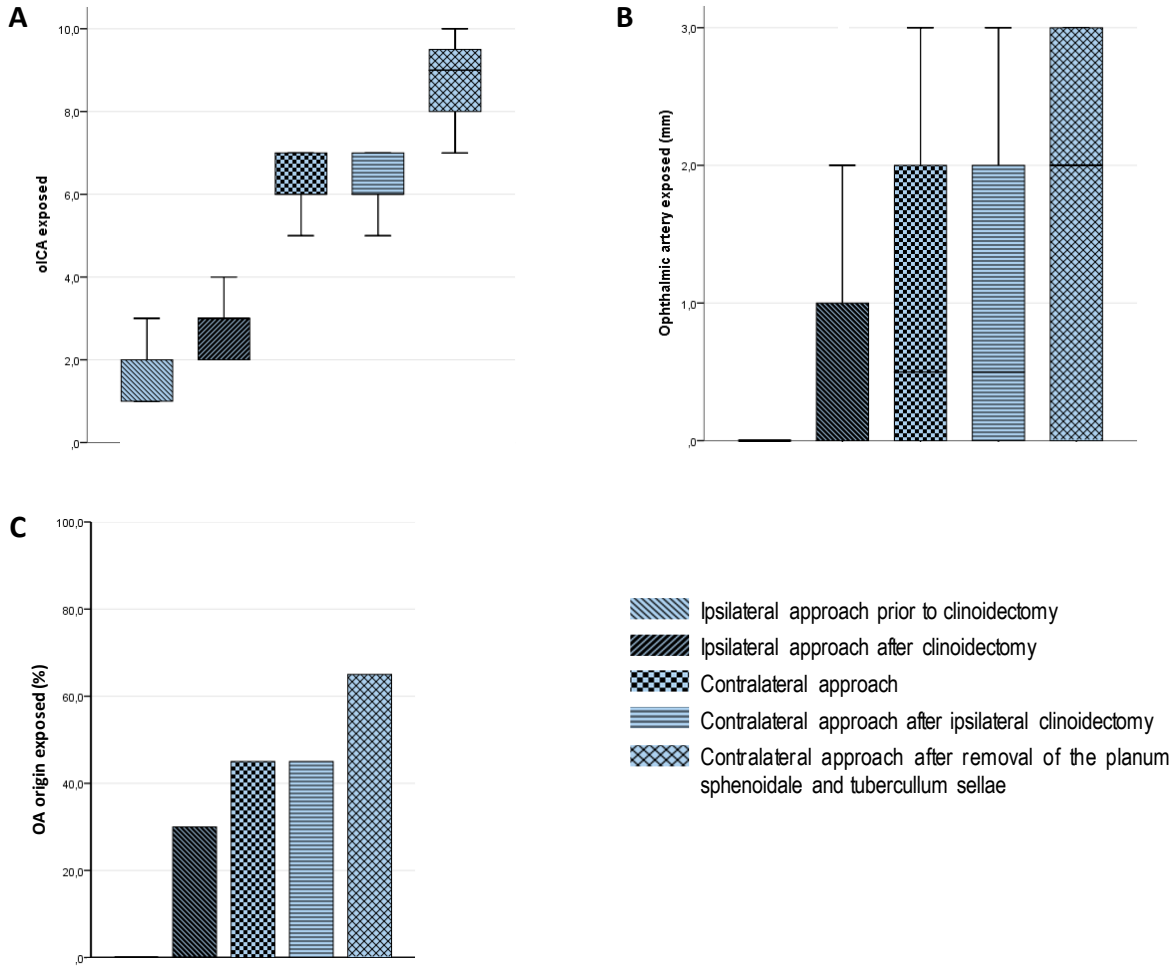

Since the observation of a segment belonging to the ophthalmic artery does not necessarily implicate the visualization of OA origin, we assessed this separately. Contralateral approaches even without bone removal increased the likelihood of visualizing the OA origin compared to ipsilateral approaches significantly [$\chi^2(1)=11.613$, $p<0.001$] (*Figure 26C*). Removal of the planum sphenoidale and tuberculum sellae did not significantly further increase visualization of OA origin ($p>0.05$). Furthermore, in virtual cases in which OA origin was visualized, oICA's exposure was significantly higher than the cases in which OA origin could not be seen. Significance of this finding was proven in separated Mann-Whitney-Wilcoxon analysis not only for ipsilateral approaches after anterior clinoidectomy ($p<0.01$), but also for contralateral approaches prior ($p<0.01$) and after planum sphenoidale/tuberculum sellae removal ($p<0.001$).

Fig. 27. Contralateral optic nerve exposure prior and after removal of the planum sphenoidale and tuberculum sellae assessed in 3D virtual dissections in the dextroscope. Removal of the contralateral half of the planum sphenoidale and tuberculum sellae increased significantly the exposure of the contralateral optic nerve. All values express mean ± 2 SD.

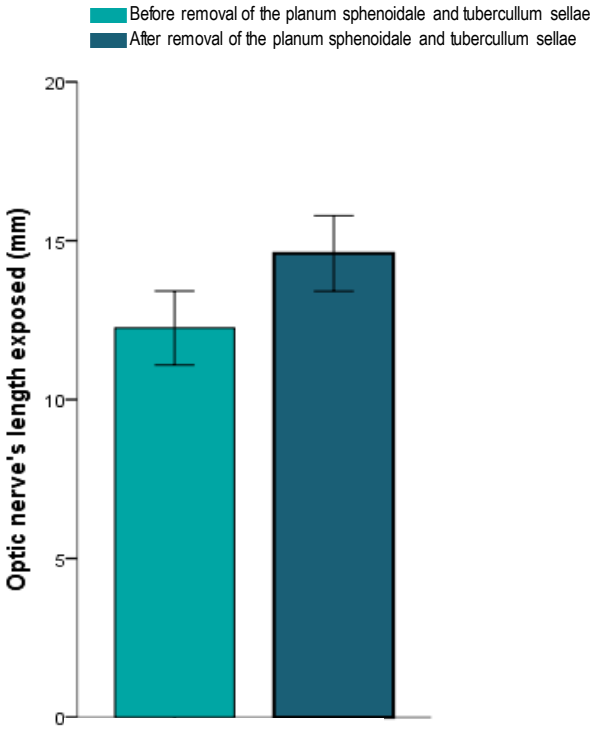

The measured distance to the contralateral optic nerve and medial wall of the oICA through the optimal subfrontal/supraorbital approach was 63.35 ± 3.360 mm and 66.05 ± 3.364 mm respectively. For contralateral approaches, the length of the exposed contralateral optic nerve was in average 12.25 ± 1.16 mm. As expected, bone removal from the contralateral half of the planum sphenoidale and tuberculum sellae significantly increased the exposed segment of the optic nerve to 14.6 ± 1.19 mm as demonstrated in separate Student-t test [$T(38)= -6,319$, $p<0.001$] (*Figure 27*).

4.2.3 Relative interoptic triangle's assessment for accessibility to the contralateral oICA and parasellar space

Following the same rationale as for cadaveric specimens, we assessed the 2-dimensional projection of the interoptic triangle on the operative microscope (*see methods*), assuming that the anatomo- morphometrical features of this space are relevant for the accessibility to the oICA and neighbor structures from the contralateral side.

The mean interoptic triangle's area calculated for approaches using the optimal subfrontal/supraorbital trajectory to the contralateral oICA was 80 ± 8.59 mm^2. As expected, ipsilateral removal of the anterior clinoid process did not influence these parameters. The removal of the contralateral half from the planum sphenoidale and tuberculum sellae in contrast significantly increased the relative interoptic triangle's area to 90.2 ± 10.5 mm^2, as shown in separate one-way ANOVA [$F(2, 57)=8.063$, $p=0.001$] (*Figure 28*).

As seen in the cadaveric part of this work, our virtual parameters in alive patients corroborated a strong positive correlation between the relative interoptic triangle's area and oICA as well as OA exposure (both $r=0.915$, $p<0.001$) (*Figure 29*). This correlation remained significant after removal of the contralateral half of the planum sphenoidale and tuberculum sellae for both parameters, oICA- ($r=0.873$, $p<0.001$) and OA exposure ($r=0.955$, $p<0.001$). The exposed length of oICA increased from 5.4 ± 0.55 mm for specimens with relative interoptic triangle areas lower than 75 mm^2, to 6 ± 0.11 mm for interoptic triangle areas between 75 and 85 mm^2 and 6.87 ± 0.35 mm for interoptic triangle areas larger than 85 mm^2. The same pattern was observed for the exposed OA length (<75 mm^2: 0 mm; 75 – 85 mm^2: 0,8 ± 0.48 mm;

>85 mm^2: 2.25 ± 0.46 mm). While relative interoptic triangle areas <75 mm^2 allowed no visualization of OA origin, for relative interoptic triangle areas between 75 and 85 mm^2 OA origin was visualized in 28% of the cases, increasing to 87% of the cases if the interoptic triangle area was >85 mm^2. Additionally, virtual cases in which OA origin could be visualized were demonstrated to have a significantly greater relative interoptic triangle's area both prior and after removal of the planum sphenoidale and tuberculum sellae as shown by separate Mann-Whitney-Wilcoxon analysis (both p<0.001) (*Figure 30*).

Fig. 28. Extension of the relative interoptic triangle area for contralateral approaches in 3D virtual dissections. All values express mean ± 2 SD.

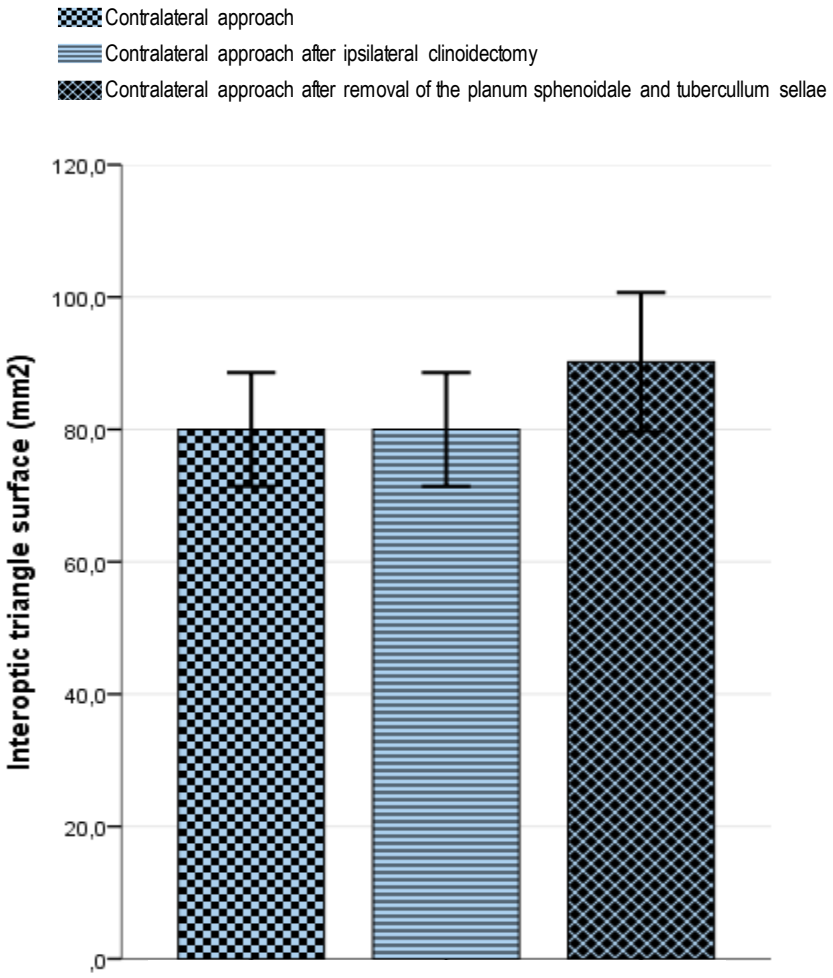

Fig. 29. Scatter plots obtained from 3D virtual dissections showing correlation patterns between relative interoptic triangle (rIOT) extension and the extent of exposure of the contralateral oICA's superomedial aspect (*A, B*) and OA length (*C, D*) previous to (*A, C*) and after (*B, D*) removal of the contralateral half of the planum sphenoidale and tubercullum sellae.

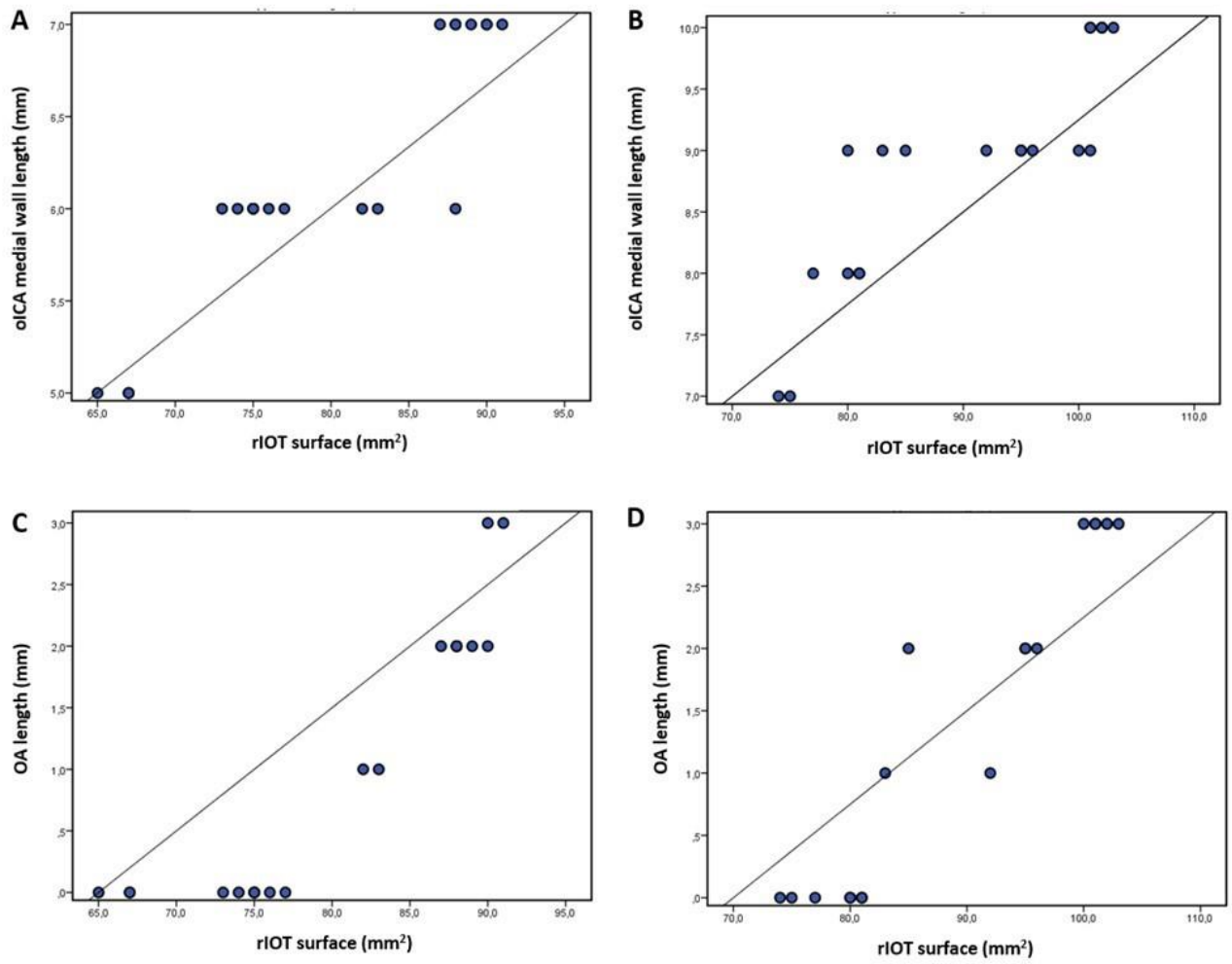

Fig. 30. Relative interoptic triangle (rIOT) area in 3D virtual dissections in which the origin of the contralateral OA could be exposed or not. The measurements were obtained again before (*A*) as well as after (*B*) removal of the contralateral half of the planum sphenoidale and tuberculum sellae. All values express median ± IQR.

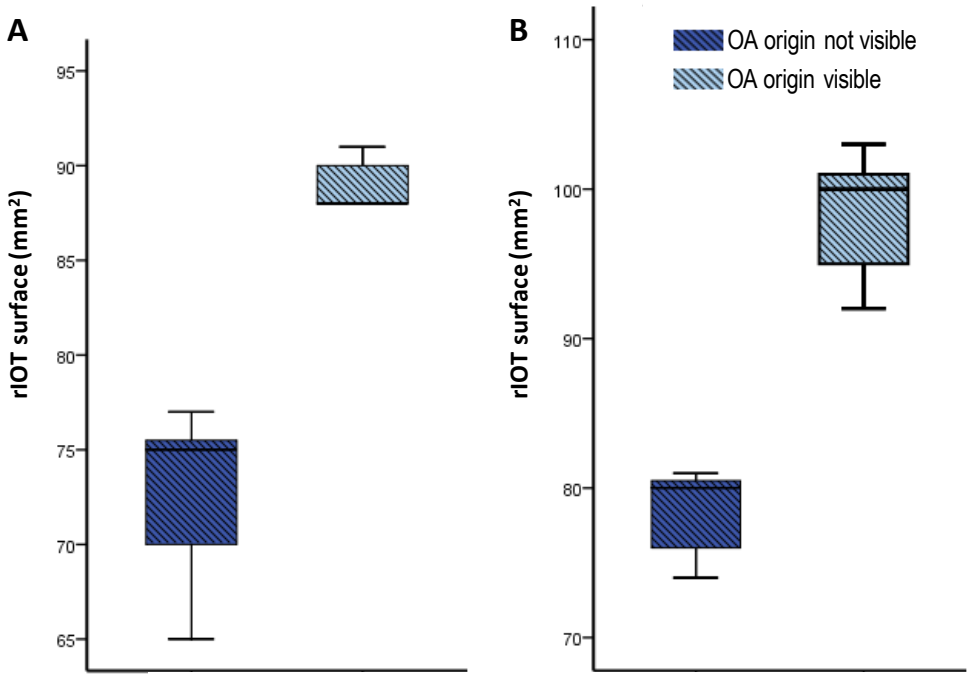

5. Discussion

5.1 Targeting the ophthalmic segment of the internal carotid artery and its branches from the ipsilateral or contralateral side requires the adoption of different approach trajectories

We determined the optimal route to the ophthalmic segment of the internal carotid artery for approaches directed from the ipsilateral and contralateral side. The corresponding findings in both cadaveric and virtual surgical studies demonstrated that given a reference line crossing the MacCarty's keyhole and the apex of the ipsilateral anterior clinoid process, the optimal approach trajectory to target the oICA from the ipsilateral side is posterior to this line and follows a route through opening the Sylvian cistern (trans-Sylvian corridor), while the optimal approach trajectory to target the oICA and its branches from the contralateral side follows a lateral subfrontal/supraorbital route anterior to the reference line. These findings validate the surgical experience propagated by Perneczky et al. that if certain anatomical conditions are given and the approach trajectory is planned carefully, aneurysms arising from the oICA can be successfully treated using a keyhole contralateral supraorbital approach even without the need of larger craniotomies (Perneczky 1985, van Lindert 1998).

When approaching the oICA from the ipsilateral side, predominantly the lateral wall of the artery is exposed, while the OA and SHA arise from the medial third of the superior part of the C4 segment (Hayreh & Dass 1962, Hayreh 1974, Rhoton 2002, Stephens & Stilwell 1969). All variants of paraclinoid ICA aneurysms (except for extremely rare anterolateral variants of clinoid aneurysms and dorsal ophthalmic segment aneurysms) require the exposure of the superior and medial aspect of the supraclinoid ICA (Hassoun-Turkmani 2016, Yasargil 1984). For this the ICA needs to be approached between its superior border and the optic nerve and, if the anterior clinoid process is not removed, the mobility of the oICA and the optic nerve is extremely limited and the exposure of oICA's superomedial aspect is very limited. The maximal exposure can be achieved by a trajectory slightly posteriorly angulated in relation to the keyhole-clinoid line. After removal of the anterior clinoid process, the mobility and with it the achievable exposure of the oICA and the optic nerve increase and the adoption of a slightly more posterior trajectory provides the best

exposition of the target area, as demonstrated by our dissections in both cadaver and virtual cases (*Figure 31*). The reason why trajectories pointing more anteriorly to the ipsilateral oICA were yielding a worse exposure of the vessel and its branches is its close anatomic relation to the optic nerve. The optic nerve is situated directly above the ICA when seen from this angle, so that a further visualization of the ICA can only be achieved by an intolerable optic nerve mobilization.

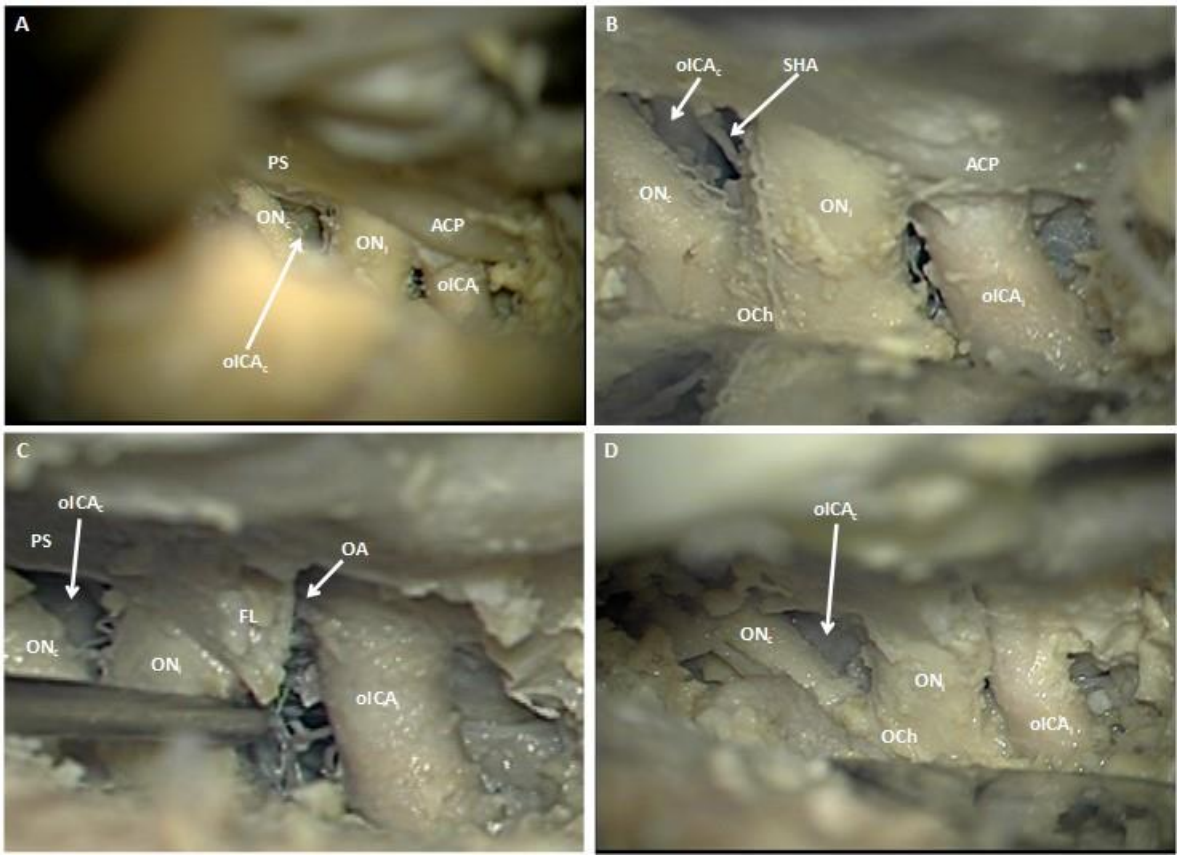

Fig. 31. The exposure of the ipsilateral internal carotid artery and optic nerve prior to anterior clinoidectomy (*A, B*) increased significantly after removal of the anterior clinoid process (*C, D*). This allowed a greater mobility of ipsilateral neurovascular structures to expose the ipsilateral ophthalmic artery, arising in this specimen from the anterior aspect of the carotid artery. *ON_i*, ipsilateral optic nerve; *ON_c*, contralateral optic nerve; *OCh,* optic chiasm; *$oICA_i$*, ophthalmic segment of the ipsilateral internal carotid artery; *$oICA_c$,* ophthalmic segment of the contralateral internal carotid artery; *FL,* falciform dural fold (ligament); *PS,* planum sphenoidale; *ACP,* ipsilateral anterior clinoid process; *OA,* ipsilateral ophthalmic artery; *SHA,* contralateral superior hypophyseal artery.

For approaches to the oICA from the contralateral side, the optimal angle to target the vessel and its branches was anterior to the keyhole-clinoid reference line as clearly demonstrated in both cadaveric and virtual dissections (*Figure 32*). Adopting this trajectory, the approach route passes above the previously smoothed orbit roof and below the orbital gyri of the frontal lobe and maximizes the visualization of the oICA and its branches through the space comprehended between both optic nerves converging into the chiasm (Clatterbuck 2005). Given that this approach profits from the window created by the interoptic space and since the anterior clinoid process on craniotomy's side is located laterally to this window, it becomes clear why anterior clinoidectomy did not influence the optimal approach angle and trajectory to the contralateral oICA in neither cadaveric nor virtual specimens. In addition, the increase in contralateral exposure of the oICA and its branches induced by removal of the contralateral half of the planum sphenoidale and tuberculum sellae was achieved only by enlargement of the relative interoptic space and not due to an optimization of the trajectory, as evidenced by insignificant differences in terms of optimal approach angles measured prior and after bone removal.

The approach from the contralateral side using the subfrontal/supraorbital trajectory enabled, in comparison to the approaches directed through the ipsilateral side, a greater exposure of the medial wall of the oICA, its perforant branches, the ophthalmic artery and the superior hypophyseal arteries concerning both origin and length. These findings from the cadaveric study were replicated in our virtual surgical approaches in alive subjects, although due to limitations in image resolution it was not possible to analyze the superior hypophyseal artery and perforant branches in the virtual part of the study.

In both cadaveric and virtual dissections, the exposure of the oICA from the contralateral side alone without the need for further manoeuvres, such as optic nerve mobilization of bone removal, was significantly greater than the approaches directed from the ipsilateral side even after anterior clinoidectomy. As the OA arises usually from the medial third of the oICA it is not surprising that a major exposure of the oICA´s medial wall achieved by contralateral approaches also significantly increase exposure of the OA which we observed in in both cadaveric and virtual dissections. Supporting our findings, Oshiro et al. reported to have identified the origin of the OA through contralateral approaches in 62% of cadaveric specimens (Oshiro 1997).

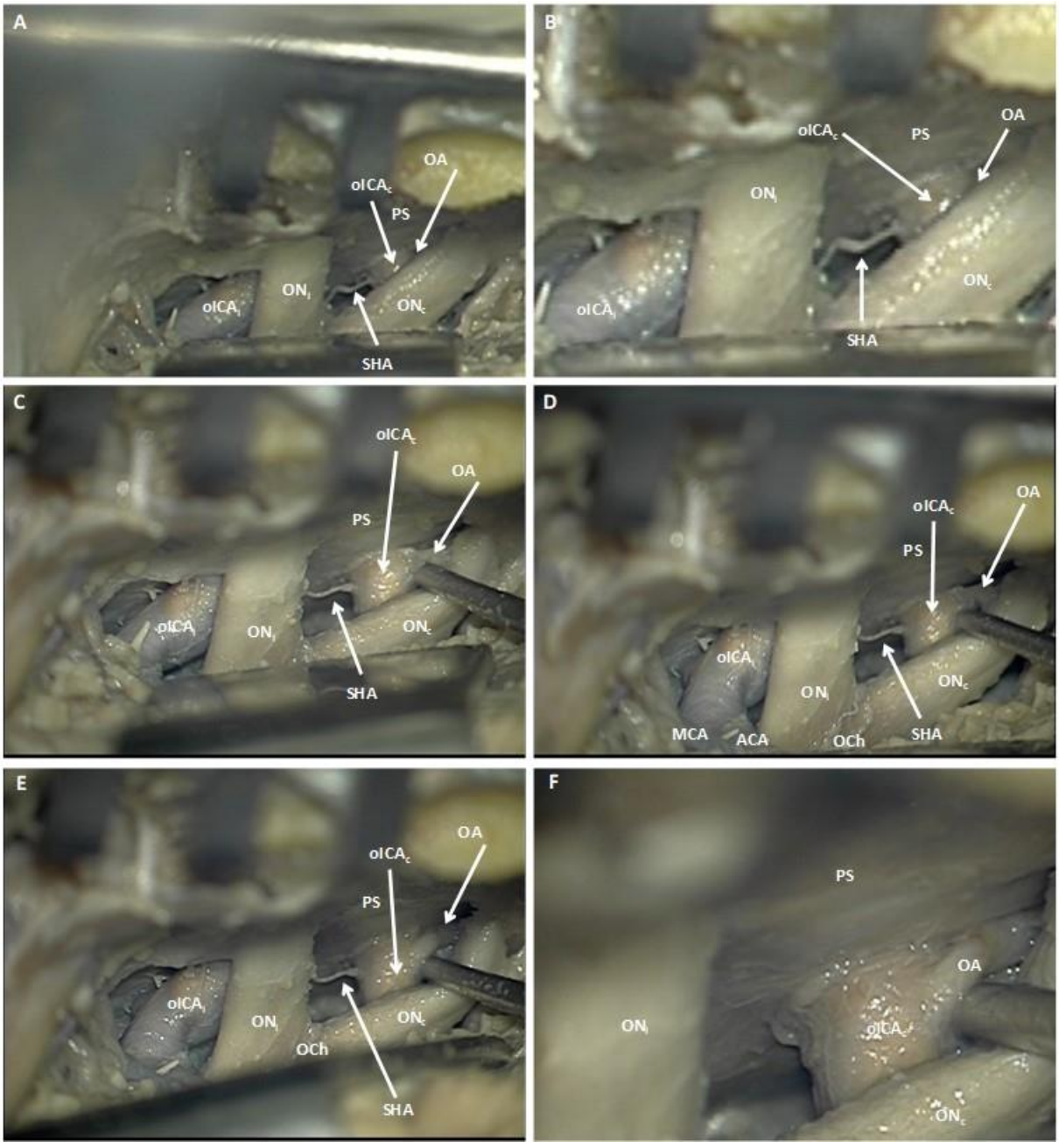

Fig. 32. Exposure of the medial aspect of the contralateral internal carotid artery, as well as the superior hypophyseal and ophthalmic arteries. In this case, the ophthalmic artery can be visualized prior to the mobilization of the contralateral optic nerve (*A, B*). Only a light optic nerve mobilization is required to increase ophthalmic artery's exposure (*C to F*). *ON$_i$,* ipsilateral optic nerve; *ON$_c$,* contralateral optic nerve; *Och,* optic chiasm; *oICA$_i$,* ophthalmic segment of the ipsilateral internal carotid artery; *oICA$_c$,* ophthalmic segment of the contralateral internal carotid artery; *PS,* planum sphenoidale; *OA,* contralateral ophthalmic artery; *SHA,* contralateral superior hypophyseal artery; *ACA,* anterior cerebral artery; *MCA,* middle cerebral artery.

A separate comparison of OA exposure through a contralateral approach without bone removal or optic nerve mobilisation to the ipsilateral approach revealed a significant advantage of contralateral against ipsilateral approaches prior to anterior clinoidectomy in both cadaver and virtual simulations. However, this trend did not reach significance level when compared with ipsilateral approaches after anterior clinoidectomy. The reason for the missing significance for this parameter is probable due to an anatomical variation: Although the ophthalmic artery arises from the antero-medial (53.6%) or supero-medial (31.5%) surfaces of the carotid artery, in 6.5% of the cases it can arise from the most anterior portion of the carotid cistern (Hayreh & Dass 1962, Hayreh 1974). Given this condition, OA visualization from the contralateral side can be difficulted by the interposition of the planum sphenoidale and tuberculum sellae as well as by the contralateral optic nerve. Accordingly, contralateral approaches after removal of the planum sphenoidale and tuberculum sellae and/or contralateral optic nerve mobilisation showed a significantly better exposure of the OA when compared with ipsilateral approaches before or after anterior clinoidectomy.

Contralateral approaches to the oICA likewise provided a greater exposure of the SHA in length and origin compared to ipsilateral approaches. Indeed, ipsilateral approaches were found to be ineffective to expose perforant arteries in both parts of the presented study even after anterior clinoidectomy. As pointed out previously, the greater exposure of oICA medial aspect achieved by contralateral approaches plays a determining role in increasing SHA exposure and its origin from the medial aspect of the oICA. Supporting these findings, several small clinical series have been reported in literature that show the effectiveness of pterional contralateral approaches to treat aneurysms arising from the SHA, taking advantage of this key anatomical feature (Chen 2013a).

Similar results were found when analyzing the effectiveness of ipsilateral and contralateral approaches regarding the exposure of perforant branches arising from the C4. Perforant arteries of the oICA arise mostly from the posterior or medial aspect of the artery and are frequently directed towards the infundibulum and stalk of the pituitary gland, the optic chiasm, or less frequent to the optic nerve, premamillary portion of the floor of the third ventricle, and the optic tract (Rhoton 2002). Hence, considering again that these branches mostly originate from the medial aspect of the

ICA and are directed towards midline structures, the greater portion of oICA´s medial wall exposed the contralateral side constitutes a key to enhance the visualization of its perforant arteries. In our cadaveric study, our median exposure of the oICA´s perforant branches through contralateral approaches was close to the total number of perforant arteries arising from this ICA portion (Rhoton 2002). On the contrary, ipsilateral approaches were rather ineffective to expose perforant branches of the oICA. The lack of data derived from our virtual dissections is owed to identical reasons as discussed above for the assessment of SHA.

5.2 The role of anterior clinoidectomy in ipsilateral approaches to the oICA

In concordance with the existing literature, our anatomic and morphometric studies in both cadaveric and virtual specimens underline the importance of anterior clinoidectomy for approaches to the C4 segment of the ICA performed from the ipsilateral side (*Figure 31 and 33*). As our morphometric characterization demonstrates, anterior clinoidectomy does not provide better exposure of the oICA compared to approaches from the contralateral side.

On ipsilateral approaches in our cadaveric study, anterior clinoidectomy tended to increase SHA and oICA superomedial aspect exposure, though this tendency did not reach statistical significance. Increase of oICA superomedial aspect exposure after clinoidectomy only reached statistical significance in virtual dissections. We also saw advantages provided by anterior clinoidectomy regarding OA visualization, optic nerve exposure and significant reduction in the need of mobilizing the optic nerve and ICA to achieve a better exposure of oICA branches, even when optic nerve's mobility was in fact increased by anterior clinoidectomy. The anterior clinoid process forms the lateral margin of the optic canal and the ICA courses along the medial aspect of this bony structure (Rhoton 2002). Therefore, anterior clinoidectomy plays a key role in ipsilateral surgical exposure of paraclinoid aneurysms (Hassoun-Turkmani 2016, Ota 2015, Chang 2009, De Jesus 1999, Huynh-Le 2004). It can be performed extradurally (Dolenc 1985) or, as preferred by many surgeons, intradurally since this allows to simultaneously observe the optic nerve and aneurysm and achieve immediate bleeding control if the aneurysm ruptures prematurely (Hassoun-Turkmani 2016).

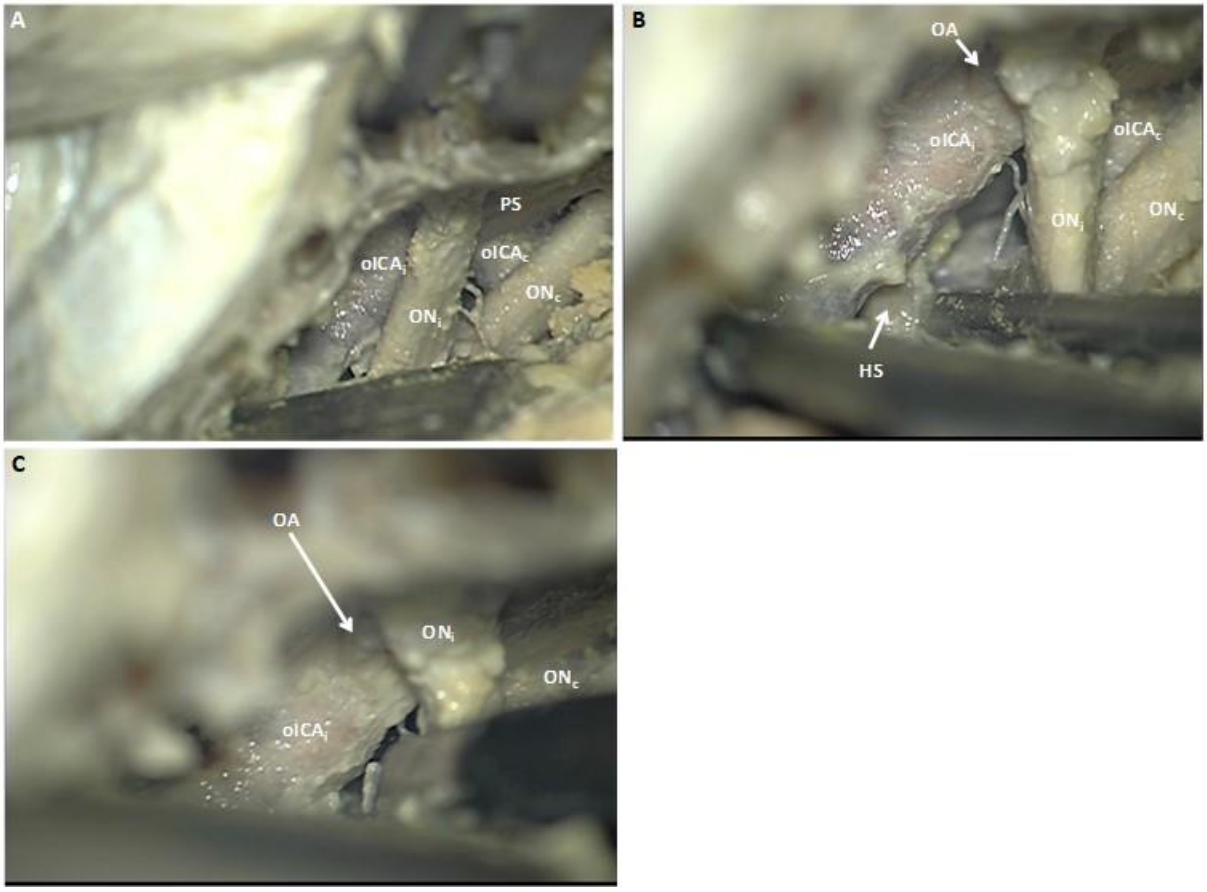

Fig. 33. Another example illustrating the exposure of the ipsilateral internal carotid artery and optic nerve after anterior clinoidectomy. The exposure of the ipsilateral ophthalmic artery and perforant branches of the internal carotid artery was enabled only after removal of the anterior clinoid process and sufficient optic nerve mobilization (*B,* C). *ON$_i$,* ipsilateral optic nerve; *ON$_c$,* contralateral optic nerve; *oICA$_i$,* ophthalmic segment of the ipsilateral internal carotid artery; *oICA$_c$,* ophthalmic segment of the contralateral internal carotid artery; *PS,* planum sphenoidale; *OA,* ipsilateral ophthalmic artery.

However, anterior clinoidectomy is not exempt from being a hazardous procedure and the factual risk of removing this bony structure should not be underestimated. The surgical treatment of paraclinoid aneurysms is known to be associated with a relatively high risk of optic apparatus injury, related to the anterior clinoidectomy (Sheikh 2000, Kassam 2007). The mechanical and thermal injury from the rotating drill, including direct cranial neuropathies with affection of the olfactory, optic, oculomotor and trochlear nerves, as well as vascular injuries are potential negative consequences of anterior clinoidectomy (Chang 2009). Drilling of the anterior clinoid

process can cause temperature elevations in the bone of up to 70°C around the drill tip (Matheus 1972, Chang 2009) and heating nerve tissue to 45 to 47°C for only 1 or 2 minutes can produce permanent electrophysiological impairments and complete destruction of myelinated and unmyelinated fibers (Xu 1994, Chang 2009). Already temperatures close to 58°C can lead to immediate axonal degeneration and cell death (Xu 1994, Chang 2009). Furthermore, even in the hands of very experienced cerebrovascular and skull-base neurosurgeons, power- drilling or rongeur bites into the aneurysm dome have been reported during clinoidectomy (Korosue 1992, Chang 2009, Hassoun-Turkmani 2016). The fact that some aneurysms erode into and through the anterior clinoid process may further enhance the risk of premature rupture (Hassoun-Turkmani 2016). Finally, the ventilated cells of the sphenoid sinus can in some cases extend into the anterior clinoid process, increasing the risk of cerebrospinal-fluid (CSF) fistula if anterior clinoidectomy is performed intradurally (Rhoton 2002). Sparing anterior clinoidectomy constitutes for the reasons mentioned a clear advantage of contralateral approaches to the oICA.

5.3 The role of removing the contralateral half of the planum sphenoidale and tuberculum sellae in contralateral approaches to the oICA

Removal of the planum sphenoidale and tuberculum sellae surrounding the oICA was performed during contralateral approaches and after acquisition of morphometrical and anatomical data on intact conditions (*Figure 34 and 35*). Bone removal resulted in a statistically significant improvement of oICA medial aspect exposure in both cadaveric and virtual dissections. Although the planum sphenoidale and tuberculum sellae removal provided also some improvement concerning OA exposure, this was not statistically significant. Values for exposure of the SHA or other perforant arteries were likewise not statistically significant in the cadaveric study. Perhaps the main advantage provided by removing the planum sphenoidale and tuberculum sellae on contralateral approaches was the enlargement of the workspace around the oICA medial aspect, between both optic nerves.

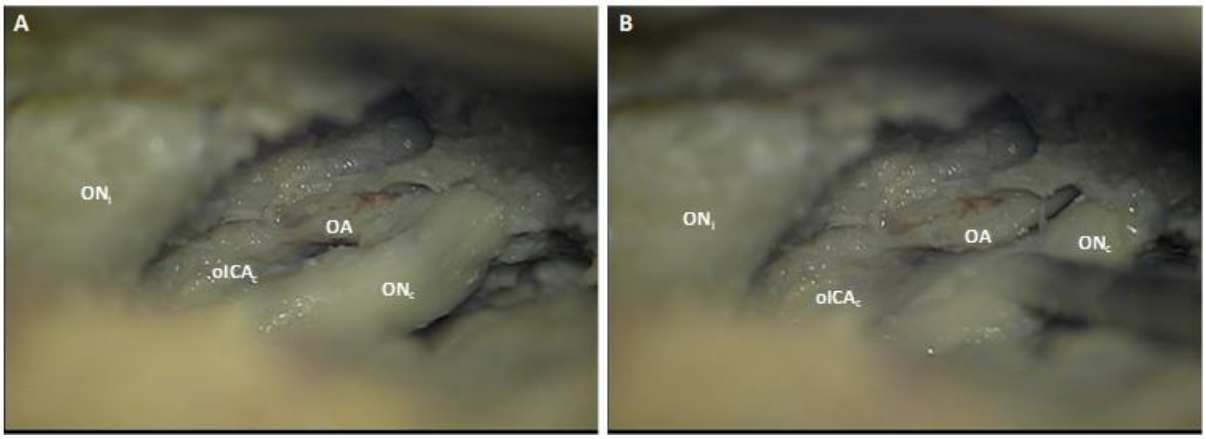

Fig. 34. Exposure of the contralateral internal carotid artery and ophthalmic artery after removal of the surrounding planum sphenoidale and tuberculum sellae (*A, B*). *ON_i,* ipsilateral optic nerve; *ON_c,* contralateral optic nerve; *$oICA_c$,* ophthalmic segment of the contralateral internal carotid artery; *OA,* contralateral ophthalmic artery.

However, our data failed to show that ipsilateral approaches in combination with partial removal of the planum sphenoidale and tuberculum sellae provided clear advantages over contralateral approaches sparing this maneuver.

Some surgeons propose that the lateral part of the tuberculum sellae can be safely drilled and removed as much as needed to mobilize the optic nerve from suprasellar lesions (Metwali 2017, Germanwala 2017). However, the same risks that are mentioned above for anterior clinoidectomy, such as nerve or vascular mechanical or thermal injury, are likewise to be expected when power drills are used on the tuberculum sellae and planum sphenoidale next to the ICA or optic nerve. Furthermore, if this procedure is performed intradurally, it can create a wide opening of the sphenoidal sinus that could be very difficult to seal, and thus increase the risk of CSF fistula. For this reason, surgeons who advocate the removal of the tuberculum sellae, recommend to carefully analyze the pneumatization of the sphenoid sinus preoperatively in bone window CT and, if it is opened intraoperatively, to reconstruct the dura with fat tissue and fibrin glue (Metwali 2017, Germanwala 2017). According to the extent of pneumatization, the sphenoid sinus can be classified in three types: conchal, presellar and sellar (Renn 1975). In the conchal type, the area below the sella is a solid block of bone without any air cavities. In the presellar type, the air cavity does not penetrate beyond a vertical

plane parallel to the anterior sellar wall. The sellar type of sphenoid sinus is the most common, and here the air cavity extends into the body of sphenoid below the sella and as far posteriorly as the clivus (Renn 1975, Rhoton 2002). In adults, 76% of the sphenoid sinus are sellar types and 24 presellar types (Renn 1975). The conchal type is only common in children before the age of 12 years, at which time pneumatization of the sphenoid begins. However, only in the conchal type, the strength of the bone separating the sella from the sphenoid reaches 10 mm or more. In this case the risk of opening the sphenoid sinus when drilling the tuberculum sellae is rather low. In our experience on cadaveric and virtual dissections, drilling of the tuberucum sellae resulted in widely opened sphenoid sinus in all cases.

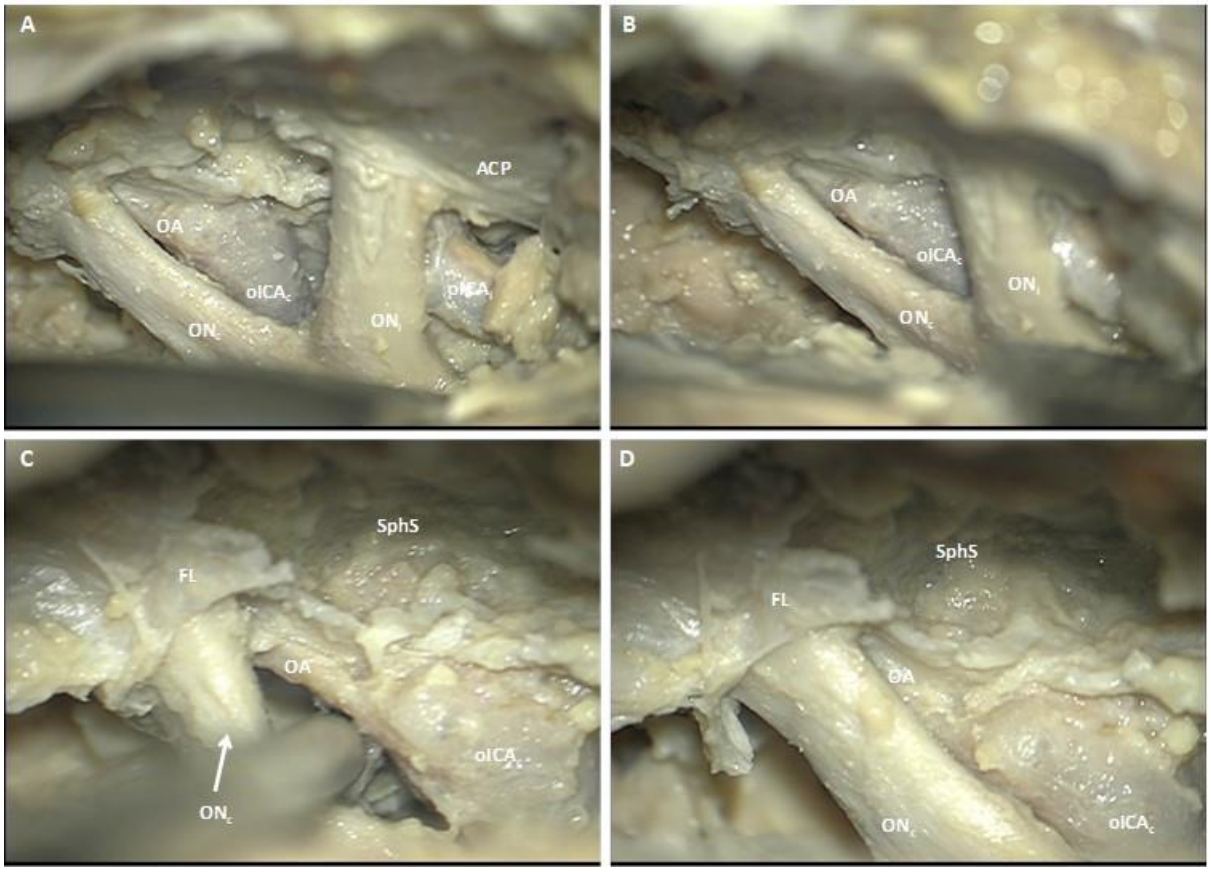

Fig. 35. Exposure of the contralateral internal carotid artery and ophthalmic artery prior (*A,* B) and after (*C, D*) removal of the surrounding planum sphenoidale and tuberculum sellae. As clearly seen in (*C, D*) the cavity of the sphenoidal sinus was widely exposed after opening the planum sphenoidale and tuberculum sellae. *ON$_i$,* ipsilateral optic nerve; *ON$_c$,* contralateral optic nerve; *oICA$_i$,* ophthalmic segment of the ipsilateral internal carotid artery; *oICA$_c$,* ophthalmic segment of the contralateral internal carotid artery; *OA,* contralateral ophthalmic artery; *FL,* falciform dural fold (ligament); *ACP,* ipsilateral anterior clinoid process; *SphS,* sphenoidal sinus.

Most of surgical series on oICA aneurysms using a contralateral approach for clipping did not report of any removal of bone from the tuberculum sellae or planum sphenoidale. However, in the series of Kakizawa et al. (2000) three out of eleven patients with paraclinoid aneurysms which were approached from the contralateral side needed some extent of bone removal around the aneurysm's neck, corresponding to the tuberculum sellae. In these three patients, aneurysms were pointing inferiorly and close to the ICA dural ring. Similar experiences have been reported by other authors, who have only seen the need of partial tuberculum sellae removal in contralateral approaches in cases of aneurysms arising from very close to the carotid cave or pointing deep inferomedially (Nishio 1985, Perneczky 1985, Sheick 2000b). In cases where the sphenoid sinus was opened, interposition of abdominal fat and fibrin glue has been reported to effectively sealing the defect and no cases of CSF fisula have been reported (Nishio 1985, Perneczky 1985, Sheick 2000b).

5.4 The role of optic nerve mobilization on contralateral approaches to the C4 segment of the internal carotid artery

For ipsilateral approaches, optic nerve mobilization was indispensable to expose the oICA superomedial aspect and its branches. As already mentioned above, the two most important branches of the oICA, namely the OA and the SHA, originate from the medial aspect of the ICA. Hence, without mobilization of the optic nerve, the origin of these vessels cannot be seen from a lateral view, respectively an ipsilateral craniotomy (Fries 1997). These findings are in accordance with the recent literature, where the necessity of optic nerve mobilization is often mentioned when approaching the sellar and parasellar region from the ipsilateral side (Kobayashi 1989, Sugita 1985, Chang 2006, Metwali 2017, Germanwala 2017, Salunke 2017, Akabane 1995). Accordingly, the surgical treatment of paraclinoid aneurysms is associated with a relatively higher risk of optic apparatus injuries (Sheikh 2000, Kassam 2007). As shown in our study, anterior clinoidectomy increased the mobility of the optic nerve while simultaneously reducing the need of mobilizing the nerve to maximally expose ICA superomedial aspect. However, anterior clinoidectomy goes with its own risk for thermal and/or mechanic injury of the optic nerve (Sheikh 2000, Kassam 2007). Unexplained visual loss after technically successful clipping of intracranial aneurysms approached ipsilaterally constitutes a real concern since the prognosis

for any recovery of vision in these cases is poor (Rizzo 1995, Zimmermann 1995, Kang 1997, McMahon 2001). Added to clinoidectomy-associated thermal injury, both direct traumatic optic nerve injury as well as occlusion of the OA can be caused by the mobilisation of these neurovascular structures during surgery.

According to our morphometrical measures in cadaveric specimens, a clear advantage of contralateral approaches was the fact that optic nerve mobilization was no prerequisite to sufficiently expose ICA medial wall and its main branches. These findings support surgical experiences of contralateral oICA aneurysm clipping reported in literature (Perneczky 1985, Vajda 1988, Hongo 2009, Chen 2013a, McMahon 2001). Specifically, in the majority of SHA aneurysms, which are typically oriented medially, it is difficult to position the clip around the aneurysmal neck from the ipsilateral side. To achieve this significant mobilization of the optic nerve is required and the risk of postoperative visual deterioration is high (de Jesus 1999). On the contrary, some experienced neurosurgeons have pointed out that by using a contralateral approach, the SHA can be identified under the optic nerve with minimal or no retraction of the overlying optic nerve (Chen 2013a). Consistently with these findings, small surgical series comparing clinical outcomes in patients operated of oICA aneurysms from the ipsilateral or contralateral side have reported that all patients with permanent postoperative visual deficits had been operated via an ipsilateral approach (Fries 1997, Nacar 2014). In the series of Kakizawa et al. in contrast, no visual deficits occurred among the 11 patients operated through a contralateral approach (Kakizawa 2000).

Although there is lack of detailed knowledge about the exact duration and amount of mobilisation that the optic nerve can tolerate during surgery, literature suggests that light and gentle mobilization may be performed without any visual impairment (Chang 2006, Metwali 2017, Germanwala 2017). Alterations on visual evoked potentials have been described during optic nerve mobilisation, although these changes not indicate permanent visual impairment in all cases (Akabane 1995). Independently of the approach selected, authors agree that optic nerve and OA mobilization should be avoided or at least the falciform dural fold should be opened to release the nerve before manipulation (Akabane 1995, Fries 1997, Oshiro 1997, Hong 2009, Chang 2006, Clatterbruck 2005, Germanwala 2017). That can be achieved in ipsi- and contralateral approaches (Oshiro 1997, Clatterbruck 2005).

5.5 The extent of the relative interoptic traiangle is determinant for the accessibility to the oICA using a contralateral approach

The interoptic space defines the way to access the C4 segment of the ICA when using a contralateral approach. Therefore, the determination of interoptic space's extension is crucial while considering approaching the oICA from the contralateral side (Yameda 1984, Fries 1997, Oshiro 1997, Kakizawa 2000). The apex of the interoptic triangle is limited by the confluence of both optic nerves into the chiasm, while the base is defined by the tuberculum sellae and planum sphenoidale linking both optic foramina, also named chiasmatic groove (Rhoton 2002). Therefore, the relationship of the chiasm to the sella and tuberculum sellae is an important determinant of the interoptic triangle's area and space through which the contralateral ICA can be approached. Most commonly, the chiasm overlies the diaphragma sellae and the pituitary gland, a prefixed chiasm is situated over the tuberculum and a postfixed chiasm over the dorsum sellae. According to older anatomic studies, in approximately 70% of the cases the chiasm is in the normal position and approximately the half of the remaining 30% are in prefixed respectively postfixed position (Renn 1975). All of our cadaveric specimens and virtual subjects presented a normal position of the chiasm.

Although the importance of the interoptic space's width to determine the accessibility to the contralateral oICA has been specially remarked previously (Kakizawa 2000, Oshiro 1997), these studies have not considered that the approach angle to the contralateral oICA is not orthogonal to the interoptic space's axis. In surgical practice the workspace available to the surgeon is smaller. Hence, after having determined in each case the optimal approach angle and trajectory through the interoptic space to the contralateral lCA, we calculated the interoptic triangle's area presented to surgeon's microscope and analysed its morphometry in regard of the exposure of the contralateral ICA and its branches. The area of this relative (orthogonal to the surgeons view) interoptic triangle correlated significantly with the accessibility and exposure of the contralateral oICA and it branches. These findings corroborate the surgical experience that sufficient interoptic space is required for the treatment of ICA pathology using a contralateral approach (Oshiro 1997, Clatterbruck 2005). The

opening of the falciform ligament above the contralateral optic nerve is a further indispensable step when manipulation the contralateral ICA, the OA and the optic nerve. It helps to avoid optic nerve injury from the sharp edge of this fold if the nerve is displaced superiorly and laterally (Oshiro 1997, Clatterbruck 2005). Furthermore, in order to evaluate the accessibility to the contralateral ICA through the interoptic triangle, the individual anatomy in relation to the optimal approach trajectory must be carefully considered preoperatively. The 3D virtual reality system dextroscope allowed us to determine the optimal contralateral approach trajectory in each individual subject and simultaneously visualize the 2-dimensional interoptic triangle's projection to surgeon's view, enabling us to determine the accessibility to the contralateral ICA and its branches in practical (surgical) terms.

5.6 Surgical applications of contralateral approaches to the oICA

Aneurysms arising from the oICA frequently point medially. This corresponds with two anatomical key features, namely the fact that the OA and the SHA arise usually from oICA's medial aspect and the limit posed by the anterior clinoid process on the lateral side. The very same anatomical key features, added to the close relationship of OA and the optic nerve superiorly, however likewise limit the accessibility of paraclinoid aneurysms via an ipsilateral approach.

Some experienced neurosurgeons have proposed the contralateral approach for paraclinoid aneurysms, since the anatomy of the paraclinoid region can be best seen from the contralateral side (van Lindert 1998, de Oliveira 1996, Fries 1997, Nakao 1981, Nishio 1985, Perneczky 1985, Shiokawa 1988, Vajda 1988). To date contralateral approaches for aneurysm clipping has been mostly applied in selected cases in the context of bilateral intracranial aneurysms of the anterior circulation as well as in the presence of aneurysms arising from the oICA medial wall with very good obliteration rates and clinical results (Nakao 1981, Milenkovic 1982, Yamada 1984, Nishio 1985, Shiokawa 1988, Vajda 1988, Oshiro 1997, Fries 1997, Kakizawa 2000, Sheick 2000b, Hongo 2001, McMahon 2001, Pereira 2006, Park 2009, Chandela 2011, Chen 2013a, Nacar 2014, Andrade-Barazarte 2015, Yu 2017). Contralateral approaches are considered feasible in selected cases of bilateral and mirror intracranial aneurysms, given its high frequency up to 9 – 10% of the cases (Campos 1998, Porter 2001, Andrade-Barazarte 2015), that can rise to

48.5 – 50% for carotid-ophthalmic aneurysms (Yasargil 1984, Andrade-Barazarte 2015). In this context, it has been shown that clipping multiple aneurysms through a unilateral craniotomy decreases the bleeding risk and the rate of complications related to multiple craniotomies as well as reduces length hospital of stay and costs (McMahon 2001, Inci 2012, Rodriguez-Hernandez 2012, Clatterbuck 2005).

However, the decision of whether the oICA should be approached from the ipsilateral or contralateral side is mostly determined by aneurysm characteristics as well as individual skull base anatomy of the patients. The aneurysm anatomy, independently of other factors plays an important role on whether the contralateral approach may be feasible or not. Most authors agree that the aneurysm dome must project medially, superiorly, superomedially or inferomedially to allow clipping from the contralateral side (de Oliveira, Clatterbuck 2005, Hong 2009, Nishio 1985, Rajesh 2010, Nacar 2014). Aneurysms arising from the lateral wall of the ophthalmic segment and projecting superolaterally or laterally should be approached via an ipsilateral craniotomy, due to the risk of optic nerve damage and poor visualization of the aneurysm (Andrade-Barazarte 2015). Additionally, most works agree that the aneurysm size should be less than 10 to 15 mm for safe clipping from the contralateral side (McMahon 2001, Kakizawa 2000, Yasargil 1984, Fries 1997, Andrade-Barazarte 2015, Hong 2009). Larger aneurysms may require complex surgical techniques, which may be dangerous especially considering the long surgical trajectory of a contralateral route, additionally they may require extreme mobilization of the contralateral optic nerve and thus increasing the risk of visual deficits. Nevertheless, some authors have reported effective obliteration of giant aneurysms with good clinical outcomes through a contralateral approach, without retracting the optic nerve and sparing of the anterior clinoid process and tuberculum sellae if the aneurysm projected medially and featured a small neck (Hongo 2001). Another important factor is aneurysm's shape. According to most authors, only saccular aneurysms with simple configurations make their clipping straightforward, using the contralateral approach (de Oliveira 1996, Clatterbuck 2005, Rajesh 2010, Andrade-Barazarte 2015).

On the other hand, patient's skull base anatomy, independently of aneurysm's morphology can be determinant for selecting an ipsilateral or contralateral approach to the oICA. While considering a contralateral approach to the oICA, the surgeon

must be aware of potential risks of injuring the optic apparatus. Our results show that the main point determining the accessibility to the contralateral ICA and its branches is the relative interoptic space's area. Several surgeons stated that, in their experience, aneurysm clipping from the contralateral side was feasible at lower risk of visual deficits compared to ipsilateral approaches, if an adequate workspace between both optic nerves exist (Fries 1997, McMahon 2001, Andrade-Barazarte 2015). In agreement with our results, previous series have reported technical difficulties during the clipping of oICA aneurysms approached contralaterally if the interoptic space is small or the chiasm is prefixed (Yasargil 1984, Nishio 1985, Oshiro 1997, Chen 2013a). Other authors have pointed out that the median prechiasmatic distance (considered from the anterior border of the chiasm to the tuberculum sellae) of 5.7 mm and a median interoptic distance (calculated between the medial aspect of both optic nerves at the entrance to the optic canal) of 10.5 mm renders the contralateral clipping technique possible (Andrade-Barazarte 2015). These findings confirm prior observations reporting the feasibility of the contralateral approach for oICA aneurysms in patients with a prechiasmatic distance of at least 5.4 mm and an interoptic distance of 10.4 mm (Kakizawa 2000).

In the present work, we confirm and extended this knowledge by proposing the concept of the `relative' interoptic triangle. The ICA is not a midline structure, it is located laterally from the sagittal axis line of the interoptic triangle (a line linking the confluence from both optic nerves into the chiasm with tuberculum sellae's midline point). Hence, to maximally visualize the oICA from contralateral side, an angulation and displacement with respect to the midline is needed. As a consequence, the more opened the angle, the more tangential becomes the trajectory line to the interoptic space and the two-dimensional projection of the triangle's area seen from the surgeons's view decreases. Therefore, considering the interoptic triangle's area with regard to the most optimal approach angle to the contralateral oICA provides a more accurate idea about the workspace available between both optic nerves to access the oICA contralaterally during surgery. This does not replace but rather complements the information about absolute interoptic space morphometry cited above. To accomplish this assessment in clinical practice, a 3-D virtual reality software for surgery planning such as the dextroscope® is of invaluable use (Fries 1997, Kockro 2016).

According to surgical reports, and given anatomical conditions, clipping of a contralateral aneurysm is possible in 95 and 97% of cases. In an illustrative case from our department we can observe that successful clipping of a medially pointing paraclinoidal aneurysm can be achieved even via a minimally invasive supraorbital approach if the patient's and aneurysm anatomy are carefully assessed preoperatively *(Figures 36 and 37)*. Possible problems include arachnoid adhesions surrounding the neck of the aneurysm or a more complex aneurysm shape than expected (Vajda 1988, Fries 1997, Oshiro 1997, Andrade-Barazarte 2015). Furthermore, removal of the anterior clinoid process and opening of the distal dural ring, essential for the ipsilateral approach, are not required during contralateral approaches which might prevent bleeding from the cavernous sinus, besides contralateral approaches require usually a shorter operation time (Kakizawa 2000).

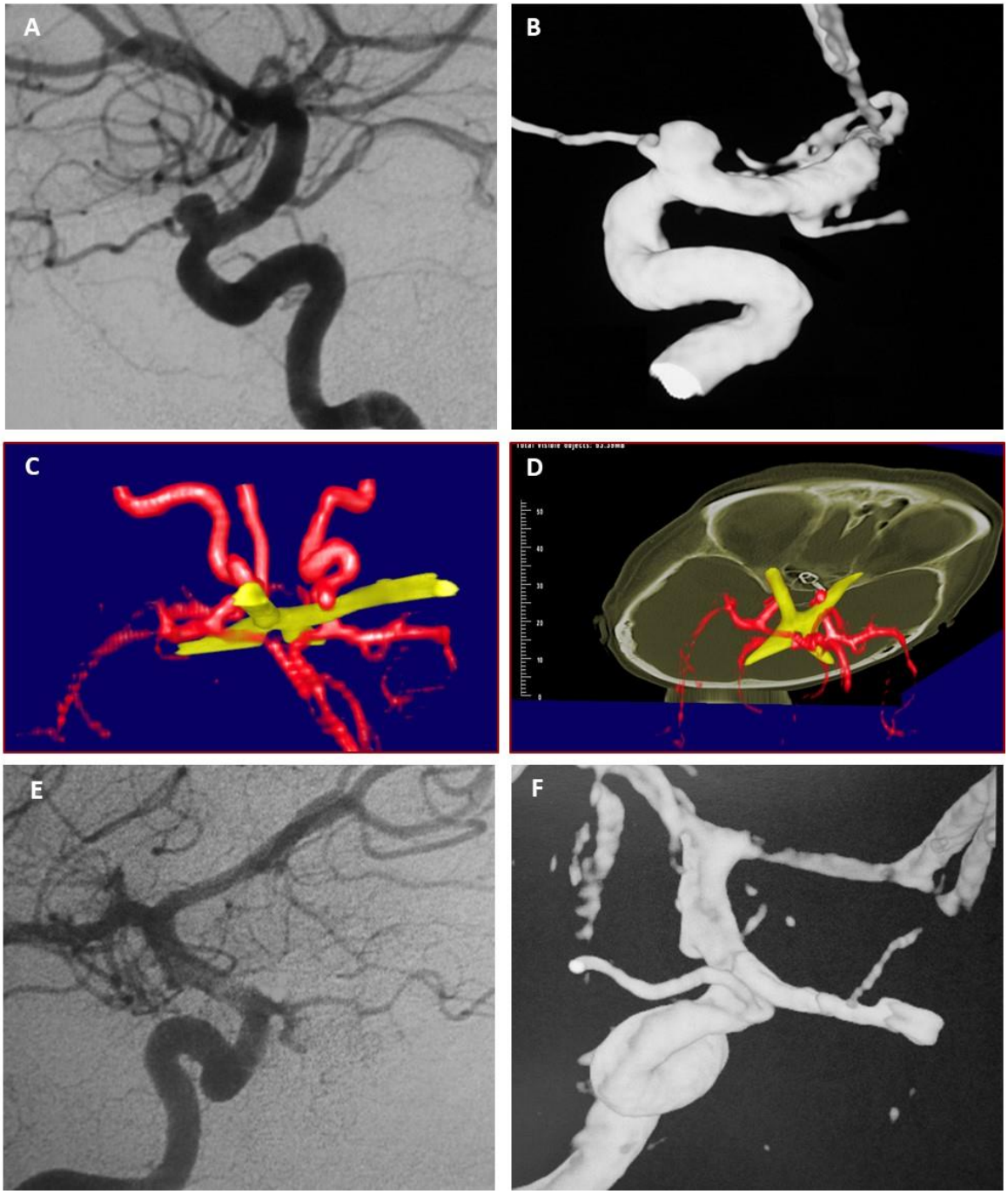

Fig. 36. An illustrative surgical case of a 41 year old woman presenting in our department with a scotoma of the right visual field caused by a medially pointing left paraclinoid aneurysm, as demonstrated in preoperative angiograms *(A, B)*. A 3D reconstruction of the optic apparatus and ist relationship with vascular structures was performed in a virtual workspace to plan the most optimal surgical approach *(C, D)*. After a careful evaluation of patient‘s and aneurysm anatomy we decided to approach the aneurysm from the contralateral side. This detailed anatomical assessment enabled us to accomplish aneurysm clipping in a minimally invasive way, using a contralateral endoscopic assisted supraorbital keyhole approach. Postoperative angiograms showed a complete aneurysm occlusion *(E, F)* and the patient recovered without adding neurological deficits or other complications.

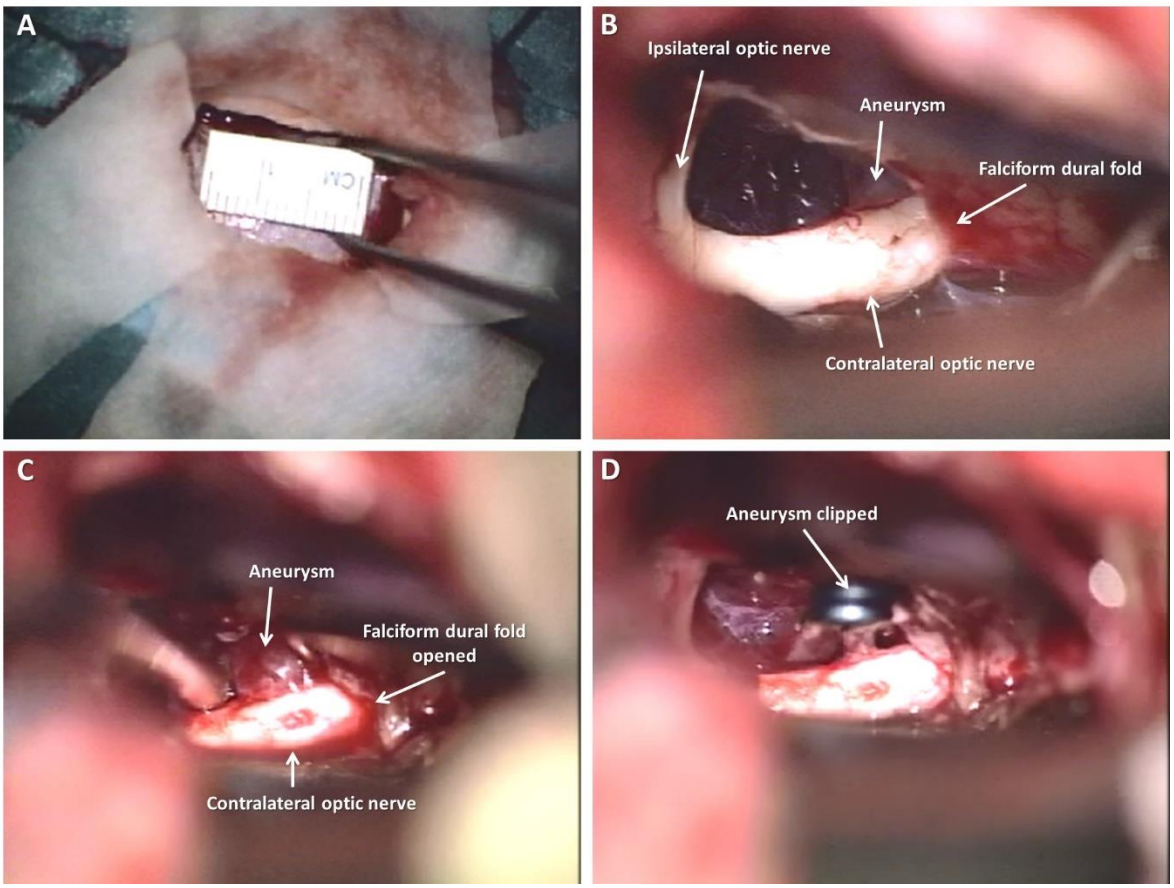

Fig. 37. Intraoperative captures showing contralateral clipping of a paraclinoid carotid aneurysm in our illustrative case *(Video available upon request)*. A supraorbital craniotomy was performed *(A)* and dissection proceeded straightforwart towards the optic apparatus. The aneurysm dome could be fully exposed through the space between both optic nerves and unroofing the contralateral optic canal enabled the minimally needed gentle and safe mobilization of the contralateral optic nerve to completely expose aneurysm's dome and neck *(B, C).* Aneurysm clipping could be performed succesfully *(D)*.

5.7 Anatomical and surgical limitations and pitfalls of contralateral approaches to the oICA

The surgical limitations of contralateral approaches to the oICA in comparison to ipsilateral ones are the need of mobilizing the olfactory nerve, working in a target area located deeper, the risk of opening the frontal sinus and difficulties to achieve proximal vascular control, particularly in clinoid segment aneurysms.

To contralaterally approach the oICA, the subfrontal/supraorbital route required the mobilization and in a few cases the sacrifice of the olfactory nerve on craniotomy's side in our cadaveric study. Due to limited image resolution it was not possible to

dissect the olfactory nerve from the brain using the dextroscope, so that we could not replicate the observations made in cadaveric specimens in our virtual surgical simulations. The trans-Sylvian trajectory to approach the oICA ipsilaterally does not present this limitation, since the minimal olfactory nerve mobilisation accompanies the slightly retraction of the frontal lobe.

Obviously, the sacrifice of the olfactory nerve leads invariably to unilateral loss of function. It has been reported that quantitative olfactory disorders can have an impact on the quality of patient's life, leading in some cases to weight loss or depression, but especially after complete bilateral loss of olfactory function (Deems 1991, Miwa 2001, Blomqvist 2004, Temmel 2002). In addition, complete olfactory loss can be associated with a markedly increased risk of exposure to hazardous events in every-day living, such as intake of spoilt food, burning of meat etc. (Santos 2004), although patients with post-traumatic anosmia have been shown to acquire an elevated gustatory threshold, which tends to compensate the deficit (Hummel 2001). Furthermore, the olfactory nerve has a remarkable capacity for neural regeneration and recovery following injury, especially if nerve's continuity is respected (Kobayashi 2009). There is lack of clinical evidence to establish the amount of mobilization that the olfactory nerve can tolerate during surgery and its quantitative functional consequences. According to our results, if gentle mobilization of the olfactory nerve is applied, the continuity of the nerve can be respected in the majority of cases while approaching the oICA contralaterally and olfaction should therefore not be impaired permanently. Nevertheless, the true impact of contralateral approaches to the oICA segment on olfactory function has not been studied in detail. In the context of unilateral approaches to bilateral aneurysms of the MCA, rates of hyposmia and anosmia were 8 and 13 % respectively (Andrade-Barazarte 2015b, Cho 2017). In the series of Yu et al. (2017), the rate of hyposmia following contralateral approaches to different aneurysm locations was 6.3%. Park et al. studied the risk of olfactory nerve dysfunction after contralateral approaches for aneurysm clipping in 12 patients, finding that rates of hyposmia and anosmia were 17% and 42% respectively (Park 2009). However, the precise aneurysm location was not reported for patients presenting olfactory dysfunction postoperatively. In this work, only 2 of the patients approached contralaterally presented oICA aneurysms, the other 10 patients had either ICA bifurcation or proximal and bifurcation MCA

aneurysms. This constitutes a relevant aspect, because contralateral approaches to more distal anterior vessel segments, such as the ICA bifurcation, ACA or MCA, require the placement of a self-retaining retractor on the inferior surface of both frontal lobes, submitting both olfactory nerves to risk of injury (Park 2009, Cho 2017). Contralateral approaches to the clinoid and oICA (the most proximal portion of the C4-carotid segment) require the mobilization of only one olfactory nerve, so that the likelihood of contralateral damage and complete loss of olfaction remains low and surgical studies do not explicitly report this issue as a frequent postoperative concern.

The possibility of frontal sinus opening with the theoretical risk of CSF fistula, mucocele and meningitis must be considered prior to performing a contralateral approach to the oICA (Meetze 2004). We observed frontal sinus opening in 25% of the cadaveric dissections and 30% of virtual cases. In our study, we extended standardly the pterional craniotomy anteriorly up to the supraorbital foramen independently of the extent of pneumatisation of the frontal sinus. Taking into account that the optimal approach angle measured in both cadaveric and virtual dissections to the contralateral oICA was about 17 ± 5° anterior to the keyhole-clinoid reference line, the anterior extension of the craniotomy can be significantly reduced without restricting approach's effectiveness and adapting it to individual frontal sinus pneumatization observed in preoperative CT to avoid its opening.

If preoperative planning is done considering this anatomical feature and avoiding sinus opening, the likelihood to induce related complications is low (van Lindert 1998). Even in the case of unintentional frontal sinus exposure during craniotomy, cranialization and sinus obliteration can be performed prior to dura incision. In surgical series of contralateral approaches to intracranial aneurysms, there are no explicit mentions regarding frontal sinus opening.

One of the major concerns of contralateral approaches to the oICA is the way to achieve proximal arterial control in case of intraoperative aneurysm rupture (Fries 1997, Chen 2013a, Aheikh 2000b, Andrade-Barazarte 2015, Spetzler 2011). Due to patient's positioning for a contralateral approach, the cervical ICA is located away from the surgical field, so that cervical carotid compression or ligation is not possible with the head fixed in the Mayfield clamp. The same applies to the exposure of ICA

petrous segment. Therefore, proximal control requires the implementation of other techniques. In case of aneurysms arising distally to the clinoid ICA, the resection of the distal dural ring of the ICA can be performed without causing major bleeding from the cavernous sinus and exposing an additional proximal segment of the ICA about 3 to 4 mm in length, which is often sufficient for achieving proximal arterial control of the ophthalmic segment (Fries 1997). For more proximally located aneurysms, balloon occlusion of the ICA in the cervical or petrous segment can be performed (Fries 1997, Chen 2013a, Sheikh 2000b). Other experienced cerebrovascular surgical teams have used adenosine-induced transitory cardiac arrest in selected cases to soften the aneurysm for safe clip placement without proximal temporary clipping, reporting no complications and excellent clinical and surgical outcomes (Luostarinen 2010, Andrade-Barazarte 2015). Finally, the use of the radiolucent Sugita head frame, which enables head rotation to easily gain contralateral cervical carotid exposure and then change head position for the craniotomy and intraoperative angiography has been reported (Chandela 2011). Anyway, since contralateral approaches are planned for unruptured aneurysms and a careful patient selection is done according to individual skull base and aneurysm anatomy, intraoperative rupture of the aneurysm approached from the contralateral side is an extreme rare event in surgical series. The only such case reported in literature is a 48-year-old woman who was intervened due to a ruptured left MCA aneurysm and during aneurysm dissection, a contralateral previously unruptured carotid-ophthalmic aneurysm suddenly ruptured, so that the surgeons were forced to clip the contralateral aneurysm first (Milenkovic 1982).

6. Schlussfolgerung

Bezüglich der Hauptfragen dieser Dissertation, die in der Einleitung formuliert wurden, können wir folgende Schlussfolgerungen ziehen:

Wir haben festgestellt, dass sich die optimalen Trajektorien zur Darstellung der medialen Wand der oICA bei kontralateralen und ipsilateralen Zugängen deutlich unterscheiden. Die beste Exposition der oICA wird bei ipsilateralen Zugängen durch einen Zugangswinkel hinter der Keyhole-Clinoid-Linie erreicht. Im Gegenteil dazu wird die kontralaterale oICA durch einen Zugangswinkel vor der Keyhole-Clinoid-Linie optimal dargestellt. Diese Feststellung ist wichtig für für die chirurgische Behandlung paraclinoidaler Aneurysmen. Erstens profitieren ipsilaterale Zugänge von pterionalen Kraniotomien mit ausreichender Exposition der Sylvischen Fissur, da nur durch die Eröffnung dieser Fissur (transsylvianer Zugang) der optimale Zugangswinkel erreicht werden kann. Bei kontralateralen Zugängen ermöglicht eine subfrontale Trajektorie eine optimale Darstellung, ohne dass die sylvische Fissur eröffnet werden muss. Demnach profitieren kontralateralen Zugänge von vorderen und begrenzten supraorbitalen oder frontolateralen Kraniotomien. Zweitens, kann bei kontralateralen Zugängen auf eine breite Öffnung Sylvischen Fissur, die ihrerseits wieder mit einer erhöhten Morbidität verbunden ist, verzichtet werden. Allerdings wird bei kontralateralen Zugängen eine vermehrte Mobilisierung des Nervus olfactorius und ein Abschleifen des Orbitadachs zur Reduktion der Frontallappen-Retraktion benötigt.

Die vorgelegte Studie erbrachte eine detallierte und ausführliche morphometrische und anatomische Charakterisierung der ipsilateralen und kontralateralen Zugänge zu der oICA. Zusammenfassend kann geschlussfolgert werden, dass kontralaterale Zugänge im Vergleich zu ipsilateralen Zugängen tatsächlich eine bessere Exposition der medialen Wand der oICA und ihre perforierenden Äste, der OA und der SHA ermöglichen. Diese chirurgischen Vorteile bestehen auch nach der Resektion des Procesus clinoideus anterior weiter. Vorausgesetzt, dass die kontralaterale Zugangstrajektorie sorgfältig geplant wurde und das Fenster zwischen beiden Nervi opticii eine ausreichende Breite aufweist, wird die notwendige Retraktion des Nervus opticus bei kontralateralen Zugängen deutlich reduziert.

Die Darstellung der oICA wird bei ispilateralen Zugängen durch die Entfernung des Processus clinoideus anterior eindeutig verbessert. Aus morphometrischer Sicht ist dieses Manöver zum Erreichen einer guten Exposition sogar unverzichtbar. Allerdings ist das Entfernen des Processus clinoideus anterior mit dem Risiko einer Verletzung der oICA und OA sowie des Nervus opticus verbunden. Daher ist es einer der deutlichen Vorteile des kontralateralen Zugangs, dass dieses Mannöver entfällt.

Obwohl das Entfernen des Planums sphenoidale/Tubercullum sellae und die Mobilisierung des kontralateralen Nervus opticus das Arbeitsfenster zwischen beiden Nervi opticii erweitern und die Darstellung der kontralateralen oICA sowie ihre Äste dadurch verbessert wird, werden beide Manöver in der Regel für nicht benötigt um die meisten Pathologien zu erreichen. Die mit diesen Mannövern einhergehenden Risiken sollten daher sorgfältig gegen die Vorteile einer noch weiter verbesserten Exposition abgewogen werden.

Die Darstellbarkeit der kontralateralen oICA und ihrer Äste wird durch das interoptischen Dreiecks determiniert. Allerdings ist hier die sich dem Chirurgen bietende Ansicht des Dreiecks nicht dessen maximale anatomische Fläche von Bedeutung, die wiederum vom gewählten Zugang abhängt. Aus diesem Grund ist die genaue präoperative Evaluierung der relevanten (also der auf den Zugangsweg des Chirurgen projezierten) Fläche, die in dieser Arbeit als rIOT-Fläche definiert wurde, von größter Bedeutung. Ein virtuelles 3D-Planungstool, wie das in dieser Studie angewendete Dextroscope®, erleichtert diese Analyse deutlich.

Conclusions

Concerning the main questions of the thesis, as formulated in the introduction section of this thesis, we can conclude the following:

We have demonstrated that the optimal trajectory to the medial wall of the oICA differs significantly between contralateral and ipsilateral approaches. The greatest exposure of the oICA using an ipsilateral approach is obtained through posterior angles to the keyhole-clinoid line. On the contrary, the contralateral oICA is better exposed though trajectories passing with anterior angles to the keyhole-clinoid line. These findings have implications for the surgery of paraclinoid aneurysms. Firstly, ipsilateral approaches will benefit from proper pterional craniotomies with sufficient exposure of the Sylvian fissure, since the opening and dissection of this fissure (transsylvian route) takes the major advantages of ipsilateral approaches to expose the oICA. For contralateral approaches, a subfrontal route allows the optimal oICA exposure, without the need of Sylvian fissure dissection. In this regard, contralateral approaches benefit from more anterior and restricted supraorbital or frontolateral craniotomies. Secondly, while the attempt of maximal oICA exposure through ipsilateral approaches implies the difficulties and risks of a wider Sylvian fissure dissection, contralateral approaches spare Sylvian fissure opening, but require a greater olfactory nerve mobilisation as well as smoothing the orbit roof to reduce the amount of frontal lobe retraction.

Our study provided detailed morphometric and anatomical characterization of ipsilateral and contralateral approaches to the oICA. Summarizing our morphometric findings we can conclude that contralateral approaches provide a greater exposure of oICA's medial wall and its perforant branches, the OA and the SHA compared to ipsilateral approaches. This advantage remains even after removal of the ipsilateral anterior clinoid process. It helps to reduce optic nerve mobilization, if the trajectory is correctly planed and the window between both optic nerves is wide enough.

The exposure of the oICA is significantly increased by removing the anterior clinoid process. From a morphometric view, this manoeuvre is required to gain a greater access to the medial wall of the ipsilateral oICA and the OA during ipsilateral approaches. However, it goes with a certain risk of vessel or optic nerve lesion. In

these terms, sparing of anterior clinoidectomy can be regarded as an advantage of contralateral approaches when targeting the oICA and its branches.

Although the removal of the contralateral half of the planum sphenoidale and tuberculum sellae as well as optic nerve mobilization enhance the workspace between both optic nerves and contribute to increase the exposure of the contralateral oICA and its branches, this is usually not required and the risks and possible complications associated to these manoeuvres should be carefully pondered against their eventual benefits.

The accessibility to the contralateral oICA and its branches is definitelly determined by the area of the interoptic triangle´s projection in the surgeon's microsurgical view (rIOT). Therefore, the preoperative assessment of the rIOT-area is of importance when considering a contralateral approach to the oICA and related structures. Further, a virtual 3D planning tool, like the Dextroscope® applied in this study, greatly facilitates this assessment.

7. Conflicts of interest

The author and supervisors of this work certify that they have NO affiliations with or involvement in any organization or entity with any financial interest in the subject matter or materials discussed in this manuscript.

8. References

Akabane, A., K. Saito, Y. Suzuki, M. Shibuya and K. Sugita (1995). "Monitoring visual evoked potentials during retraction of the canine optic nerve: protective effect of unroofing the optic canal." J Neurosurg 82(2): 284-287.

al-Rodhan, N. R., D. G. Piepgras and T. M. Sundt, Jr. (1993). "Transitional cavernous aneurysms of the internal carotid artery." Neurosurgery 33(6): 993-996; discussion 997-998.

Andrade-Barazarte, H., J. Kivelev, F. Goehre, B. R. Jahromi, F. Hijazy, N. Moliz, A. Gauthier, R. Kivisaari, J. E. Jaaskelainen, H. Lehto and J. A. Hernesniemi (2015). "Contralateral Approach to Internal Carotid Artery Ophthalmic Segment Aneurysms: Angiographic Analysis and Surgical Results for 30 Patients." Neurosurgery 77(1): 104-112; discussion 112.

Barami, K., V. S. Hernandez, F. G. Diaz and M. Guthikonda (2003). "Paraclinoid Carotid Aneurysms: Surgical Management, Complications, and Outcome Based on a New Classification Scheme." Skull Base 13(1): 31-41.

Batjer, H. H., T. A. Kopitnik, C. A. Giller and D. S. Samson (1994). "Surgery for paraclinoidal carotid artery aneurysms." J Neurosurg 80(4): 650-658.

Blomqvist, E. H., A. Bramerson, P. Stjarne and S. Nordin (2004). "Consequences of olfactory loss and adopted coping strategies." Rhinology 42(4): 189-194.

Boari, N., A. Spina, L. Giudice, F. Gorgoni, M. Bailo and P. Mortini (2017). "Fronto-orbitozygomatic approach: functional and cosmetic outcomes in a series of 169 patients." J Neurosurg: 1-9.

Campos, C., A. Churojana, G. Rodesch, H. Alvarez and P. Lasjaunias (1998). "Multiple Intracranial Arterial Aneurysms: A Congenital Metameric Disease? Review of 113 Consecutive Patients with 280 AA." Interv Neuroradiol 4(4): 293-299.

Chandela, S., S. Chakraborty, G. M. Ghobrial, A. Jeddis, C. Sen and D. J. Langer (2011). "Contralateral mini-craniotomy for clipping of bilateral ophthalmic artery aneurysms using unilateral proximal carotid control and Sugita head frame." World Neurosurg 75(1): 78-82; discussion 41-72.

Chandela, S., S. Chakraborty, G. M. Ghobrial, A. Jeddis, C. Sen and D. J. Langer (2011). "Contralateral mini craniotomy for clipping of bilateral ophthalmic artery aneurysms using unilateral proximal carotid control and sugita head frame." World neurosurgery 75(1): 78-82.

Chang, D. J. (2009). "The "no-drill" technique of anterior clinoidectomy: a cranial base approach to the paraclinoid and parasellar region." Neurosurgery 64(3 Suppl): ons96-105; discussion ons105-106.

Chang, H. S., M. Joko, J. S. Song, K. Ito, T. Inoue and H. Nakagawa (2006). "Ultrasonic bone curettage for optic canal unroofing and anterior clinoidectomy. Technical note." J Neurosurg 104(4): 621-624.

Chen, S., Y. Kato, A. Kumar, R. Sinha, D. Oguri, J. Oda, T. Watabe, S. Imizu, H. Sano and Y. Hirose (2013a). "Contralateral approach to unruptured superior hypophyseal artery aneurysms." J Neurol Surg A Cent Eur Neurosurg 74(1): 18-24.

Chen, Z., Y. Yang, H. Miao, F. Li, J. Zhang, H. Feng and G. Zhu (2013b). "Experiences and complications in endovascular treatment of paraclinoid aneurysms." J Clin Neurosci 20(9): 1259-1263.

Cho, M. J., C. W. Oh, O.-K. Kwon, H. S. Byoun, S. U. Lee, T. Kim, Y. S. Chung, S. P. Ban and J. S. Bang (2017). "Comparison of Unilateral and Bilateral Craniotomy for the Treatment of Bilateral Middle Cerebral Artery Aneurysms: Anatomic and Clinical Parameters and Surgical Outcomes." World neurosurgery 108: 627-635.

Clatterbuck, R. E. and R. J. Tamargo (2005). "Contralateral approaches to multiple cerebral aneurysms." Neurosurgery 57(1 Suppl): 160-163; discussion 160-163.

Day, A. L. (1990). "Aneurysms of the ophthalmic segment. A clinical and anatomical analysis." J Neurosurg 72(5): 677-691.

De Jesús, O., L. N. Sekhar and C. J. Riedel (1999). "Clinoid and paraclinoid aneurysms: surgical anatomy, operative techniques, and outcome." Surgical neurology 51(5): 477-488.

de Oliveira, E., H. Tedeschi, M. G. Siqueira, M. Ono, C. Fretes, A. L. Rhoton, Jr. and D. A. Peace (1996). "Anatomical and technical aspects of the contralateral approach for multiple aneurysms." Acta Neurochir (Wien) 138(1): 1-11; discussion 11.

Deems, D. A., R. L. Doty, R. G. Settle, V. Moore-Gillon, P. Shaman, A. F. Mester, C. P. Kimmelman, V. J. Brightman and J. B. Snow, Jr. (1991). "Smell and taste disorders, a study of 750 patients from the University of Pennsylvania Smell and Taste Center." Arch Otolaryngol Head Neck Surg 117(5): 519-528.

Dolenc, V. V. (1985). "A combined epi- and subdural direct approach to carotid-ophthalmic artery aneurysms." J Neurosurg 62(5): 667-672.

Fries, G., A. Perneczky, E. van Lindert and F. Bahadori-Mortasawi (1997). "Contralateral and ipsilateral microsurgical approaches to carotid-ophthalmic aneurysms." Neurosurgery 41(2): 333-342; discussion 342-333.

Fujii, K., C. Lenkey and A. L. Rhoton, Jr. (1980). "Microsurgical anatomy of the choroidal arteries: lateral and third ventricles." J Neurosurg 52(2): 165-188.

Gelber, B. R. and T. M. Sundt, Jr. (1980). "Treatment of intracavernous and giant carotid aneurysms by combined internal carotid ligation and extra- to intracranial bypass." J Neurosurg 52(1): 1-10.

Germanwala, A. V., R. Hofler, C. Lagman, L. K. Chung, A. A. Khalessi, G. Zada, Z. A. Smith, N. S. Dahdaleh, A. M. Bohnen, J. M. Cho, C. B. Colen, E. Duckworth, P. Kan, S. Lam, C. Y. Kim, G. Li, M. Lim, J. H. Sherman, V. Y. Wang and I. Yang (2017). "Neurosurgery concepts: Key perspectives on endoscopic versus microscopic resection for pituitary adenomas, surgical decision-making in tuberculum sellae meningiomas, optic nerve mobilization during resection of craniopharyngiomas, and evaluation of headache and quality of life after endoscopic transphenoidal surgery for pituitary adenomas." Surg Neurol Int 8: 52.

Giannotta, S. L. (2002). "Ophthalmic segment aneurysm surgery." Neurosurgery 50(3): 558-562.

Gibo, H., C. Lenkey and A. L. Rhoton, Jr. (1981). "Microsurgical anatomy of the supraclinoid portion of the internal carotid artery." J Neurosurg 55(4): 560-574.

Harris, F. S. and A. L. Rhoton (1976). "Anatomy of the cavernous sinus. A microsurgical study." J Neurosurg 45(2): 169-180.

Hassoun-Turkmani, A. (2016). Microsurgery of paraclinoid aneurysms. Neurological Surgery 7th Edition. Youmans and Winn. 4: 3298-3306.

Hayreh, S. (1974). The ophthalmic artery. Section I. Normal gross anatomy. Radiology of the Skull and Brain. D. G. P. T. H., Mosby, St. Louis. II, Book 2: Arteries: 1333-1350.

Hayreh, S. and R. Dass (1962). "The ophthalmic artery. I. Origin and intracranial and intra-canalicular course." Brit. J. Ophthal 46: 65-98.

Heros, R. C. (2002). "Anterior paraclinoid aneurysms." J Neurosurg 96(6): 981-982; discussion 982.

Hong, T. and Y. Wang, Unilateral approach to clip bilateral multiple intracranial aneurysms. Surg Neurol, 2009. 72 Suppl 1: p. S23-8; discussion S28.

Hongo, K., N. Watanabe, N. Matsushima and S. Kobayashi (2001). "Contralateral pterional approach to a giant internal carotid-ophthalmic artery aneurysm: technical case report." Neurosurgery 48(4): 955-959.

Hummel, T., C. Nesztler, S. Kallert, G. Kobal, M. Bende and S. Nordin (2001). "Gustatory sensitivity in patients with anosmia." Chem Senses 26: 118.

Huynh-Le, P., Y. Natori and T. Sasaki (2004). "Surgical anatomy of the anterior clinoid process." J Clin Neurosci 11(3): 283-287.

Inci, S., A. Akbay and T. Ozgen (2012). "Bilateral middle cerebral artery aneurysms: a comparative study of unilateral and bilateral approaches." Neurosurg Rev 35(4): 505-517; discussion 517-508.

Kakizawa, Y., Y. Tanaka, Y. Orz, T. Iwashita, K. Hongo and S. Kobayashi (2000). "Parameters for contralateral approach to ophthalmic segment aneurysms of the internal carotid artery." Neurosurgery 47(5): 1130-1137.

Kang, S., Y. Yang, T. Kim and J. Kim (1997). "Sudden unilateral blindness after intracranial aneurysm surgery." Acta Neurochir (Wien) 139(3): 221-226.

Kassam, A. B., P. A. Gardner, A. Mintz, C. H. Snyderman, R. L. Carrau and M. Horowitz (2007). "Endoscopic endonasal clipping of an unsecured superior hypophyseal artery aneurysm. Technical note." J Neurosurg 107(5): 1047-1052.

Kinouchi, H., K. Mizoi, Y. Nagamine, N. Yanagida, S. Mikawa, A. Suzuki, T. Sasajima and T. Yoshimoto (2002). "Anterior paraclinoid aneurysms." J Neurosurg 96(6): 1000-1005.

Kobayashi, M. and R. M. Costanzo (2009). "Olfactory nerve recovery following mild and severe injury and the efficacy of dexamethasone treatment." Chem Senses 34(7): 573-580.

Kobayashi, S., K. Kyoshima, H. Gibo, S. A. Hegde, T. Takemae and K. Sugita (1989). "Carotid cave aneurysms of the internal carotid artery." J Neurosurg 70(2): 216-221.

Kockro, R. A., T. Killeen, A. Ayyad, M. Glaser, A. Stadie, R. Reisch, A. Giese and E. Schwandt (2016). "Aneurysm Surgery with Preoperative Three-Dimensional Planning in a Virtual Reality Environment: Technique and Outcome Analysis." World Neurosurg 96: 489-499.

Korosue, K. and R. C. Heros (1992). ""Subclinoid" carotid aneurysm with erosion of the anterior clinoid process and fatal intraoperative rupture." Neurosurgery 31(2): 356-359; discussion 359-360.

Lanzino, G., E. Crobeddu, H. J. Cloft, R. Hanel and D. F. Kallmes (2012). "Efficacy and safety of flow diversion for paraclinoid aneurysms: a matched-pair analysis compared with standard endovascular approaches." AJNR Am J Neuroradiol 33(11): 2158-2161.

Liu, Q. and A. L. Rhoton, Jr. (2001). "Middle meningeal origin of the ophthalmic artery." Neurosurgery 49(2): 401-406; discussion 406-407.

Loumiotis, I., P. I. D'Urso, R. Tawk, H. J. Cloft, D. F. Kallmes, V. Kairouz, R. Hanel and G. Lanzino (2012). "Endovascular treatment of ruptured paraclinoid aneurysms: results, complications, and follow-up." AJNR Am J Neuroradiol 33(4): 632-637.

Luostarinen, T., R. S. Takala, T. T. Niemi, A. J. Katila, M. Niemela, J. Hernesniemi and T. Randell (2010). "Adenosine-induced cardiac arrest during intraoperative cerebral aneurysm rupture." World Neurosurg 73(2): 79-83; discussion e79.

MacCarty, C. S. (1972). "Meningiomas of the sphenoidal ridge." J Neurosurg 36(1): 114-120.

Matthews, L. S. and C. Hirsch (1972). "Temperatures measured in human cortical bone when drilling." JBJS 54(2): 297-308.

McMahon, J. H., M. K. Morgan and M. A. Dexter (2001). "The surgical management of contralateral anterior circulation intracranial aneurysms." Journal of clinical neuroscience 8(4): 319-324.

Meetze, K., J. N. Palmer and R. J. Schlosser (2004). "Frontal sinus complications after frontal craniotomy." Laryngoscope 114(5): 945-948.

Metwali, H., V. Gerganov and R. Fahlbusch (2016). "Optic nerve mobilization to enhance the exposure of the pituitary stalk during craniopharyngioma resection: early experience." J Neurosurg 125(3): 683-688.

Milenković, Z., H. Gopić, P. Antović, V. Joviĉić and B. Petrović (1982). "Contralateral pterional approach to a carotid-ophthalmic aneurysm ruptured at surgery: Case report." Journal of neurosurgery 57(6): 823-825.

Miwa, T., M. Furukawa, T. Tsukatani, R. M. Costanzo, L. J. DiNardo and E. R. Reiter (2001). "Impact of olfactory impairment on quality of life and disability." Archives of Otolaryngology–Head & Neck Surgery 127(5): 497-503.

Nacar, O. A., A. Rodriguez-Hernandez, M. O. Ulu, R. Rodriguez-Mena and M. T. Lawton (2014). "Bilateral ophthalmic segment aneurysm clipping with one craniotomy: operative technique and results." Turk Neurosurg 24(6): 937-945.

Nakao, S., H. Kikuchi and N. Takahashi (1981). "Successful clipping of carotid-ophthalmic aneurysms through a contralateral pterional approach: Report of two cases." Journal of neurosurgery 54(4): 532-536.

Nishio, S., T. Matsushima, M. Fukui, K. Sawada and K. Kitamura (1985). "Microsurgical anatomy around the origin of the ophthalmic artery with reference to contralateral pterional surgical approach to the carotid-ophthalmic aneurysm." Acta Neurochir (Wien) 76(3-4): 82-89.

Oikawa, S., K. Kyoshima and S. Kobayashi (1998). "Surgical anatomy of the juxta-dural ring area." J Neurosurg 89(2): 250-254.

Oshiro, E. M., D. A. Rini and R. J. Tamargo (1997). "Contralateral approaches to bilateral cerebral aneurysms: a microsurgical anatomical study." J Neurosurg 87(2): 163-169.

Ota, N., R. Tanikawa, T. Miyazaki, S. Miyata, J. Oda, K. Noda, T. Tsuboi, R. Takeda, H. Kamiyama and S. Tokuda (2015). "Surgical microanatomy of the anterior clinoid process for paraclinoid aneurysm surgery and efficient modification of extradural anterior clinoidectomy." World Neurosurg 83(4): 635-643.

Park, J., S. H. Lee, D. H. Kang and J. S. Kim (2009). "Olfactory dysfunction after ipsilateral and contralateral pterional approaches for cerebral aneurysms." Neurosurgery 65(4): 727-732; discussion 732.

Paullus, W. S., T. G. Pait and A. I. Rhoton, Jr. (1977). "Microsurgical exposure of the petrous portion of the carotid artery." J Neurosurg 47(5): 713-726.

Pereira, R. S. and L. Casulari (2006). "Surgical treatment of bilateral multiple intracranial aneurysms: review of a personal experience in 69 cases." Journal of neurosurgical sciences 50(1): 1.

Perneczky, A., E. Knosp, P. Vorkapic, T. Czech (1985). “Direct surgical approach to infraclinoidal aneurysms.” Acta Neurochir (Wien). 76(1-2):36-44.

Porter, P., M. Mazighi, G. Rodesch, H. Alvarez, N. Aghakhani, P. David and P. Lasjaunias (2001). "Endovascular and surgical management of multiple intradural aneurysms: Review of 122 patients managed between 1993 and 1999." Interventional Neuroradiology 7(4): 291-302.

Raco, A., A. Frati, A. Santoro, T. Vangelista, M. Salvati, R. Delfini and G. Cantore (2008). "Long-term surgical results with aneurysms involving the ophthalmic segment of the carotid artery." J Neurosurg 108(6): 1200-1210.

Renn, W. H. and A. L. Rhoton, Jr. (1975). "Microsurgical anatomy of the sellar region." J Neurosurg 43(3): 288-298.

Rhoton, A.I., Jr., Cranial anatomy and surgical approaches. Neurosurgery, 2002. 53: p. 1-746.

Rizzo, J. F., 3rd (1995). "Visual loss after neurosurgical repair of paraclinoid aneurysms." Ophthalmology 102(6): 905-910.

Rodriguez-Hernandez, A., A. Gabarros and M. T. Lawton (2012). "Contralateral clipping of middle cerebral artery aneurysms: rationale, indications, and surgical technique." Neurosurgery 71(1 Suppl Operative): 116-123; discussion 123-114.

Rosner, S. S., A. L. Rhoton, Jr., M. Ono and M. Barry (1984). "Microsurgical anatomy of the anterior perforating arteries." J Neurosurg 61(3): 468-485.

Rozen, W. M., D. Chubb, D. L. Stella, G. I. Taylor and M. W. Ashton (2009). "Evaluating anatomical research in surgery: a prospective comparison of cadaveric and living anatomical studies of the abdominal wall." ANZ J Surg 79(12): 913-917.

Salunke, P., A. Singh and A. N. Deepak (2016). "Shattering the Rock: Technique of Bilateral Optic Nerve Mobilization and Drilling Heavily Calcified Craniopharyngiomas for Its Excision." World Neurosurg 95: 292-298.

Santos, D. V., E. R. Reiter, L. J. DiNardo and R. M. Costanzo (2004). "Hazardous events associated with impaired olfactory function." Arch Otolaryngol Head Neck Surg 130(3): 317-319.

Shapiro, S. S. and M. B. Wilk (1965). "An Analysis of Variance Test for Normality (Complete Samples)." Biometrika 52: 591-&.

Sheikh, B., K. Ohata, A. El-Naggar, M. Baba, B. Hong and A. Hakuba (2000). "Contralateral approach to junctional C2-C3 and proximal C4 aneurysms of the internal carotid artery: microsurgical anatomic study." Neurosurgery 46(5): 1156-1160; discussion 1160-1151.

Sheikh, B., K. Ohata, A. El-Naggar, B. Hong, N. Tsuyuguchi and A. Hakuba (2000). "Contralateral approach to carotid cave aneurysms." Acta Neurochir (Wien) 142(1): 33-37.

Shimizu, K., H. Imamura, Y. Mineharu, H. Adachi, C. Sakai and N. Sakai (2016). "Endovascular Treatment of Unruptured Paraclinoid Aneurysms: Single-Center Experience with 400 Cases and Literature Review." AJNR Am J Neuroradiol 37(4): 679-685.

Shiokawa, Y., N. Aoki, I. Saito and H. Mizutani (1988). "Combined contralateral pterional and interhemispheric approach to a subchiasmal carotid-ophthalmic aneurysm." Acta neurochirurgica 93(3): 154-158.

Stephens, R. and D. Stilwell (1969). Arteries and Veins of the Human Brain. S. I. Thomas.

Sugita, K. (1985). Microneurosurgical Atlas, Berlin: Springer-Verlag: 16-91.

Sun, Y., Y. Li and A. M. Li (2011). "Endovascular treatment of paraclinoid aneurysms." Interv Neuroradiol 17(4): 425-430.

Temmel, A. F., C. Quint, B. Schickinger-Fischer, L. Klimek, E. Stoller and T. Hummel (2002). "Characteristics of olfactory disorders in relation to major causes of olfactory loss." Arch Otolaryngol Head Neck Surg 128(6): 635-641.

Thornton, J., V. A. Aletich, G. M. Debrun, A. Alazzaz, M. Misra, F. Charbel and J. I. Ausman (2000). "Endovascular treatment of paraclinoid aneurysms." Surg Neurol 54(4): 288-299.

Vajda, J., J. Juhasz, E. Pasztor and I. Nyary (1988). "Contralateral approach to bilateral and ophthalmic aneurysms." Neurosurgery 22(4): 662-668.

van den Brand, C. L., T. Tolido, A. H. Rambach, M. G. Hunink, P. Patka and K. Jellema (2017). "Systematic review and meta-analysis: is pre-injury antiplatelet therapy associated with traumatic intracranial hemorrhage?" Journal of neurotrauma 34(1): 1-7.

van Lindert, E., A. Perneczky, G. Fries and E. Pierangeli (1998). "The supraorbital keyhole approach to supratentorial aneurysms: concept and technique." Surg Neurol 49(5): 481-489; discussion 489-490.

Wang, Y., Y. Li, C. Jiang, F. Jiang, H. Meng, A. H. Siddiqui and X. Yang (2013). "Endovascular treatment of paraclinoid aneurysms: 142 aneurysms in one centre." J Neurointerv Surg 5(6): 552-556.

Xu, D. and M. Pollock (1994). "Experimental nerve thermal injury." Brain 117(2): 375-384.

Yamada, K., T. Hayakawa, Y. Oku, Y. Ushio, T. Yoshimine and R. Kawai (1984). "Contralateral pterional approach for carotid-ophthalmic aneurysm: usefulness of high resolution metrizamide or blood computed tomographic cisternography." Neurosurgery 15(1): 5-8.

Yaşargil, M. G. (1984). Clinical considerations, surgery of the intracranial aneurysms and results, Thieme.

Yu, L. H., H. C. Shang-Guan, G. R. Chen, S. F. Zheng, Y. X. Lin, Z. Y. Lin, P. S. Yao and D. Z. Kang (2017). "Monolateral Pterional Keyhole Approaches to Bilateral Cerebral Aneurysms: Anatomy and Clinical Application." World Neurosurg 108: 572-580.

Zimmerman, C. F., P. D. Van Patten, K. C. Golnik, T. A. Kopitnik, Jr. and R. Anand (1995). "Orbital infarction syndrome after surgery for intracranial aneurysms." Ophthalmology 102(4): 594-598.

9. Acknowledgements

First of all, I want to thank to the directors and mentors of this project for their great supervision during all steps of this doctoral work. Without you this work would not have been possible. Thanks very much to all those who contributed to set up the lab and provided material for this work, as well as to the ones who instructed me in the use of the Dextroscope.

I want to thank my family, specially my father, brother and my mother, who supported me unconditionally during my medical studies in Argentina and further postgraduate studies in Germany. I know mama that you are still giving me wisdom and encouraging me to be a better man even from heaven now. And to my new family in Germany, thank's for receiving me with open and lovely arms after long hours in the lab or writing this thesis.

Above all, I want to dedicate this work to my best friend and the love of my life. Thank you for your great support, patience, encouragement and love.